



UNIVERSITÀ DELLA CALABRIA



**UNIVERSITA' DELLA CALABRIA**

Dipartimento di Farmacia e Scienze della Nutrizione e della Salute

**Dottorato di Ricerca in**

Biochimica Cellulare ed Attività dei Farmaci in Oncologia

*Con il contributo di FSE-Regione Calabria*

**CICLO XXVI**

**Leptin as a Novel Mediator of Tumor/Stroma Interaction  
Promotes the Invasive Growth of Breast Cancer**

**Settore Scientifico Disciplinare MED/05**

**Coordinatore:** Ch.mo Prof. Diego Sisci

**Tutor:** Ch.mo Prof.ssa Catalano Stefania

**Dottorando:** Dott. Luca Gelsomino

*"La presente tesi è cofinanziata con il sostegno della Commissione Europea, Fondo Sociale Europeo e della Regione Calabria. L'autore è il solo responsabile di questa tesi e la Commissione Europea e la Regione Calabria declinano ogni responsabilità sull'uso che potrà essere fatto delle informazioni in essa contenute".*

# Table of Contents

<b><i>Introduction</i></b>	Pag. 6
<b><i>Materials and Methods</i></b>	Pag. 8
<i>Reagent and Antibodies</i>	Pag. 13
<i>Plasmids</i>	Pag. 13
<i>Cell Culture</i>	Pag. 13
<i>CAFs Isolation</i>	Pag. 14
<i>Conditioned Medium System</i>	Pag. 14
<i>ERE-Luciferase Reporter Assay</i>	Pag. 14
<i>Expression Microarray Analysis</i>	Pag. 15
<i>Immunoblot Analysis</i>	Pag. 15
<i>Immunofluorescence</i>	Pag. 16
<i>Reverse Transcription and Real-Time Transcriptase PCR assays</i>	Pag. 18
<i>Cell proliferation Assays (MTT Assasy, Tripan Blue Assays, Soft Agar Assasy)</i>	Pag. 18
<i>Wound-Healing Scratch Assays</i>	Pag. 19
<i>Transmigration Assays</i>	Pag. 19
<i>Invasion Assays</i>	Pag. 19
<i>Leptin measurement by radioimmunoassay</i>	Pag. 19
<i>Leptin-immunodepleted conditioned media</i>	Pag. 19
<i>Aromatase Activity Assays</i>	Pag. 20
<i>Synthesis and Characterization of Peptide LDFI</i>	Pag. 20
<i>Tumor Xenografts</i>	Pag. 20
<i>Statistical Analysis</i>	Pag. 21

## ***Evaluation of the Mechanisms Underlying Tumor-Stroma Interaction in ER $\alpha$ -positive breast cancer (Aim 1).***

<i>Tumor/Stroma Interactions Stimulate Cell Proliferation and Motility</i>	Pag. 23
<i>Gene Transcription Patterns of WT and K303R ER<math>\alpha</math>-overexpressing Cells</i>	Pag. 24
<i>K303R ER<math>\alpha</math>-overexpressing Cells Exhibit Increased Leptin Signaling Activation</i>	Pag. 27
<i>K303R ER<math>\alpha</math> mutation and leptin hypersensitivity</i>	Pag. 29
<i>Leptin is responsible for CAFs-induced Cell Growth and Motility</i>	Pag. 31
<i>Tumor/Stroma Interactions in SKBR3 Breast Cancer Cells</i>	Pag. 32
<i>Effects of Breast Cancer Cell-secreted Factors on CAFs Phenotype</i>	Pag. 33

## ***Evaluation of the Potential Role of Leptin in Driving Aromatase Inhibitor Resistance in Breast Cancer (Aim 2).***

<i>Generation of Anastrozole-Resistant Breast Cancer Cells</i>	Pag. 37
<i>AnaR Cells Exhibits Increased Activation of Leptin Signalings</i>	Pag. 39
<i>CAFs enhance Growth and Motility of AnaR Cells</i>	Pag. 40
<i>Enhanced Recruitment and Protumor Activation of Macrophages from AnaR Cell through Leptin Signalings</i>	Pag. 41
<i>Macrophages Promotes Growth and Migration of AnaR Cells.</i>	Pag. 43

## ***Evaluation of the Efficacy of a Novel Peptide to Block Leptin Action in Breast Cancer (Aim 3).***

<i>Design, Synthesis and Characterization of Peptide LDFI</i>	Pag. 45
<i>Peptide LDFI Reduces Leptin-induced Cell Growth and Motility</i>	Pag. 48
<i>Peptide LDFI Antagonizes Leptin Signaling Pathways</i>	Pag. 49
<i>Peptide LDFI Abolishes Leptin-induced Up-regulation of the Ob Gene</i>	Pag. 49
<i>Efficacy of PEG-LDFI Treatment in Breast Cancer Xenografts</i>	Pag. 50

*Discussion*

Pag. 53

*References*

Pag. 60

## Introduction

For the past 3 decades, cancer research focused predominantly on the characteristics of breast cancer cells. Recently, clinical and experimental studies revealed that both tumor initiation and progression are related to the complex interactions that transpire within the tumor microenvironment. The stromal compartment is composed of mesenchymal cells (fibroblasts, adipocytes, blood cells) and extracellular matrix (ECM; lamin, fibronectin, collagen, proteoglycans, and so on), and signals from these cells come as soluble secreted factors, ECM components, or direct cell–cell contacts (Fig. 1).

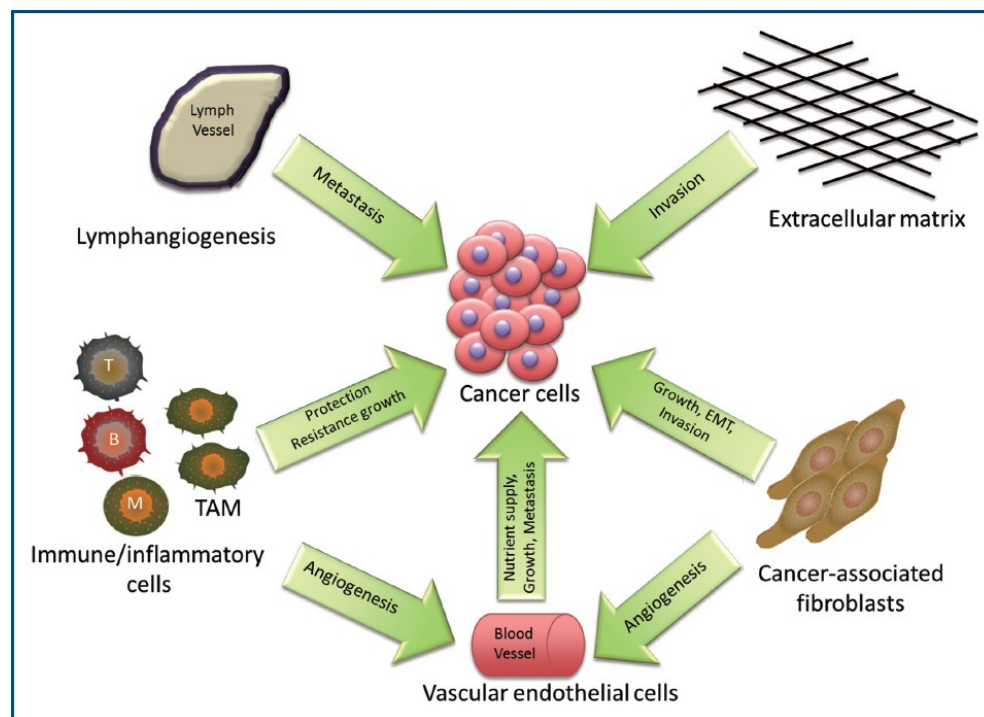


**Figure 1. A schematic representation of tumor microenvironment.**

Growth factors, cytokines, adipokines, proteases, and vascular-stimulating factors are involved in stroma-mediated procancerous activities (1–4). The chemokines CXCL12, CXCL14, and CCL7 stimulated tumor cell proliferation and invasion *in vitro* and *in vivo* and increased tumor angiogenesis and macrophage presence at tumor sites (5–7). The interleukins (IL)-1 and -8 induced cancer progression by enhancing metastasis and cachexia (8, 9).

As important adipocyte-derived endocrine and paracrine mediator, the adipokine leptin has been correlated with breast cancer occurrence. Indeed, leptin synthesis and plasma levels increase with obesity, a pandemic condition that influences both risk and prognosis of breast cancers (10).

The processes of heterotypic signaling involve a constant bidirectional cross-talk between stromal cells and malignant cells. Stromal cells influence tumor invasiveness and malignancy, whereas at the onset and during breast cancer progression the microenvironment is reorganized by cancer cells (11). Tumors recruit stromal fibroblasts in a process referred to as the desmoplastic reaction, and these carcinoma-associated fibroblasts (CAFs) are reprogrammed to produce growth factors, cytokines, and ECM-remodeling proteins, that acting in autocrine and paracrine fashion support tumor proliferation and invasion into surrounding tissues (4). Moreover, in the microenvironment of most neoplastic tissue, as those of the breast, an inflammatory component is present an included infiltration of white blood cells, essentially tumor associated macrophages (TAMs). The majority of TAMs exhibits alternatively activated M2 properties, produce abundant anti-inflammatory factors and facilitate tumor development. Accumulating evidences from both patient biopsies and experimental animal models have shown that TAMs function in tumor angiogenesis and vessel abnormalization in a density- and phenotype-dependent manner (12). Multiple clinical studies compellingly indicate the association between high TAMs influx and poor prognosis in patients with breast cancers (13). Also, the pro-inflammatory microenvironment is associated with the obese state (14-16), specifically highlighting the involvement of obesity-associated hormones/growth factors in the cross-talk between macrophages, adipocytes, and epithelial cells in many cancers. Moreover, a variety of these factors may activate estrogen receptor alpha (ER $\alpha$ ) (17).

Estrogens and its receptor play a crucial role in regulating breast cancer growth and differentiation. Variant forms of ER $\alpha$  due to alternative splicing or gene mutation have been reported, but their clinical significance is still unresolved (18, 19). A naturally occurring mutation at nucleotide 908, introducing a lysine to arginine transition at residue 303 within the hinge domain of the receptor (K303R ER $\alpha$ ) (Fig. 2), was identified in one third of premalignant breast hyperplasias and one half of invasive breast tumors.



**Figure 2. Tridimensional structure of Estrogen Receptor alpha (ER $\alpha$ ) and schematic representation of the different domains within ER $\alpha$ , AF-1 and (activation function-1), DBD (DNA binding domain), Hinge region, HBD (hormone binding domain)/AF-2.**

This mutation is correlated with poor outcomes, older age, larger tumor size, and lymph node–positive disease (20, 21) (Table 1).

	K303R (n=133)	WT (n=134)	P value
<b>Age (y), (%)</b>			
≤50	20.3	33.6	<b>0.015</b>
>50	79.7	66.4	
<b>Tumor Size (cm) (%)</b>			
0-2	24.2	42.9	<b>0.002</b>
>2-5	61.4	51.1	
>5	14.4	6.0	
<b>Nodes, (%)</b>			
Node Negative	42.1	78.4	<b>&lt;0.0001</b>
Node Positive			
1-3	31.6	13.4	
>3	26.3	8.2	

**Table 1. Clinical characteristics of breast cancer cases expressing wild-type (WT) or K303R ER $\alpha$  mutation.**

Other studies did not detect the mutation in invasive cancers (22–25), but our data suggest that the detection method used might be insensitive. However, K303R expression was found at low frequency in invasive breast tumors by Conway and colleagues (26).

K303R mutation allows ER $\alpha$  to be more highly phosphorylated by different kinases, and it alters the dynamic recruitment of coactivators and corepressors (27–29). Mutant overexpression in MCF-7 breast cancer cells increased sensitivity to subphysiologic levels of estrogen and decreased tamoxifen responsiveness when elevated growth factor signaling was present (20, 30). K303R ER $\alpha$  mutation also conferred resistance to the aromatase inhibitor anastrozole (28, 31), suggesting a pivotal role for this mutation in more aggressive breast cancers.

Resistance to hormone therapy remains a major clinical challenge in the treatment of the ER-positive breast cancers. Despite the efficacy of inhibiting ER $\alpha$  action by using the antiestrogen tamoxifen or reducing estrogen production with the aromatase inhibitors (AIs), letrozole, anastrozole or exemestane (Fig. 3), a large number of patients fail to respond to initial therapy (*de novo resistance*) or develop resistance after prolonged treatment (*acquired resistance*) that limit the usefulness of these drugs.

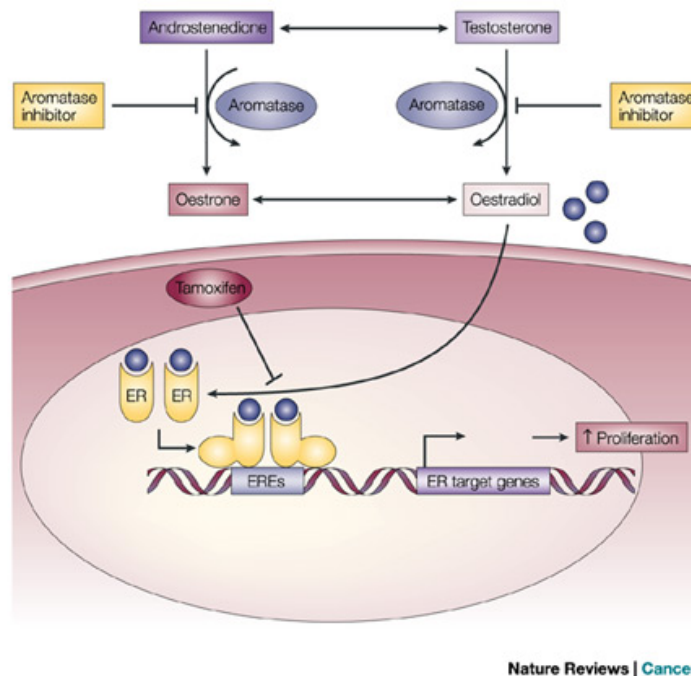


**Figure 3. Schematic action of Tamoxifen and Aromatase Inhibitors.**

The mechanisms responsible for the development of resistance remain poorly defined. Several mechanisms have been proposed (Fig. 4), including the loss of ER $\alpha$  expression or function (32), alterations in the balance of regulatory cofactors, increased oncogenic kinase signaling (33), and deregulated cell proliferation (34). Resistance may also result from altered expression of growth



- 2) **to investigate the potential role of leptin in driving AI resistance in breast cancer, in the context of tumor microenvironment.** Specifically, we evaluated whether the activation of leptin signaling pathway may provide AI resistant tumors with alternative proliferative and survival advantage and how CAFs may influence AI resistant behavior through leptin. Then, we explored if AI resistant breast cancer cells through the proinflammatory cytokine leptin may control the phenotype of macrophages, to further support breast cancer progression.
- 3) **to test the ability of a newly synthesized peptide to block leptin action in breast cancer in *in vitro* and *in vivo* experimental models.**

# **Materials and Methods**

## **Materials and Methods**

### *Reagents and antibodies.*

The following reagents and antibodies were used: leptin, 17 $\beta$ -estradiol, and epidermal growth factor (EGF), anastrozole, androstenedione from Sigma; ICI182780 from Tocris Bioscience; Gentamicin from Invitrogen. AG490, AG1478, PD98059, and LY294002 from Calbiochem; ER $\alpha$ , ER $\beta$ , glyceraldehyde-3-phosphate dehydrogenase (GAPDH), ObR1, ObRs, Ob, Akt, and pAkt<sup>Ser437</sup>, Cyclin D1 antibodies from Santa Cruz Biotechnology; and mitogen-activated protein kinase (MAPK), Janus-activated kinase (JAK)2, STAT3, pMAPK<sup>Thr202/Tyr204</sup>, pJAK2<sup>Tyr1007/1008</sup>, pSTAT3<sup>Tyr705</sup>/pER $\alpha$ <sup>Ser118</sup>, and pER $\alpha$ <sup>Ser167</sup> from Cell Signaling Technology, Aromatase from Serotec.

### *Plasmids.*

YFP-WT and YFP-K303R-ER $\alpha$ , was provided by Dr. Fuqua, Baylor College of Medicine, Houston, Texas. XETL plasmid, containing an estrogen-responsive element, was provided by Dr. Picard, University of Geneva, Geneva, Switzerland.

### *Cell culture.*

Breast cancer epithelial ER-positive MCF-7 cell line was cultured in DMEM medium containing 10% FBS, 1% L-glutamine, 1% Eagle's nonessential amino acids, and 1 mg/ml penicillin-streptomycin at 37 °C with 5% CO<sub>2</sub> air.

Breast cancer epithelial ER-negative SKBR3 cell line was cultured in phenol red-free RPMI medium containing 10% FBS, 1% L-glutamine, 1% Eagle's nonessential amino acids, and 1 mg/ml penicillin-streptomycin.

The murine macrophage RAW 264.7 cell line was cultured in DMEM medium containing 10% FBS, 1% L-glutamine, 1% Eagle's nonessential amino acids, and 1 mg/ml penicillin-streptomycin.

YFP-WT and YFP-K303R ER $\alpha$  stably expressing MCF-7 cells, MCF-7 and SKBR3 pools stably transfected with YFP-WT and YFP-K303R ER $\alpha$  were generated as described (28, 31). Immortalized normal human foreskin fibroblasts BJ1-hTERT were provided by Dr Lisanti, Jefferson University, Philadelphia, PA. MCF-7 aro cells stably expressing the aromatase enzyme were generated as previously described (31).

Anastrozole-resistant MCF-7 cells (AnaR) cells were generated by culturing MCF-7 aro cells in MEM with 10% FBS, 1% L-glutamine, 1% Eagle's nonessential amino acids, 1mg/ml penicillin/streptomycin, zeocin 0.2mg/ml and anastrozole 1 $\mu$ M. Cells were routinely maintained in 1 $\mu$ M anastrozole for longer than one year. Every 4 months, cells were authenticated by single tandem repeat analysis at our Sequencing Core; morphology, doubling times, estrogen sensitivity, and mycoplasma negativity were tested (MycoAlert, Lonza).

*CAF isolation.*

Human breast cancer specimens were collected in 2011 from primary tumors of patients who signed informed consent. Following tumor excision, small pieces were digested (500 IU collagenase in Hank's balanced salt solution; Sigma; 37 $^{\circ}$ C for 2 hours). After differential centrifugation (90 g for 2 minutes), the supernatant containing CAFs was centrifuged (500 g for 8 minutes), resuspended, and cultured in RPMI-1640 medium supplemented with 15% FBS and antibiotics. CAFs between 4 and 10 passages were used, tested by mycoplasma presence, and authenticated by morphology and fibroblast activation protein (FAP) expression.

*Conditioned medium systems.*

CAF and RAW 264.7 cells were incubated with regular full media (48–72 hours). Conditioned media were collected, centrifuged to remove cellular debris, and used in respective experiments. Alternatively, conditioned media were collected from WT- and K303R ER $\alpha$ -expressing MCF-7 cells or MCF-7 aro and AnaR cells incubated in media supplemented with 5% charcoal-stripped FBS (72 hours).

*ERE-Luciferase reporter assay*

Cells were transiently transfected using the FuGENE 6 reagent as recommended by the manufacturer with XETL reporter plasmid (0.5  $\mu$ g/well) and TK Renilla luciferase plasmid (25 ng/well). After transfection cells were treated as indicated. The firefly and Renilla luciferase activities were measured using a dual luciferase kit (Promega). The firefly luciferase data for each sample were normalized on the basis of transfection efficiency measured by Renilla luciferase activity.

*Expression microarray analysis.*

Expression profiles were determined with Affymetrix GeneChip Human Genome U133 plus 2.0 arrays. Data quality and statistical analyses were conducted as described in the work of Barone and colleagues (28). Microarray study followed MIAME (Minimum Information About a Microarray Experiment) guidelines.

*Immunoblot analysis.*

Cells were grown to 50–60% confluence and treated as indicated before lysis in 500 $\mu$ l of 50 mM Tris-HCl, 150 mM NaCl, 1% NP-40, 0.5% sodium deoxycholate, 2 mM sodium fluoride, 2 mM EDTA, 0.1% SDS, containing a mixture of protease inhibitors (aprotinin, phenylmethylsulfonyl fluoride, and sodium orthovanadate) for protein extraction. Protein extracts from frozen tumors were prepared by homogenizing the tissue in lysis buffer supplemented with 10% glycerol, and protease inhibitors (0.1 mM Na<sub>3</sub>VO<sub>4</sub>, 1% PMSF, 20  $\mu$ g/ml aprotinin). Tumor lysates were collected, sonicated (5 $\times$  for 5s on ice), and microcentrifuged at 14000 $\times$ g for 20 min at 2°C. Supernatants of the lysates were aliquoted and stored at –80°C.

Equal amounts of cell extracts were resolved under denaturing conditions by electrophoresis in 8% to 10% polyacrylamide gels containing SDS (SDS-PAGE), and transferred to nitrocellulose membranes by electroblotting. After blocking the transferred nitrocellulose membranes were incubated with primary antibodies overnight at 4°C. The antigen-antibody complex was detected by incubation of the membranes with peroxidase-coupled goat anti-mouse, goat anti-rabbit and revealed using the ECL System. To ensure equal loading all membranes were stripped and incubated with anti GAPDH or  $\beta$ -actin antibodies for total extracts. The bands of interest were quantified by Scion Image laser densitometry scanning program.

*Immunofluorescence.*

Cells were fixed with 4% paraformaldehyde, permeabilized with PBS  $\pm$  0.2% Triton X-100 followed by blocking with 5% bovine serum albumin (1 hour at room temperature), and incubated with anti-ObR antibody (4°C, overnight) and with fluorescein isothiocyanate–conjugated secondary antibody (30 minutes at room temperature). IgG primary antibody was used as negative control. 4,6-Diamidino-2-phenylindole (DAPI; Sigma) staining was used for

nuclei detection. Fluorescence was photographed with OLYMPUS BX51 microscope, 100 objective.

*Reverse transcription and real-time reverse transcriptase PCR assays.*

Total RNA was extracted from cells using TRIzol reagent and the evaluation of Ob, FAP, cyclin D1, ps2, cathepsin and 36B4 gene expression was performed by the reverse transcription-PCR method using a RETROscript kit.

Analysis gene expression of the other genes used in this study was performed by Real-time reverse transcription-PCR. Total RNA (2µg) was reverse transcribed with the RETROscript kit; cDNA was diluted 1:3 in nuclease-free water and 5µl were analysed in triplicates by real-time PCR in an iCycler iQ Detection System (Bio-Rad, USA) using SYBR Green Universal PCR Master Mix with 0.1 mmol/l of each primer in a total volume of 30 µl reaction mixture following the manufacturer's recommendations. Negative control contained water instead of first strand cDNA was used. Each sample was normalized on its GAPDH mRNA content.

The relative gene expression levels were normalized to a calibrator that was chosen to be the basal, untreated sample. Final results were expressed as n-fold differences in gene expression relative to GAPDH mRNA and calibrator, calculated using the  $\Delta\text{Ct}$  method as follows:

$n\text{-fold} = 2^{- (\Delta\text{Ct}_{\text{sample}} - \Delta\text{Ct}_{\text{calibrator}})}$  where  $\Delta\text{Ct}$  values of the sample and calibrator were determined by subtracting the average Ct value of the GAPDH mRNA reference gene from the average Ct value of the gene analysed.

Primers used for the amplification were reported in Table 1.

<i>Gene Name</i>	<i>Gene Symbol</i>		<i>Primer Sequences</i>
Fibroblast activation protein	<i>FAP</i>	Forward Reverse	5'-AGAAAGCAGAACTGGATGG-3' 5'-ACACACTTCTTGCTTGGAGGAT-3'
36B4	<i>36B4</i>	Forward Reverse	5'-CTCAACATCTCCCCCTTCTC-3' 5'-CAAATCCCATATCCTCGT-3'
Leptin Receptor Long Isoform	<i>ObRl</i>	Forward Reverse	5'-GATAGAGGCCAGGCATTTTTTA-3' 5'-ACACACTCTCTCTTTTTTGATTGA-3'
Leptin Receptor Short Isoform	<i>ObRs</i>	Forward Reverse	5'-ATTGTGCCAGTAATTATTTCTCTTCC-3' 5'-CCACCATATGTAACTCTCAGAAGTTCAA-3'
Chemokine (C-X-C motif) receptor 4	<i>CXCR4</i>	Forward Reverse	5'-AATCTTCTGCCACCATCT-3' 5'-GACGCCAACATAGACCACCT-3'
Insulin Receptor	<i>IR</i>	Forward Reverse	5'-AGGAGCCCAATGGTCTGA-3' 5'-AGACGCAGAGATGCAGC-3'
Interleukin 2 Receptor	<i>IL2R</i>	Forward Reverse	5'-GGCCATGGCTGAAGAAGGT-3' 5'-CTGGACGTCTCCTCCATGCT-3'
Interleukin 6 Receptor	<i>IL6R</i>	Forward Reverse	5'-TGAGCTCAGATATCGGGCTGAAC-3' 5'-CGTCGTGGATGACACAGTGATG-3'
Epidermal growth factor receptor	<i>EGFR</i>	Forward Reverse	5'-GGACTCTGGATCCCAGAAGGTG-3' 5'-GCTGGCCATCACGTAGGCTT-3'
Insulin growth factor-1 receptor	<i>IGF1R</i>	Forward Reverse	5'-CACGACGGCGAGTGCAT-3' 5'-ACAGACCTTCGGCAAGGA-3'
Fibroblast growth factor receptor 3	<i>FGFR3</i>	Forward Reverse	5'-TGCTGAATGCCTCCCACG-3' 5'-CGTCTTCGTTCATCTCCCGAG-3'
Estrogen receptor	<i>ERα</i>	Forward Reverse	5'-TGATTGGTCTCGTCTGGCG-3' 5'-CATGCCCTCTACACATTTCCC-3'
Cyclin D1	<i>CD1</i>	Forward Reverse	5'-TCTAAGATGAAGGAGACCTATC-3' 5'-GCGGTAGTAGGACAGGAAGTT-3'
18s rRNA	<i>18s</i>	Forward Reverse	5'-CCCACTCCTCCACCTTTGAC-3' 5'-TGTTGCTGTAGCCAAATTCGTT-3'
Cathepsin D	<i>CD</i>	Forward Reverse	5'-AACAACAGGGTGGGCTTC-3' 5'-TTTGAGTAGTCAAAGTCAGAGC-3'
Trefoil factor 1/pS2	<i>pS2</i>	Forward Reverse	5'-TTCTATCCTAATACCATCGACG-3' 5'-TTTGAGTAGTCAAAGTCAGAGC-3'

<i>Gene Name</i>	<i>Gene Symbol</i>		<i>Primer Sequences</i>
Leptin	<i>Ob</i>	Forward Reverse	5'-GAGACCTCCTCCATGTGCTG-3' 5'-TGAGCTCAGATATCGGGCTGAAC-3'
Epidermal Growth Factor	<i>EGF</i>	Forward Reverse	5'-CCCTAAGTCGAGACCGGAAGT-3' 5'-CAAGAGTACAGCCATGATTCCAAA-3'
Interleukin-6	<i>IL-6</i>	Forward Reverse	5'-CCAGGAGCCAGCTATGAAC-3' 5'-CCAGGGAGAAGGCAACTG-3'
Insulin	<i>INS</i>	Forward Reverse	5'-TCAGAAGAGGCCATCAAGCA-3' 5'-AGATGCTTCACGAGCCCAGC-3'
Transforming Growth Factor Beta	<i>TGFβ</i>	Forward Reverse	5'-ATCCTGTCCAAACTAAGGCTCG-3' 5'-ACCTCTTTAGCATAGTAGTCCGC-3'
Small mothers against decapentaplegic	<i>Smad3</i>	Forward Reverse	5'-GGATCCATGTGTCCTCATCTGCCC-3' 5'-GAATTCCTAAGACACACTGGAACAGCGGATG-3'
Interleukin-10	<i>IL-10</i>	Forward Reverse	5'-CTGGACAACATACTGCTAACCG-3' 5'-GGGCATCACTTCTACCAGGTAA-3'
Interleukin-12	<i>IL-12</i>	Forward Reverse	5'-TGGTTTGCCATCGTTTTGCTG-3' 5'-ACAGGTGAGGTTCACTGTTTCT-3'
Arginase	<i>Argi</i>	Forward Reverse	5'-CTCCAAGCCAAAGTCCTTAGAG-3' 5'-AGGAGCTGTCATTAGGGACATC-3'
Inducible nitric oxide synthase	<i>iNOS</i>	Forward Reverse	5'-GTTCTCAGCCCAACAATACAAGA-3' 5'-GTGGACGGGTCGATGTCAC-3'

**Table 1. Oligonucleotide primers used in this study.**

#### Cell proliferation assays.

#### MTT assays.

Cell viability was determined by using 3-(4,5-Dimethylthiazol-2-yl)-2,5-Diphenyltetrazolium Bromide (MTT) reagent following the recommendation of the manufacturer.

#### Trypan blue cell count assays.

Cell numbers were evaluated by trypsin suspension of samples followed by microscopic evaluation using a hemocytometer.

#### Soft agar growth assays.

Cells (25000/well) were plated in 4 ml of 0.35% agarose with 5% charcoal-stripped FBS in phenol red-free media, in a 0.7% agarose base in six-well plates. Two days after plating, media containing control vehicle or treatments was added to the top layer, and the media was replaced every two days. After 14 days, 150 µl of MTT was added to each well and allowed to incubate at

37°C for 4h. Plates were then placed in 4°C overnight and colonies > 50 µm diameter from triplicate assays were counted.

*Wound-healing scratch assays.*

Cell monolayers were scraped and treated as indicated. Wound closure was monitored over 24 hours; cells were fixed and stained with Coomassie brilliant blue. Images represent 1 of 3 independent experiments (10 contrast microscopy).

*Transmigration assays.*

Cells untreated or treated as indicated were placed in the upper compartments of Boyden chamber (8-µm membranes; Corning Costar). Bottom well contained the specific chemoattractant as indicated. After 24 hours, migrated cells were fixed and stained with Coomassie brilliant blue. Migration was quantified by viewing 5 separate fields per membrane at 20 magnifications and expressed as the mean number of migrated cells.

*Invasion assays.*

Matrigel-based invasion assay was conducted in invasion chambers (8-µm membranes) coated with Matrigel (BD Biosciences; 0.4 µg/mL). Cells treated with or without leptin were seeded into top Transwell chambers, whereas regular full medium was used as chemoattractant in lower chambers. After 24 hours, invaded cells were evaluated as described for transmigration assays.

*Leptin measurement by radioimmunoassay.*

Leptin was measured by a competitive in-house immunoassay (Chematil) following manufacturer's protocol. Results are presented as nanograms per cell.

*Leptin-immunodepleted conditioned media.*

Protein G-agarose beads were incubated with anti-leptin or IgG antibodies. Antibody-beads complexes were incubated with CAF conditioned media and centrifuged. Leptin immunodepletion was verified by radioimmunoassay (RIA).

*Aromatase activity assays.*

The aromatase activity was measured by the tritiated water release assay using 0.5  $\mu\text{M}$  [ $1\beta$ - $^3\text{H}$ ]androst-4-ene-3,17-dione as substrate (40). The incubations were performed at 37 °C for 5 h under an air/ $\text{CO}_2$  (5%) atmosphere. The results obtained were expressed as picomole/h and normalized to mg of protein (pmol/h/mg of protein).

*Synthesis and characterization of peptide LDFI.*

Peptide LDFI (4 amino acids residues, leucine, aspartate, phenylalanine, isoleucine) and a scrambled version of this peptide (leucine, leucine, leucine, alanine) were synthesized by CEM-Liberty microwave-assisted automated-synthesizer and characterized by  $^1\text{H}$ -NMR spectroscopy.

*Tumor xenografts.*

*In vivo* studies were conducted in 45-day-old female nude mice (nu/nu Swiss). At day 0, the animals were fully anesthetized by i.m. injection of 1.0 mg/kg Zoletil (Virbac) and 0.12% Xylor (Xylazine) to allow the s.c. implantation of estradiol (E2) pellets (1.7 mg per pellet, 60-day release; Innovative Research of America, Sarasota, FL) into the intrascapular region of mice. The day after, exponentially growing MCF-7 WT and K303R ER $\alpha$  cells ( $5.0 \times 10^6$  per mouse) were inoculated s.c. in 0.1 mL of Matrigel. Leptin treatment was started 24 h later, when animals were injected i.p. with either solutions: recombinant human leptin (230  $\mu\text{g}/\text{kg}$ ) diluted in saline + 0.3% bovine serum albumin (BSA) or saline + 0.3% BSA only (control). The treatment was done for 5 days a week until the 8th week. All the procedures involving animals and their care have been conducted in conformity with the institutional guidelines at the Laboratory of Molecular Oncogenesis, Regina Elena Cancer Institute in Rome.

For peptide LDFI experiments, mice were inoculated with exponentially growing SKBR3 cells ( $5.0 \times 10^6$  per mouse) and injected i.p. with either solutions: LDFI peptide (10mg/kg/day) diluted in saline 0.3% bovine serum albumin (BSA) or saline. The treatment was done for 5 days a week until the 4th week. All animals were maintained and handled in accordance with the recommendation of the Guidelines for the Care and Use of Laboratory Animals and were approved by the Animal Care Committee of University of Calabria.

Tumor development was followed twice a week by caliper measurements along two orthogonal axes: length (L) and width (W). The volume (V) of tumors was estimated by the following

formula:  $V = L (W^2) / 2$ . At the time of killing, tumors were dissected out from the neighboring connective tissue, frozen and stored in nitrogen for further analysis.

*Statistical analysis*

Each datum point represents the mean  $\pm$  SD of three different experiments. Data were analyzed for statistical significance with 2-tailed Student t test using GraphPad Prism 4. Survival curves were computed by Kaplan–Meier method and compared using 2-sided log-rank tests.

## AIM 1

*Evaluation of the mechanisms  
underlying tumor-stroma interactions  
in ER $\alpha$ -positive breast cancer*

### **Tumor/Stroma Interactions Stimulate Cell Proliferation and Motility.**

Epithelial-stromal interactions support tumor cell proliferation and invasion. Thus, we first investigated the role of tumor microenvironment in influencing breast cancer phenotype in relation to the expression of wild-type (WT) or K303R ER $\alpha$  mutant receptor.

We used as experimental models for breast cancer ER $\alpha$ -positive MCF-7 cells stably transfected with YFP-WT or YFP-K303R ER $\alpha$  expression vectors. We chose this approach because WT receptor was present along with K303R ER $\alpha$  in invasive breast tumors (21). Stable clones were screened for ER $\alpha$  expression using immunoblot analysis (Fig. 1A). Two clones stably expressing YFP-WT (WT1-2) or YFP-K303R ER $\alpha$  (K303R1-2) are shown along with WT or mutant receptor stable pools (WT P and K303R P). As stromal cells, we employed cancer-associated fibroblasts (CAFs), isolated from biopsies of primary breast tumors. CAFs possessed the basic fibroblast characteristics of long and spindle-shaped morphology, and highly expressed the fibroblast activation protein-FAP (Fig. 1B). To create *in vitro* conditions that can mimic the complex *in vivo* microenvironment, we used co-culture experiments. Breast cancer cells were incubated with regular-full media (FM), CAFs-derived conditioned media (CM) or normal fibroblasts (NFs)-CM and growth was evaluated by soft agar assays (Fig. 1C, upper panel). As previously shown by Barone et al (28, 31) control basal growth of mutant-expressing cells was elevated compared to WT-expressing cells. CAFs-CM significantly increased colony numbers in both WT and K303R ER $\alpha$ -expressing cells; however, CAFs-CM enhanced K303R-expressing cell growth at a higher extent compared to WT-expressing cells. We then examined the ability of CAFs-CM to promote WT- and K303R-expressing cell movement in wound-healing scratch assays (Fig. 1C, lower panel). The mutant cells moved the farthest in either direction to close the gap compared to WT-expressing cells. CAFs-CM promoted net movement of WT-expressing cells compared to FM; but K303R-expressing cells exposed to CAFs-CM moved at higher rate to close the gap in the cell bed. As expected, CAFs possessed a higher ability to enhance both proliferation and motility of breast cancer cells than normal fibroblast (NFs) (Fig. 1C). CAFs-CM-induced cell growth and migratory potential was blocked by inhibition of the classic cytokine JAK2/STAT3 signaling cascade (AG490) and the ER $\alpha$  signaling inhibitor (ICI182,780), although to a higher extent in K303R clones (Fig. 1D). All functional effects described so far are the results of exposure to the total complement of CAFs-secreted proteins. However, it is desirable albeit experimentally difficult to define the contribution of a single

factor. Thus, we addressed which CAFs-secreted factor may promote breast cancer cell growth and motility.

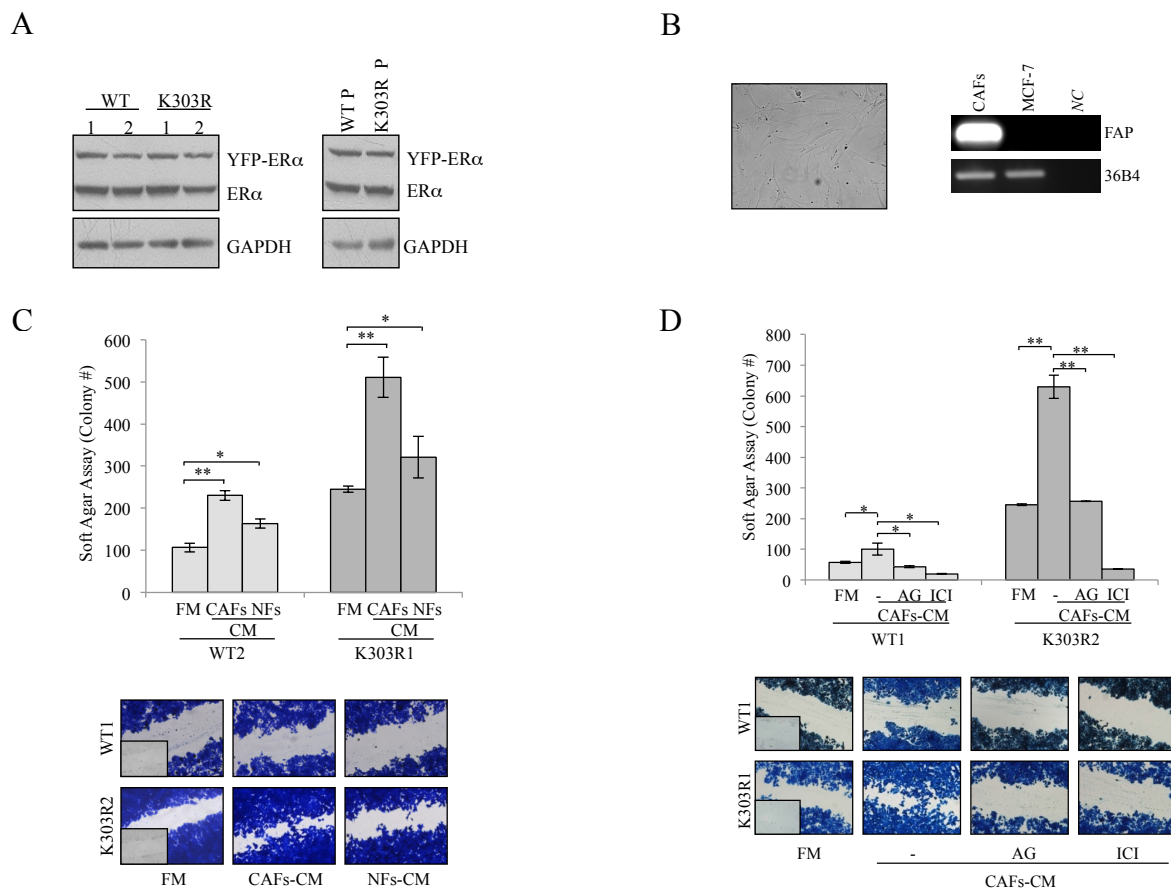


**Figure 1. CAF-induced breast cancer cell growth and motility.** **A**, immunoblotting for ER $\alpha$  expression in YFP-WT and YFP- K303R ER $\alpha$  stably expressing MCF- 7 cells. GAPDH (glyceraldehyde-3- phosphate dehydrogenase) was used as loading control. **B**, CAF morphology in monolayer growth using phase contrast microscopy. RT-PCR for FAP and 36B4 (internal standard). NC, negative control. **C**, soft agar (upper panel) and scratch assays (lower panel) in cells treated with regular full media (FM), CAF-derived conditioned media (CAF-CM), or normal fibroblasts- derived conditioned media (NF-CM). **D**, soft agar (upper panel) and scratch assays (lower panel) in cells treated with FM, CAF-CM with or without AG490 (AG, 10 mmol/L) or ICI182760 (ICI, 1 mmol/L). \*P < 0.05; \*\*P < 0.005. Small squares, time 0.

### Gene Transcription Patterns of WT and K303R ER $\alpha$ -overexpressing Cells.

Diffusible growth factors, interleukins, chemokines and adipokines implicated as mediators of stromal-epithelial interactions are involved in breast carcinoma initiation and progression. To determine changes in gene expression for the different receptors of CAFs-secreted factors, that may be responsible of the different sensitivity of WT and mutant clones to CAFs-CM exposure, we performed microarray analysis. Gene expression profile comparing RNA isolated from K303R-expressing with WT-expressing cells is shown in Table 1 and Table 2. K303R ER $\alpha$

expression induced several genes potentially involved into tumor/stroma interactions; however, the leptin receptor (ObR) gene was the most highly induced (2.4 fold, Table 1).

Gene name	Gene symbol	Parametric P	Fold change in K303R clones
<u>Leptin receptor</u>	<i>ObR/LepR</i>	<1e-07	<u>2.4</u>
Interleukin 28 receptor $\alpha$	<i>IL28RA</i>	<1e-07	1.9
Chemokine (C-X-C motif) receptor 4	<i>CXCR4</i>	<1e-07	1.9
Insulin receptor	<i>IR</i>	1.7e-06	1.68
Interleukin 17 receptor C	<i>IL17RC</i>	7e-07	1.6
Insulin-like growth factor 2 receptor	<i>IGF2R</i>	1e-07	1.57
Interleukin 15 receptor $\alpha$	<i>IL15RA</i>	3e-07	1.5
Macrophage stimulating receptor 1	<i>MSR1</i>	9.2e-06	1.44
Hepatocyte growth factor receptor	<i>MET</i>	1.69e-05	1.39
Interleukin 1 receptor, type I	<i>IL1R1</i>	0.0004	1.38
Chemokine (C-C motif) receptor 7	<i>CCR7</i>	0.0001	1.3
Chemokine (C-X3-C motif) receptor 1	<i>CX3CR1</i>	7.9e-05	1.32
Interleukin 2 receptor $\beta$	<i>IL2RB</i>	3.57e-05	1.25
Interleukin 9 receptor	<i>IL9R</i>	0.0002	1.23
Interleukin 10 receptor $\beta$	<i>IL10RB</i>	0.0003	1.21
Interleukin 6 receptor	<i>IL6R</i>	0.01	1.2
Interleukin 21 receptor	<i>IL21R</i>	0.0006	0.8
Interleukin 4 receptor	<i>IL4R</i>	0.0007	0.7
Epidermal growth factor receptor	<i>EGFR</i>	7.6e-06	0.7
Insulin-like growth factor 1 receptor	<i>IGF1R</i>	0.0006	0.7
Fibroblast growth factor receptor 3	<i>FGFR3</i>	0.0005	0.7

**Table 1. Gene expression profile comparing RNA isolated from K303R-expressing with WT-expressing cells.**

<i>Gene name</i>	<i>Gene Symbol</i>
Interleukin 2 receptor $\alpha$ , interleukin 2 receptor $\gamma$ , interleukin 7 receptor, interleukin 8 receptor $\beta$ , interleukin 10 receptor $\alpha$ , interleukin 12 receptor $\beta$ 2, interleukin 13 receptor $\alpha$ 2, interleukin 18 receptor 1, interleukin 22 receptor $\alpha$	IL2RA, IL2RG, IL7R, IL8RB, IL10RA, IL12RB2, IL13RA2, IL18R1, IL22RA
Colony stimulating factor 3 receptor, colony stimulating factor 2 receptor	CSF3R, CSF2R
Platelet derived growth factor receptor $\beta$	PDGFRB
Nerve growth factor receptor	NGFR
Tumor necrosis factor receptor, member 8, 9, 10 and 17	TNFR8, TNFR9, TNFR10, TNFR17
Chemokine (C-X-C motif) receptor 3, chemokine (C-X-C motif) receptor 6, chemokine (C-C motif) receptor 2, chemokine (C-C motif) receptor 3, chemokine (C-C motif) receptor 5, chemokine (C-C motif) receptor 6	CXCR3, CXCR6, CCR2, CCR3, CCR5, CCR6

**Table 2. Unchanged genes in the receptor family of CAFs-secreted factors among WT and K303R ER $\alpha$ -expressing MCF-7 breast cancer cells.**

We also observed increased expression of different leptin signaling downstream effectors such as JAK2, the transcription factors fos, STAT, as well as the suppressor of cytokine signaling 3 (Table 3).

<i>Gene name</i>	<i>Gene Symbol</i>	<i>Parametric P-value</i>	<i>Fold change in K303R clones</i>
Janus Kinase 2	<i>JAK2</i>	<1e-07	3,7
Signal Transducer and Activator of Transcription	<i>STAT</i>	<1e-07	15,1
v-fos FBJ Murine Osteosarcoma Viral Oncogene Homolog	<i>FOS</i>	4e-07	5,2
Suppressor of Cytokine Signaling 3	<i>SOCS3</i>	0.009	1,2

**Table 3. Selection of relevant up-regulated genes in the leptin signaling pathway in K303R ER $\alpha$ -expressing MCF-7 breast cancer cells.**

To validate the microarray study, YFP-WT and YFP-K303R ER $\alpha$ -expressing cells were evaluated for a panel of genes using real-time PCR (Fig. 2A). K303R-associated induction could be confirmed for all of them, and, again, the gene encoding the long and short leptin receptor isoforms (ObRl/ObRs) was the most highly up-regulated in mutant-expressing cells. However, we did not detect any differences in IGF1R mRNA expression levels between the two cells, although microarray analysis showed a significant decrease of IGF1R. ER $\alpha$  RNA levels were similar between K303R and WT ER $\alpha$ -expressing cells.

The increase in both ObRl and ObRs was then confirmed by evaluating protein levels using immunoblotting analysis (Fig. 2B) and immunofluorescence staining of WT and K303R ER $\alpha$ -expressing cells (red, Fig. 2C).

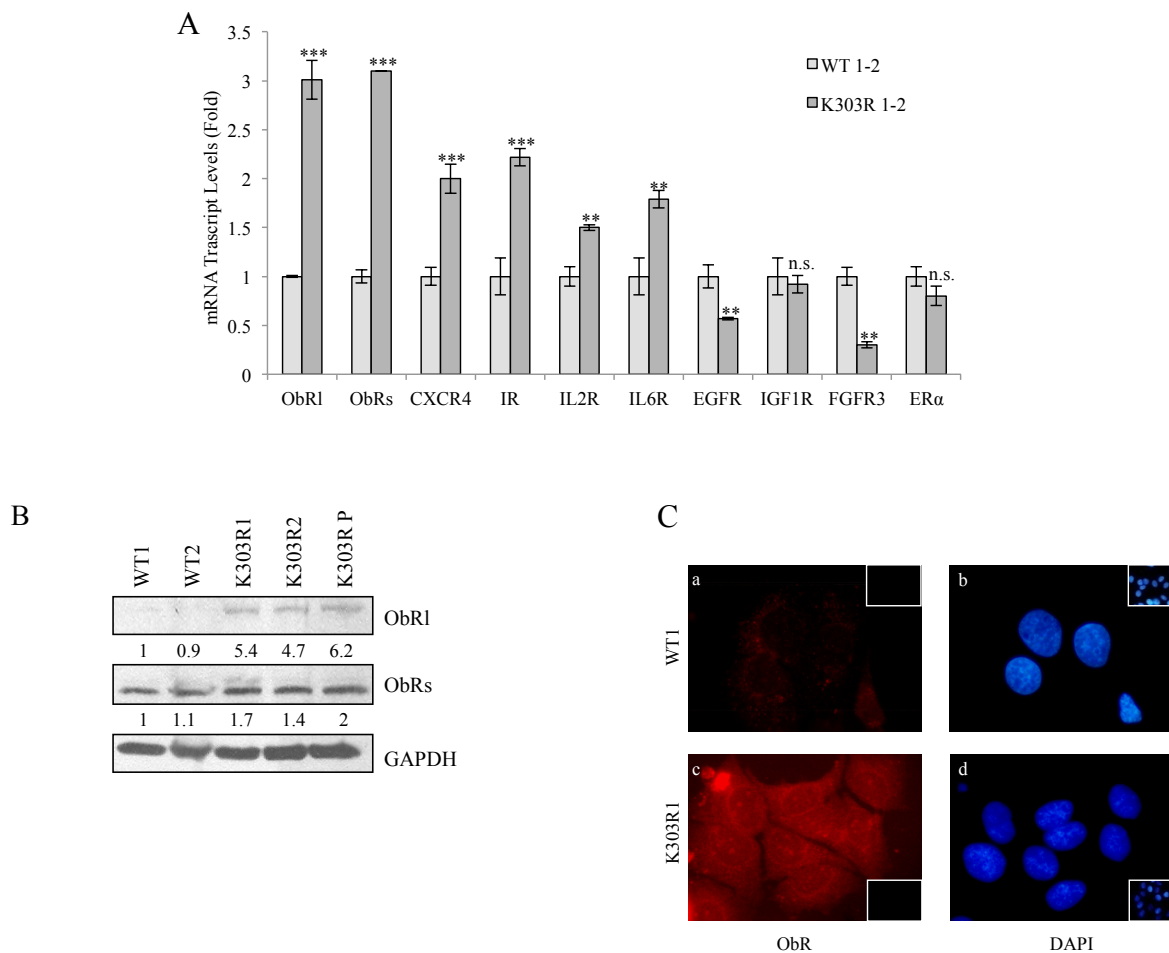


**Figure 2. Increased leptin receptor expression in mutant cells.** **A**, real-time RT-PCR for different receptors of CAF-secreted factors. n.s., nonsignificant; \*\* $P < 0.01$ ; \*\*\* $P < 0.005$ . **B**, immunoblotting showing leptin receptor long and short isoforms (ObR1/ObRs). GAPDH, loading control. Numbers represent the average fold change in ObR1 and GAPDH and ObRs and GAPDH levels. **C**, immunofluorescence of ObR (a and c) and DAPI (b and d). Small squares, negative controls.

### K303R ERα-overexpressing Cells Exhibit Increased Leptin Signaling Activation.

Given the gene expression profile identified in the microarray study, we defined the impact that a single factor-leptin may have on K303R ERα breast cancer cell progression. First, time-course response studies were performed to analyze phosphorylation of leptin downstream effectors using immunoblot analysis (Fig. 3A). WT-expressing cells exhibited low basal levels of phosphorylated JAK2, STAT3, Akt and MAPK that were increased in a time-dependent manner after leptin treatment. In contrast, K303R-expressing cells showed elevated constitutive phosphorylation of these signaling molecules in control-vehicle conditions that was slightly increased after leptin treatment. Thus, the mutant ERα expression was associated with increased leptin signaling activation.

Leptin directly activates ER $\alpha$  in the absence of its own ligand in MCF-7 breast cancer cells (41). As a consequence of the enhanced leptin signaling, we found increased ER $\alpha$ -transcriptional activity (Fig. 3B) and up-regulated mRNA levels of the classical ER $\alpha$ -target genes Cyclin D1, pS2 and Cathepsin D in both control and leptin-treated conditions in K303R ER $\alpha$ -expressing cells (Fig. 3C). In addition, the mutant exhibited elevated pS118 and pS167 YFP-ER $\alpha$  levels

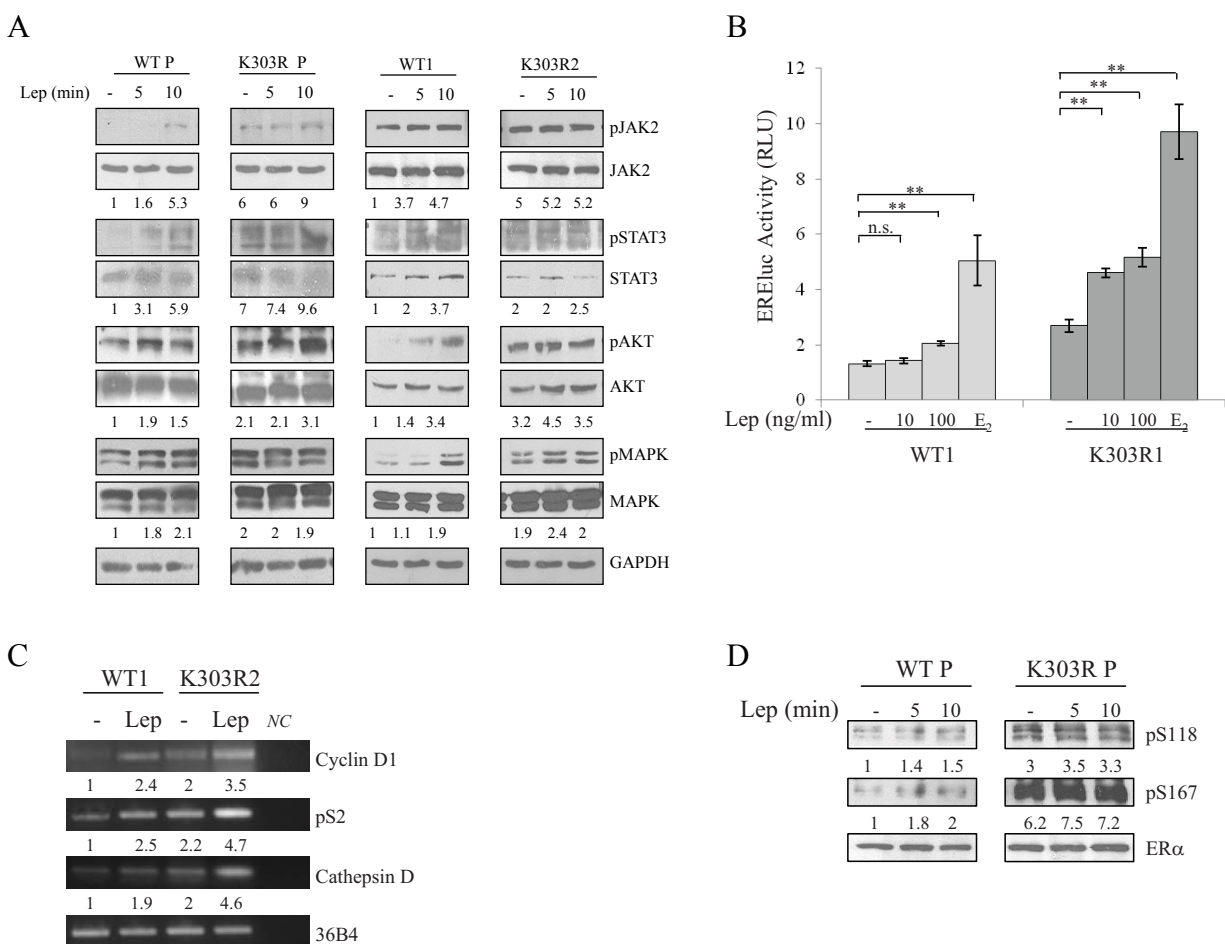


**Figure 3. Leptin signaling activation in mutant cells.** **A**, immunoblotting of phosphorylated (p) JAK2/STAT3/AKT/MAPK and total proteins from cells treated with vehicle (-) or leptin (Lep 100 ng/mL, 5 and 10 minutes). GAPDH, was used as loading control. Numbers represent the average fold change between phospho-, total, and GAPDH levels. **B**, ER $\alpha$ -transactivation assay in cells treated with vehicle (-), Lep at 10 and 100 ng/ml or 17- $\beta$  estradiol (E<sub>2</sub> 10nM, positive control). Data are reported as Relative Lights Units (RLU). n.s.=nonsignificant, \*\* $P$ <0.01. **C**, mRNA expression of Cyclin D1, pS2, Cathepsin D and 36B4 (internal standard) by RT-PCR in cells treated with vehicle (-) or Lep 100ng/ml for 24 hours. NC, negative control. Numbers represent the average fold change between Cyclin D1, pS2 or Cathepsin D and 36B4 levels. **D**, total extracts from cells treated with Lep 100ng/ml for 5 and 10 min were analyzed for phosphorylation of serines 118 and 167 (pS118 and pS167) and expression of ER $\alpha$  by immunoblot analysis. Numbers below the blots represent the average fold change between pER $\alpha$  levels and ER $\alpha$  total protein expression.

### **K303R ER $\alpha$ Mutation and Leptin Hypersensitivity.**

We next used these stably transfected clones as model systems to study leptin sensitivity, in relation to mutant receptor expression. First, we evaluated leptin effects on growth using anchorage-independent growth assays (Fig. 4A). Leptin treatments at 100 and 1000 ng/ml concentrations enhanced colony numbers in all four clones tested, even though to a higher extent in mutant-expressing cells. Moreover, leptin at 10 ng/ml increased anchorage-independent growth only in K303R cells. The increase in colony numbers induced by leptin was reversed by the JAK2/STAT3 inhibitor AG490 (Fig. 4B). We also used the antiestrogen ICI182,780 and found that this treatment suppressed anchorage-independent growth of both cell lines, indicating that ER expression remains important in growth regulation of these cells (Fig. 4B).

We next evaluated the ability of increasing doses of leptin to influence cell migration in wound-healing scratch assays (Fig. 4C). Again, the mutant cells moved farthest in either direction to close the gap compared to WT-expressing cells. Leptin treatments at 100 and 1000 ng/ml promoted cell motility in both WT and K303R-expressing cells, although to a higher extent in mutant cells. Interestingly, leptin at 10ng/ml stimulated migration only in K303R-expressing cells. Then, the capacity of cells to migrate across uncoated membrane in transmigration assays or to invade an artificial basement membrane-Matrigel in invasion assays was tested in the presence of leptin (Fig. 4D). While WT cells exhibited little motile and no invasive behaviour *in vitro*, our data clearly demonstrated that mutant receptor expression increased both motility and invasion of cells. High doses of leptin increased the number of migrated and invaded cells in both clones and again low doses of leptin stimulated motility and invasion only of cells expressing the K303R receptor. As expected, treatment with AG490 and ICI182,780 resulted in a clear reduction of both control-untreated and leptin-induced cell motility in wound-healing scratch assays, especially in K303R-expressing cells (Fig. 4E). In a previously work, Barone et al published that K303R ER $\alpha$  MCF-7 xenograft tumors grew faster than WT ER $\alpha$  tumors (31). In addition, MCF-7 xenograft tumors doubled control value after 13 weeks of leptin exposure (42). Thus, we determined if the mutant receptor-expressing breast cancer cells might exhibit an increased sensitivity to leptin stimulation also *in vivo*. We found that in mice treated with leptin, all xenografts derived from cells with K303R ER $\alpha$  expression doubled in size within 6 weeks of treatment, while none of xenografts from WT ER $\alpha$ -expressing cells doubled in size during this experiment (Fig. 4F). Thus, expression of the mutant generated a leptin hypersensitive phenotype *in vitro* and *in vivo*.

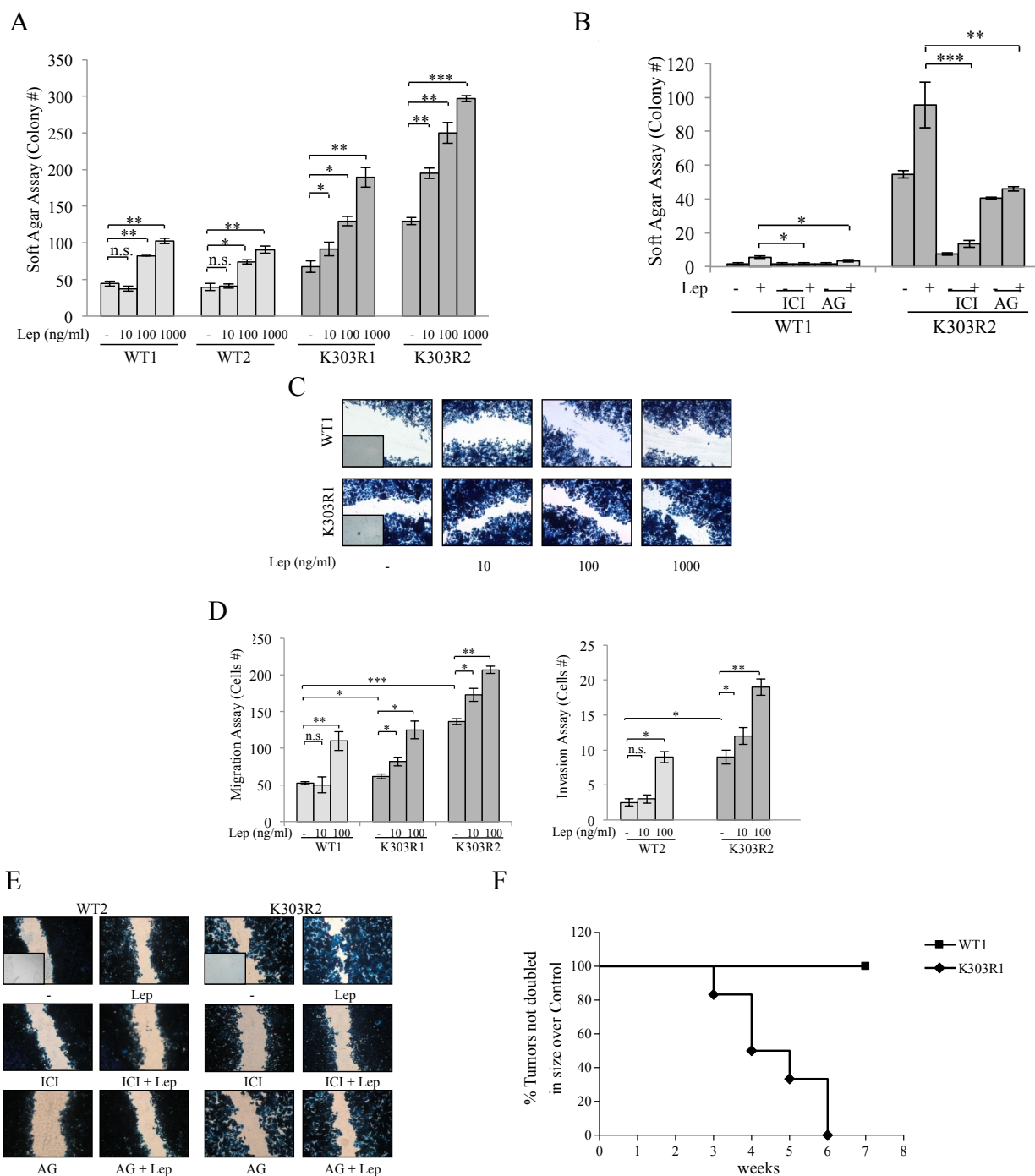


**Figure 4. The K303R ER $\alpha$  mutation generates a leptin hypersensitive phenotype.** **A**, soft agar assay in cells treated with vehicle (-) or leptin (Lep 10, 100 and 1000 ng/mL). **B**, soft agar assay in cells treated with vehicle (-) or leptin (Lep; 100 ng/mL), with or without ICI182760 (ICI, 1  $\mu$ mol/L) or AG490 (AG, 10  $\mu$ mol/L). Scratch (**C**) and transmigration and invasion (**D**) assays in cells treated as indicated. n.s., nonsignificant; \* $P < 0.05$ ; \*\* $P < 0.005$ ; \*\*\* $P < 0.001$ . **E**, scratch assay in cells treated with vehicle (-) or 100 ng/mL leptin, with or without ICI182760 or AG490. Small squares, time 0. **F**, WT- and K303R ER $\alpha$ - expressing cells were injected into mice ( $n=6$  per group) supplemented with E $_2$  and 230  $\mu$ g/kg leptin OR vehicle (control). Survival curves [shown as percentage (%) of mice in which tumors had not doubled in size] are graphed as the time in weeks from treatment to a 2-fold increase in total tumor volume over baseline (time to tumor doubling).

### Leptin is Responsible for CAFs-induced Cell Growth and Motility.

We next assessed the role of leptin in the context of heterotypic signalings working in tumor/stroma interactions. First, RIA measurement in CAFs-CM showed that leptin secretion varied from  $10 \pm 4.5 \text{ ng}/200.000 \text{ cells}$ . RT-PCR evidenced Ob mRNA expression in CAFs (Fig. 5A); CAFs also expressed ObR long isoform, but they did not express ObR short isoform, ER $\alpha$ , or ER $\beta$  (Fig. 5B). Leptin was then immunodepleted from CAFs-CM by leptin specific antibodies and resulting media were tested for the ability to induce anchorage-independent growth and migration of breast cancer cells. Leptin-depletion (CM+LepAb) significantly decreased growth and migration-promoting activities of CAFs-CM, particularly in K303R-expressing cells (Fig. 6A). CM treated with a non specific mouse IgG had not effects, suggesting that the neutralizing effects of leptin antibodies were specific. Our results identify leptin as a main molecular player that mediates CAFs effects on tumor cell growth and migration.

Leptin activates via JAK2 the MAPK and PI3K/Akt pathways (43). Thus, we investigated the specific signaling involved in the CAFs/breast cancer cells interaction, and found that the PI3K/Akt inhibitor LY294002 was more effective in inhibiting CAFs-induced proliferation and migration than the MEK1 inhibitor PD98059 (Fig. 6B).

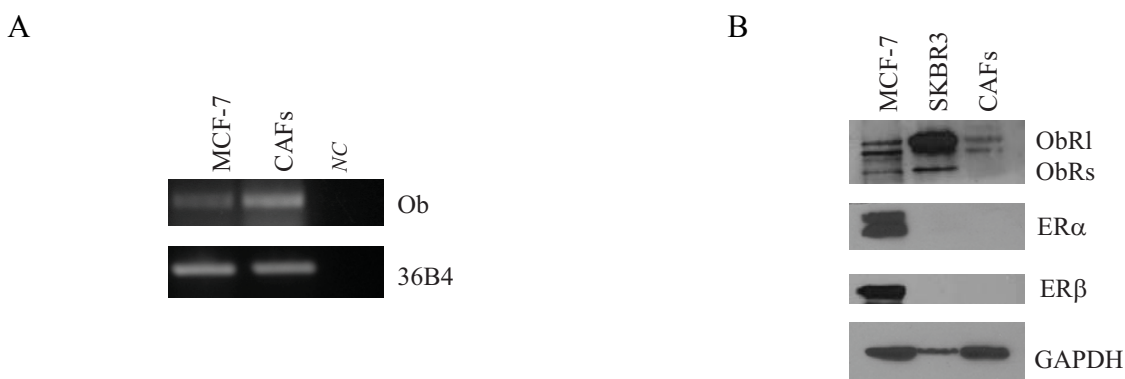


**Figure 5. Expression of Leptin and its receptor in Cancer Associated Fibroblasts (CAFs).** **A**, RT-PCR for leptin (Ob) and 36B4 (internal standard) mRNA expression. *NC*, negative control. **B**, Immunoblotting analysis of whole-cell lysates from MCF-7, SKBR3 and CAFs cells for ObR long and short isoforms, ER $\alpha$  and ER $\beta$  expression. GAPDH was used as a control for equal loading and transfer.

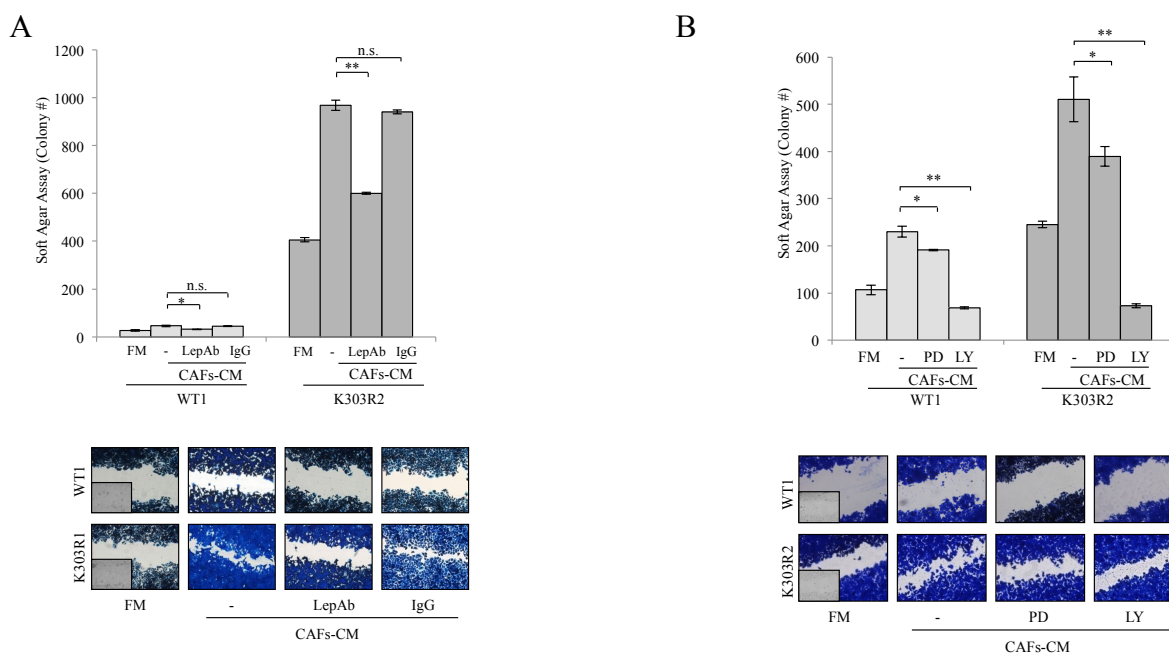


**Figure 6. Leptin immunodepletion reduces CAF-induced cell growth and migration.** **A**, soft agar (upper panel) and scratch assays (lower panel) in cells treated with full media (FM), CAF-derived conditioned media (CAF-CM), or leptin-depleted conditioned media (CM + LepAb). Conditioned media treated with a nonspecific IgG as a control (CM IgG). **B**, soft agar (upper panel) and scratch assays (lower panel) in cells treated with FM, CAF-CM with or without PD98059 (PD, 10  $\mu$ mol/L) or LY294002 (LY, 10  $\mu$ mol/L). n.s., nonsignificant; \* $P < 0.05$ ; \*\* $P < 0.005$ . Small squares, time 0.

### Tumor/Stroma Interactions in SKBR3 Breast Cancer Cells

To extend the results obtained, we generated pools of YFP-WT and YFP-K303R ER $\alpha$  stable transfectants in ER $\alpha$ -negative SKBR3 breast cancer cells (Fig. 7A). As previously shown for MCF-7 cells, we found a significant increase in both long and short leptin receptor isoforms mRNA in mutant-expressing cells (Fig. 7B). Again, treatment with leptin at 100 and 1000ng/ml significantly increased colony numbers of WT clones, and to a higher extent of K303R-expressing cells; however 10 ng/ml of leptin enhanced anchorage-independent growth only in K303R-expressing clones (Fig. 7C). Similarly, low leptin promoted migration only in mutant cells (Fig. 7D). Finally, we tested CAFs-CM for its effects on cell growth and migration. We found a great induction of anchorage-independent growth and motility after treatment with CM, especially in K303R-expressing SKBR3 pools (Fig. 7E and 7F). Leptin-immunodepleted CM strongly reduced CM-proliferative and migratory-promoting activities on K303R cells, confirming that leptin hypersensitive phenotype was associated with K303R ER $\alpha$  expression in different cellular backgrounds.

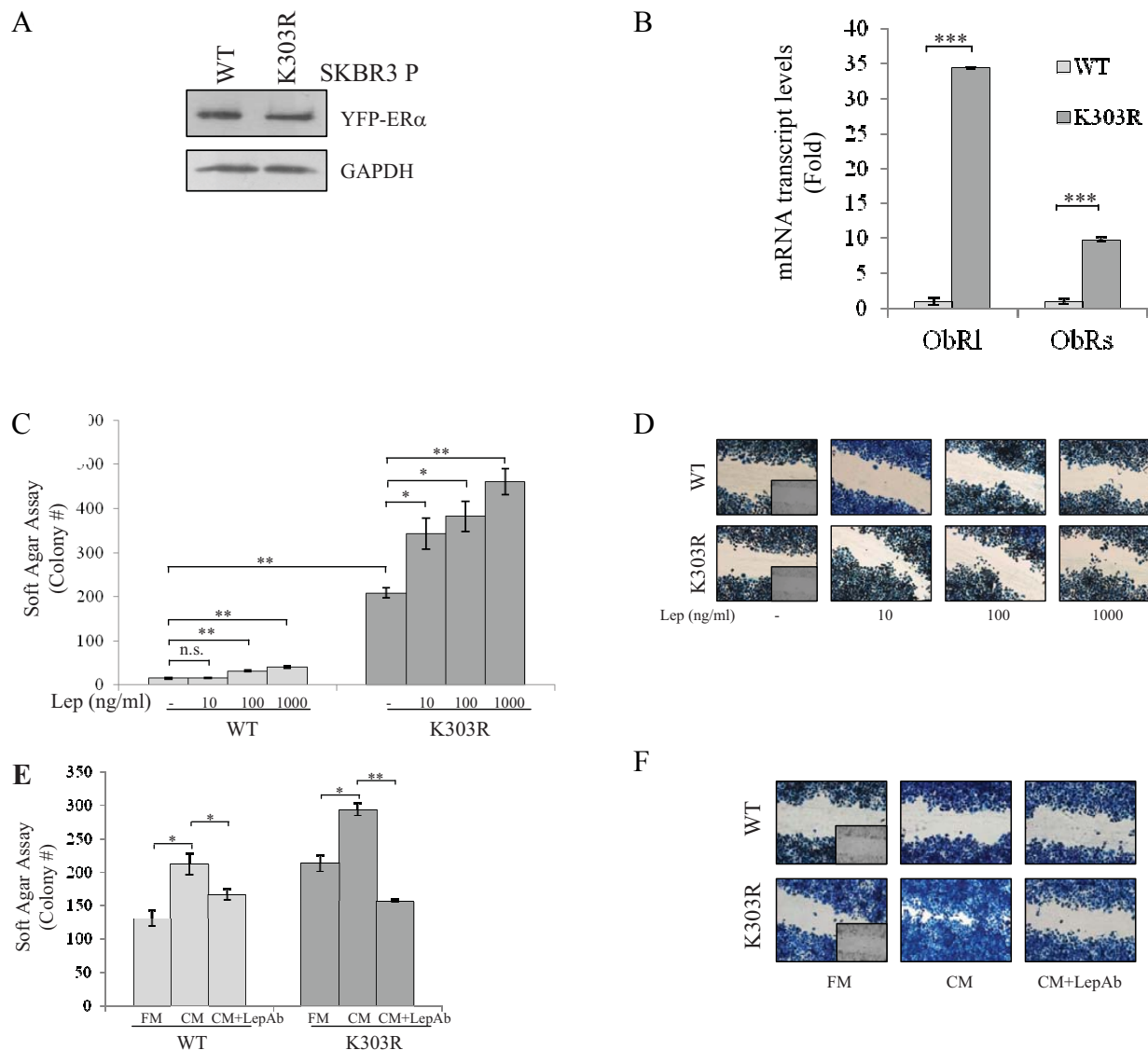


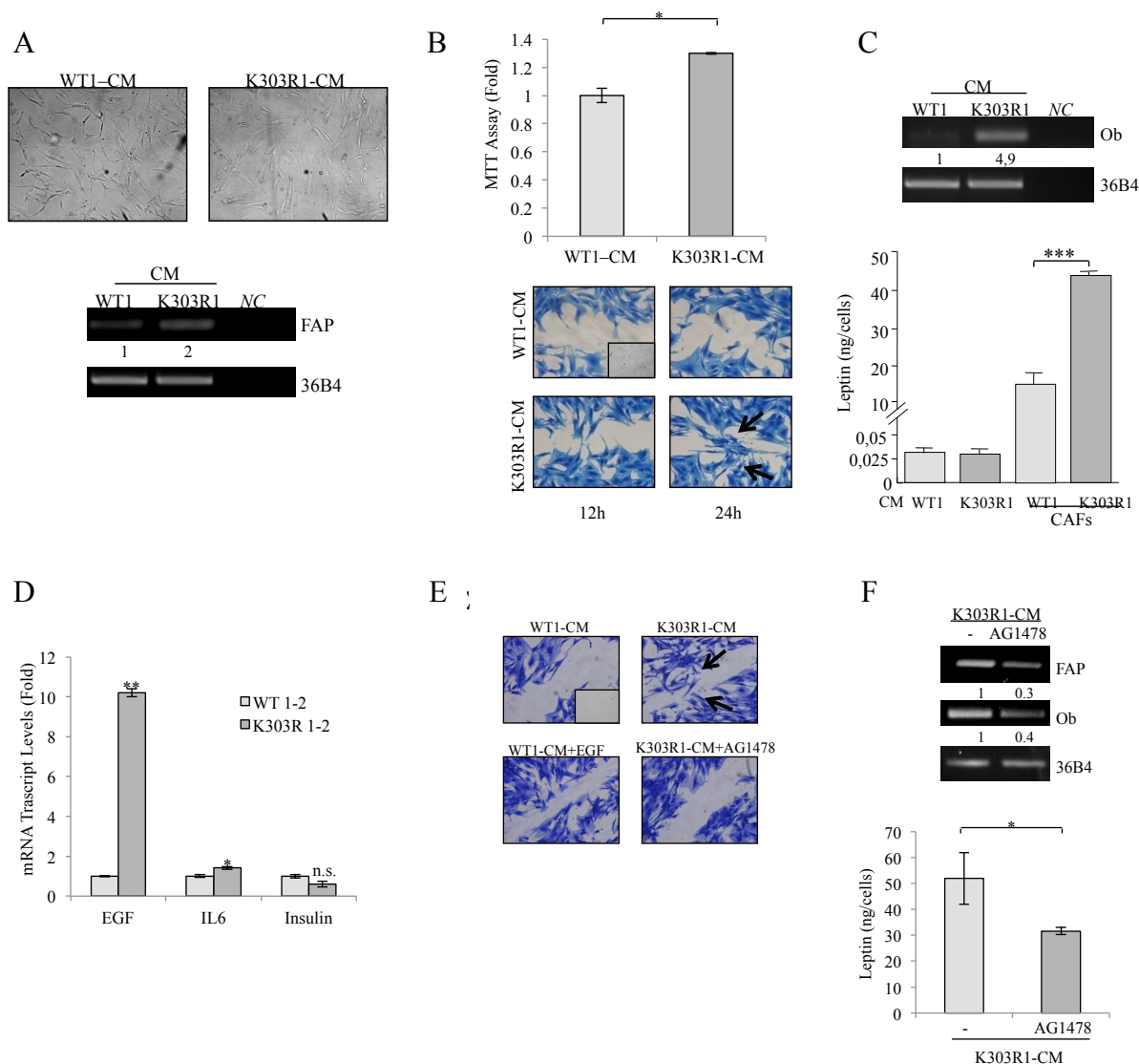
**Figure 7. Leptin increases growth and migration in K303R ER $\alpha$  SKBR3 cells.** **A**, immunoblotting analysis for ER $\alpha$  and GAPDH in YFP-WT and YFP-K303R ER $\alpha$  stable transfected SKBR3 pools. **B**, real-time RT-PCR for ObR1 and ObRs. \*\*\*P<0.0001. Soft agar (**C**) and scratch assays (**D**) in cells treated as indicated. Soft agar (**E**) and scratch assays (**F**) in cells treated with full media (FM), CAFs-derived conditioned media (CM) or leptin-depleted CM (CM+LepAb). n.s.=nonsignificant, \*P<0.05, \*\*P<0.005. Small squares represent time 0 of treatment.

### Effects of Breast Cancer Cell-secreted Factors on CAFs Phenotype.

CAFs and tumor cells cross-talk via different soluble factors, whose effects on both subpopulations determine the final outcome of the tumorigenic process. Thus, as a final step of this study we defined the effects of CM from WT and K303R ER $\alpha$ -expressing breast cancer cells on CAFs phenotype. Treatment with K303R-CM elicited a dramatic alteration in the shape of CAFs *in vitro*, accompanied by an increased FAP mRNA expression (Fig. 8A). K303R-CM also

stimulated CAFs viability and motility compared to WT-CM effects (Fig. 8B), suggesting how soluble K303R ER $\alpha$  cell-secreted factors may generate a more activated CAFs phenotype. Since leptin synthesis is influenced by different humoral factors (44-46), we evaluated the effects of breast cancer-derived CM in modulating leptin secretion from CAFs. Incubation of CAFs with K303R-CM increased leptin mRNA expression and leptin release compared with WT-CM, while no differences were detected in leptin levels among WT and K303R-CM (Fig. 8C). Finally, to investigate the paracrine factor by which breast cancer cells may affect CAFs phenotype, we used microarray analyses to measure the expression of different genes known to be associated with CAFs and/or leptin secretion (11, 44-47). Our results showed that the genes encoding for EGF (2,8 fold), IL6 (1,2 fold) and Insulin (1,2 fold) were induced in mutant cells, and realtime PCR confirmed that the EGF gene was the most highly upregulated (Fig. 8D). Thus, we evaluated the role of EGF. First, addition of EGF in WT-CM mimicked the induction of K303R-CM on CAF motility, and the EGFR signaling inhibitor (AG1478) reduced K303R-CM effects (Fig. 8E). Second, treatment with AG1478 reversed K303R-CM stimulated FAP mRNA expression (Fig. 8F, upper panel). Third, Ob mRNA expression and leptin secretion from CAFs co-cultured with K303R-CM was significantly decreased in the presence of AG1478 (Fig. 8F, lower panel).

Our data show that K303R ER $\alpha$ -expressing breast cancer cells through their soluble secreted factors may take advantage of the plastic nature of reactive surrounding cell populations, as CAFs, to generate a tumor enhancing microenvironment.



**8. CAFs activated phenotype after K303R ER $\alpha$  cell-derived conditioned media exposure.** **A**, phase contrast microscopy for CAF morphology and RT-PCR for FAP and 36B4 (internal standard) after treatment with conditioned media from WT- or K303R ER $\alpha$ -expressing cells. *NC*, negative control. **B**, MTT growth (upper panel) and scratch assays (lower panel) in CAFs treated with WT-derived conditioned media and K303R-derived conditioned media. **C**, RT-PCR for leptin/Ob and 36B4 and leptin release by RIA. **D**, real-time RT-PCR for EGF, IL-6, and insulin. **E**, scratch assays in CAFs treated with WT-derived conditioned media with or without 100 ng/mL EGF or K303R-derived conditioned media with or without AG1478 10  $\mu$ mol/L. **F**, RT-PCR (upper panel) for FAP, leptin/Ob, and 36B4, and leptin release (lower panel) from CAFs by RIA. Numbers represent the average fold change of FAP/36B4 and Ob/ 36B4 levels. n.s. nonsignificant; \* $P < 0.05$ ; \*\* $P < 0.005$ ; \*\*\* $P < 0.0001$ . Small squares, time 0.

## AIM 2

*Evaluation of the potential role of leptin  
in driving Aromatase Inhibitor resistance  
in breast cancer*

### **Generation of Anastrozole-Resistant Breast Cancer Cells.**

In the first part of our work we demonstrated the functional importance of tumor–host cross-talk in impacting malignant behavior of estrogen-receptor positive breast cancer cells. Next, we investigated the potential role of tumor microenvironment in supporting the phenotype of breast cancer cells resistant to aromatase inhibitors (AIs).

To this aim, as an adequate aromatase/ER positive model system to study aromatase inhibitor response, parental human MCF-7 breast cancer cells stably transfected with an aromatase expression vector (MCF-7 aro) (31) were used to establish a therapy refractory cancer cell line by culturing them continuously in the presence of the non-steroidal AI Anastrozole (AnaR). As shown by immunoblotting analysis (Fig. 1A), these cells did not show any major changes in ER $\alpha$  or aromatase protein expression. To test for AI resistance, we examined the effects of Anastrozole in different *in vitro* assays. Anchorage-independent MTT assay revealed that growth of MCF-7 aro cells was significantly enhanced by androstenedione (AD), which aromatase converts to estrogen, after four days of treatment and as expected Ana completely blocked this stimulation (Fig. 1B). In contrast, in AnaR cells AD enhanced growth at two days of treatment and Ana was unable to inhibit AD-induced effects. To extend the MTT data, we performed anchorage-independent soft agar growth assays (Fig. 1C). Again, inhibition of aromatase activity by Ana completely abrogated AD-stimulated growth only in parental cells. Concomitantly, in ERE-luciferase reporter assays treatment with Ana did not affect AD-induced ER $\alpha$  transcriptional activity in the resistant cell line we generated (Fig. 1D). To evaluate the real ability of anastrozole to inhibit the aromatase activity, we performed water released assays and we found a strong reduction of aromatase activity by Ana in both cells (Fig. 1E), suggesting that AIR cannot be explained by an intrinsic insensitivity of the aromatase enzyme itself to Ana.

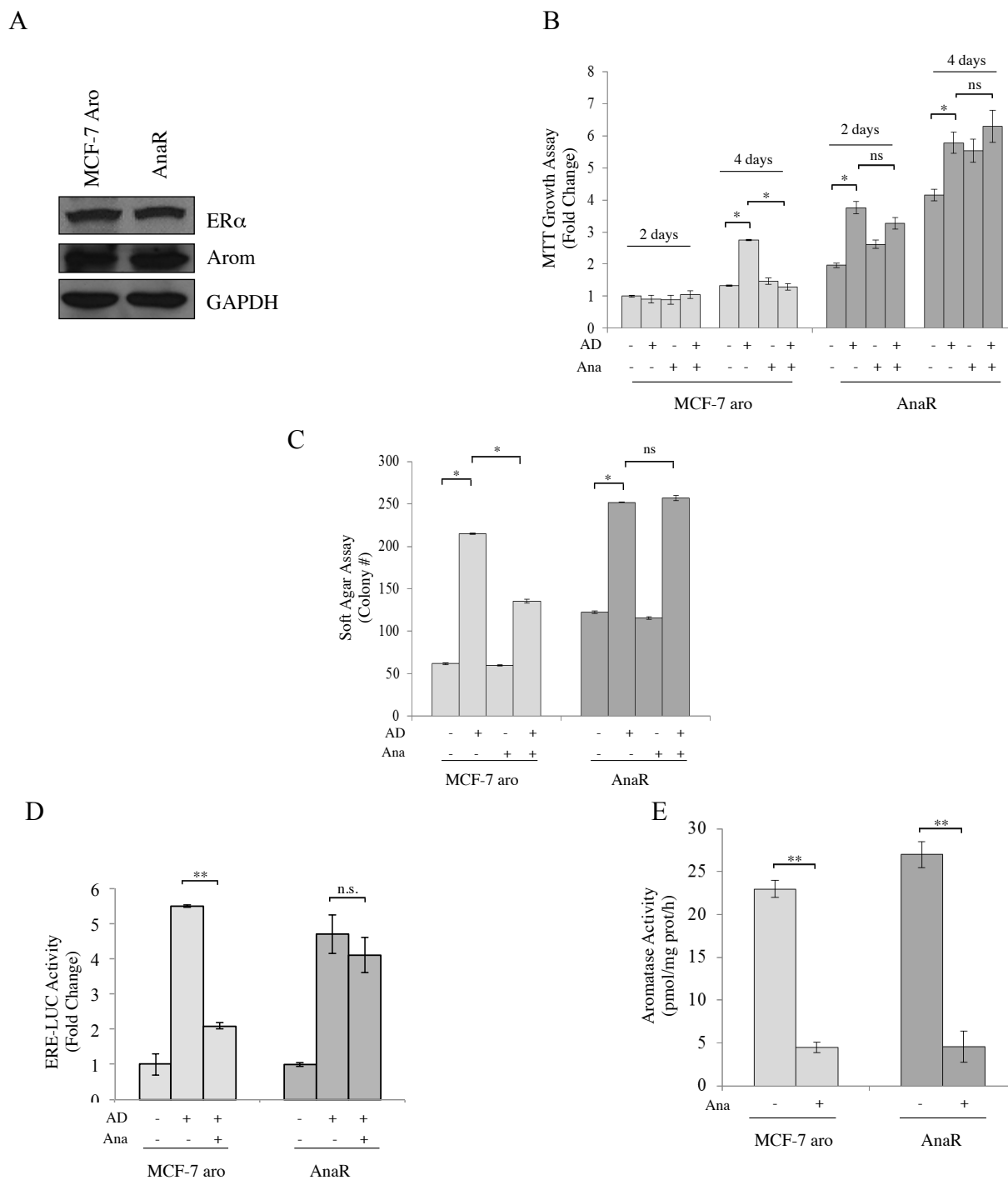


**Figure 1. Characterization of AnaR breast cancer cells.** **A**, immunoblotting for expression of endogenous ER $\alpha$  along with aromatase. GAPDH was used as loading control. **B**, Anchorage-dependent MTT growth assays in MCF-7 aro and AnaR cells treated with the aromatase substrate androstenedione (AD, 10 nMol/L), in the presence or not of anastrozole (Ana, 1  $\mu$ M) for 2 and 4 days. **C**, soft agar growth assays in MCF-7 aro and AnaR breast cancer cells, stimulated for 14 days with AD and/or Ana. **D**, cells were transiently transfected with ERE-LUC reporter gene and after 24 hours were treated with AD alone or in combination with Ana. **E**, aromatase activity in cell treated as indicated. n.s., non significant, \* $P < 0.01$ , \*\* $P < 0.001$ .

### AnaR cells Exhibits Increased Activation of Leptin Signalings.

Once confirmed the AIR phenotype, we investigated the potential role of leptin in the development of anastrozole resistance. First, we evaluated by real-time PCR specific transcript levels of leptin and the short and long receptor isoforms in MCF-7 aro at different time points (1-4 months) after the first treatment with Ana (Fig. 2A). We observed during the months of treatment a phenotypic shift characterized at the 4<sup>th</sup> month, when the *in vitro* assays performed have demonstrated the acquisition of Ana resistance, by an higher mRNA expression of leptin and its receptors in AnaR cells compared to MCF-7 aro cells. This may imply that an enhanced autocrine feedback loop exist in AnaR cells. As a consequence, resistant cells exhibited increased constitutive phosphorylation levels of the leptin downstream effectors JAK2, STAT3, AKT, MAPK (Fig. 2B) along with an increased anchorage-independent growth and motility (Fig. 2C and 2D).

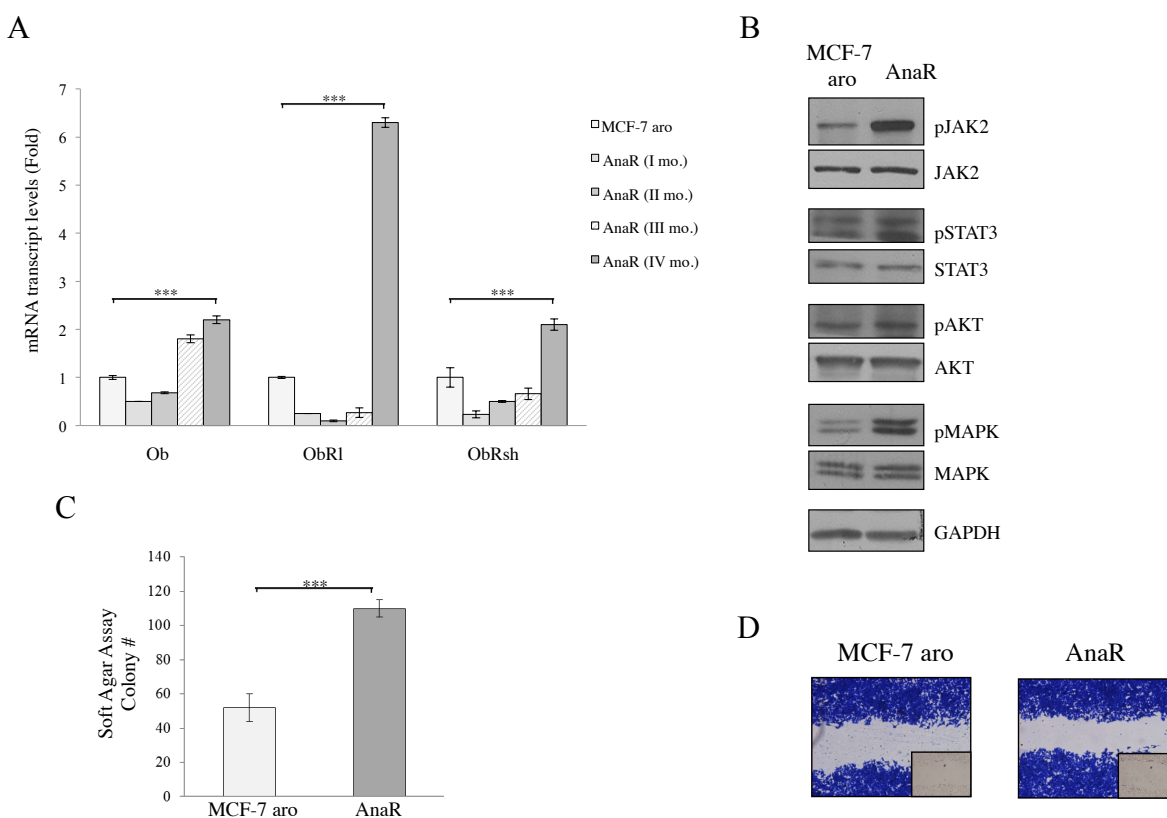


**Figure 2. Increased leptin signaling activation in AnaR cells.** **A**, quantitative real-time RT-PCR for mRNA expression of Ob (Leptin) and its receptors (long-l and short-sh isoforms of ObR) in MCF-7 aro and AnaR cells along the different months (mo.) of treatment with anastrozole. **B**, immunoblotting for phosphorylation levels (p) of JAK2, STAT3, Akt and MAPK in MCF-7 aro and AnaR breast cancer cells. GAPDH was used as loading control. **C**, soft agar growth assays in MCF-7 aro and AnaR breast cancer cells. \*\*\*P<0.0001. **D**, Cells were subjected to “in vitro” scratch assay with images captured at 0 and 24 h using phase-contrast microscopy. Small squares, time 0.

The described effects were reduced in the presence of the inhibitor of the classic cytokine JAK2/STAT3 signaling cascade, AG490 (Fig. 3). But, what is worth to underline is that low doses of AG4900 were able to specifically decrease the proliferation (at about 80%) and migration of AnaR cells, indicating a selective dependency on the leptin signaling for these cells.

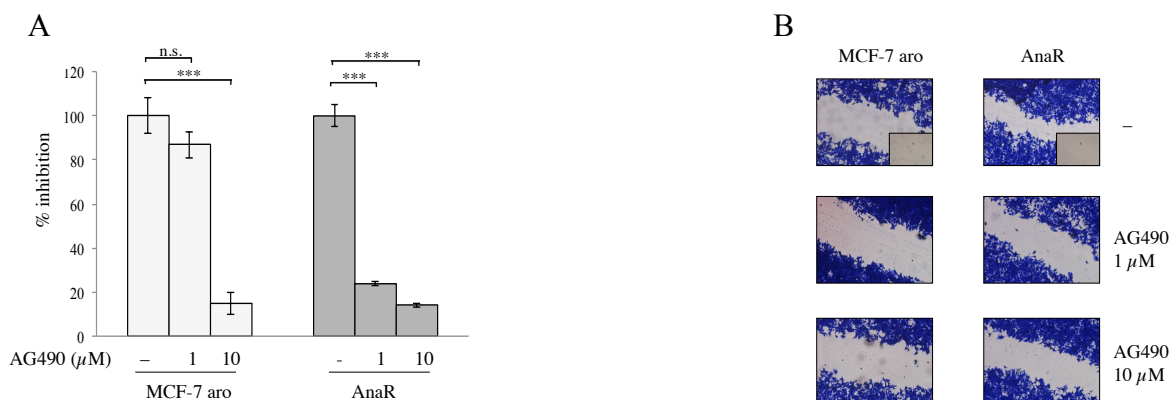


**Figure 3. Inhibition of leptin signaling reduces growth and motility in AnaR cells.** **A**, soft agar growth assays in MCF-7 aro and AnaR breast cancer cells stimulated for 14 days with increasing doses of AG490. n.s., nonsignificant, \*\*\* $P < 0.0001$ . **B**, Cells were subjected to “in vitro” scratch assay with images captured at 0 and 24 h after incubation with AG490 using phase-contrast microscopy. Small squares, time 0.

### CAFs Enhance Growth and Motility of AnaR Cells.

We have previously shown that CAFs, via leptin production, promote the growth of ER-positive breast cancer cells. Also, it has been demonstrated that CAFs could lead to tamoxifen resistance, with activation of AKT and MAPK, and phosphorylation of ER $\alpha$  (39). To further assess the role of leptin on phenotypic behavior of our model system, we co-cultured AnaR cells with CAFs. Either sensitive and resistant cells were incubated with CAFs-derived conditioned media (CAF-CM), with or without anastrozole or AG490 and growth and motility were evaluated (Fig. 4). CAF-CM significantly increased colony numbers in both cells; but it induced a greater increase in the anchorage-independent growth of resistant breast cancer cells and also AnaR cells exposed to CAF-CM moved at higher rate to close the gap in the cell bed in a wound healing scratch assay. Ana treatment did not counteract CM-induced effects in resistant cells, but AG490 was able to reduce growth and migration-promoting activities of CAFs-CM. Thus, stromal fibroblasts may support resistance in breast cancer cells likely through increased leptin signalings.

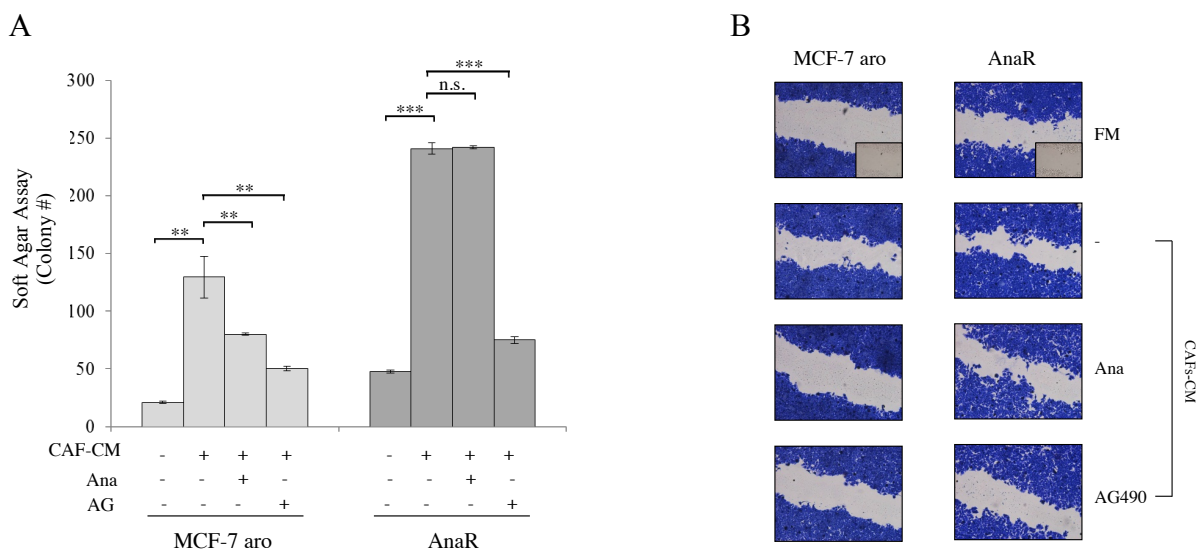


**Figure 4. Increased growth and motility in AnaR cells induced by CAFs.** **A**, soft agar growth assays in MCF-7 aro and AnaR breast cancer cells treated for 14 days with conditioned medium derived from CAFs (CAF-CM), with or without anastrozole (Ana, 1  $\mu\text{mol/L}$ ), or AG490 (10  $\mu\text{mol/L}$ ). n.s., nonsignificant,  $**P < 0.001$ ,  $***P < 0.0001$ . **B**, Cells were subjected to “in vitro” scratch assay with images captured at 0 and 24 h after incubation with regular full media (FM), CAFs-CM,  $\pm$  Ana or AG, using phase-contrast microscopy. Small squares, time 0.

### Enhanced Recruitment and Protumor Activation of Macrophages from AnaR Cells through Leptin Signalings.

Inflammation is now considered a hallmark of cancer and can play a role in virtually all aspects of tumor biology, including initiation, promotion, angiogenesis, and metastasis (48). It has been reported that leptin is a mediator of the inflammatory response. Indeed, this adipokine activates proinflammatory cells, promotes T-helper 1 response and mediates the production of the other proinflammatory cytokines, such as tumor necrosis factor  $\alpha$ , interleukin -2 and -6 (49). Thus, we investigated whether an enhanced production of leptin from AnaR cells may impact the phenotype of immune cells such as macrophages to further support malignant progression. For this aim, first the murine macrophage cell line RAW 264.7 was exposed to CM from Ana-sensitive and resistant cells and the capacity of cells to migrate across uncoated membrane in transmigration assays was tested. Our data clearly showed that CM derived from AnaR cells enhanced macrophages motility at higher extent than CM derived from MCF-7 aro cells (Fig. 5A). This effect is dependent on leptin signaling activation since AnaR cell-secreted factors did not induce any significant migration when RAW cells were exposed when AnaR-CM depleted of leptin by using specific antibody was used as chemoattractant (Fig. 5B). Moreover, exposure of macrophages to AnaR-CM leads to a regulation of a number of genes associated with macrophage polarization (Fig. 5C). Real Time RT-PCR analysis revealed that expression levels

of ArgI and IL-10 were induced, while expression levels of iNos and IL-12 were decreased, as typically observed in TAMs. In addition, we found no modification in the TGF $\beta$ /SMAD3 pathway, whose role in macrophage function is still controversial. Therefore, the mechanisms underlying aggressive behavior of anastrozole resistant breast tumors appears to be not only intrinsic to cancer cells but it also may rely on their ability to control the phenotype of macrophage, promoting their rapid recruitment to epithelial structures and their subsequent activation.

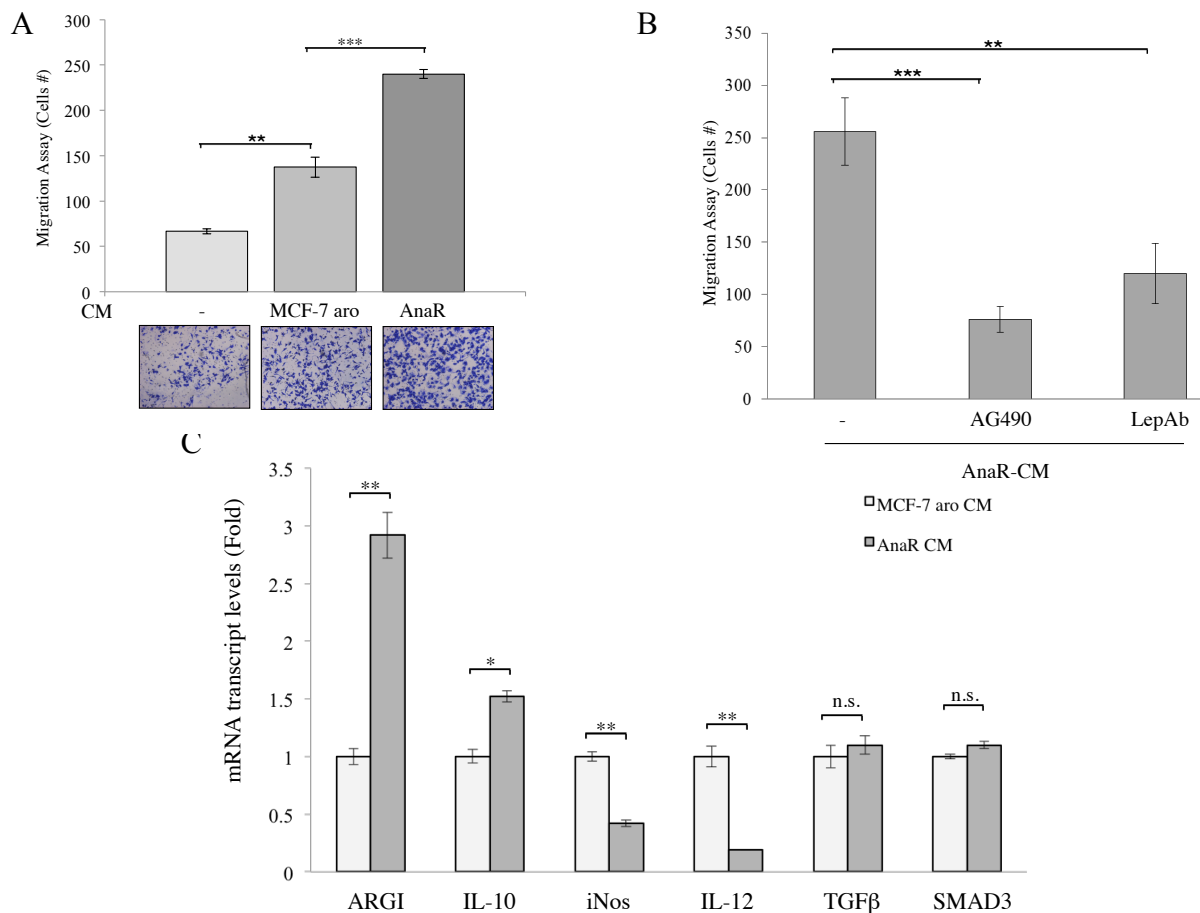


**Figure 5. AnaR cells recruit and activate macrophages through leptin.** **A**, transmigration assay in RAW cells using as chemoattractant charcoal-stripped serum media (-) and conditioned media (CM) derived from MCF-7 aro or AnaR cells. Images are representative of one random microscopic field of view within each membrane. **B**, transmigration assay in RAW cells treated or not with AG490 (10  $\mu$ mol/L) using as chemoattractant AnaR-CM or AnaR-CM in which leptin was immunodepleted by incubation with a mouse monoclonal specific antibody against leptin (LepAb) **C**, quantitative real-time RT-PCR for mRNA expression of ARG1 (Arginase I), IL-10 (Interleukin-10), TGF- $\beta$  (Transforming Growth Factor  $\beta$ ), SMAD3, markers of pro-tumor macrophages and IL-12 (Interleukin-12), iNOS (inducible Nitric Oxide Synthase), markers of tumor-inhibitory macrophages, in RAW cells after incubation with CM derived from MCF-7 aro or AnaR cells. \*P<0.01; \*\*P<0.001; \*\*\*P<0.0001 n.s., nonsignificant.

### Macrophages Promote Growth and Migration of AnaR Cells.

As a final step of this study, we examined the effects of soluble factors of activated macrophages on growth and migration of breast cancer cells. As revealed by soft agar (Fig. 6A) we found an enhanced number of colonies in AnaR cells, after incubation with RAW-CM. Accordingly, the capacity of AnaR cells to migrate across the uncoated membrane in transmigration assay was increased in the presence of RAW-CM (Fig. 6B). These data, highlight the existence of an enhanced bidirectional crosstalk between anastrozole resistant breast cancer cells and macrophages.

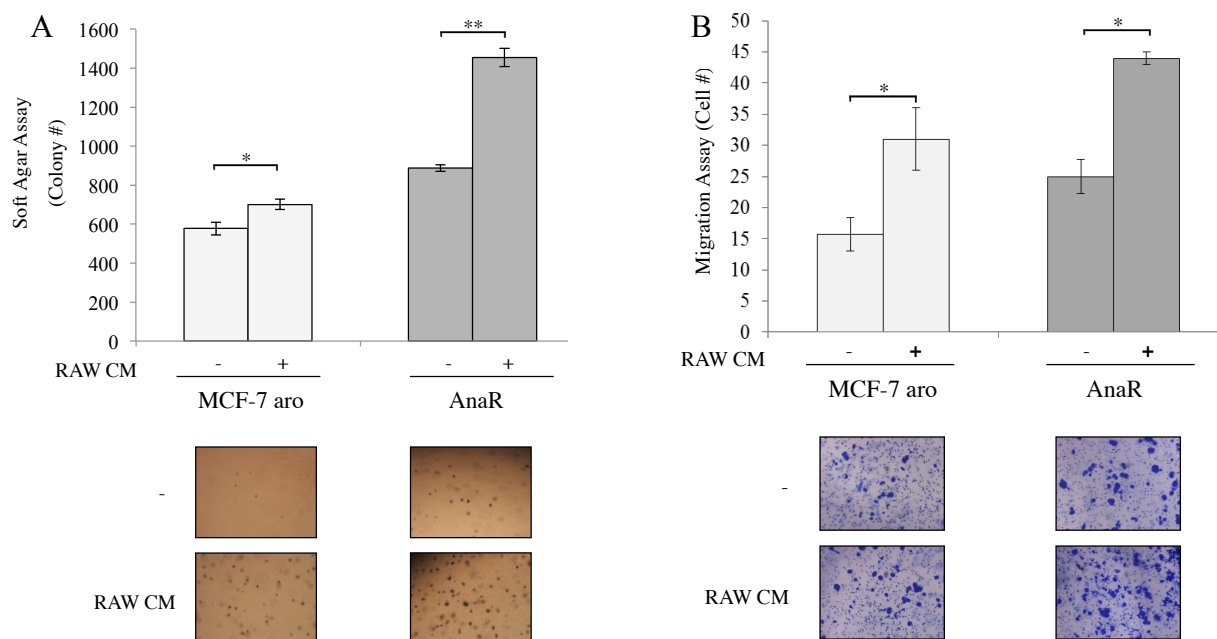


**Figure 6. Activated macrophages support AnaR aggressive phenotype.** **A**, soft agar growth assays in MCF-7aro and AnaR breast cancer cells treated as indicated. A typical well for each condition is shown. **B**, transmigration assay in MCF-7 aro and AnaR breast cancer cells using as chemoattractant regular growth media (-) or conditioned media derived from RAW cells (RAW-CM). Images are representative of one random microscopic field of view within each membrane. \* $P < 0.01$ , \*\* $P < 0.001$ .

## AIM 3

*Evaluation of the efficacy of a novel  
peptide to block leptin action  
in breast cancer*

### Design, Synthesis and Characterization of Peptide LDFI.

The critical role played by leptin in mammary tumorigenesis have generated a great interest in the design and development of several potential therapeutic approaches that could interfere with the action of leptin and thereby prevent or delay breast cancer development and progression. In this regard, we synthesized an unmodified leptin peptide (LDFI) and investigated its ability to inhibit leptin receptor function in breast cancer cells using *in vitro* and *in vivo* experimental models. Peptide LDFI synthesized in collaboration with Prof. Liguori (Laboratory of Chemistry), is a four-amino acids-long peptide, corresponding to amino acids 39-42 (leucine (L), aspartate (D), phenylalanine (F), isoleucine (I)) analog of ObR binding site III, that appears to be crucial for the formation of an active leptin-leptin receptor complex and its subsequent activation. Peptide LDFI was obtained by automated solid phase peptide synthesis and characterized by  $^1\text{H-NMR}$  and HPLC/MS. Molecular structure and  $^1\text{H-NMR}$  spectrum profile are shown in figure 1.

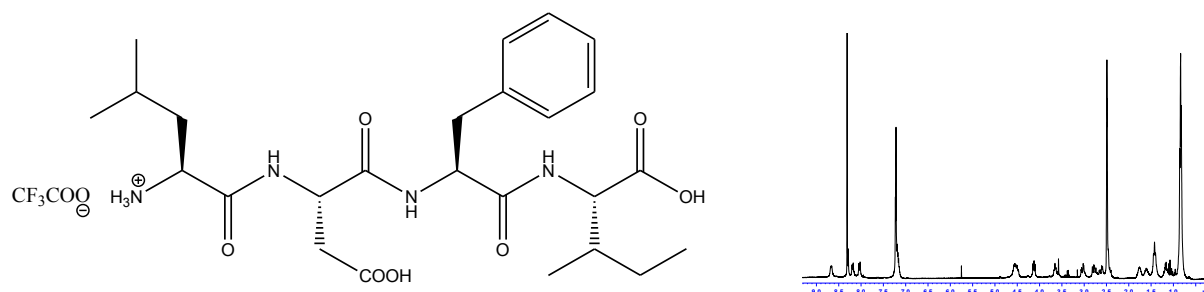
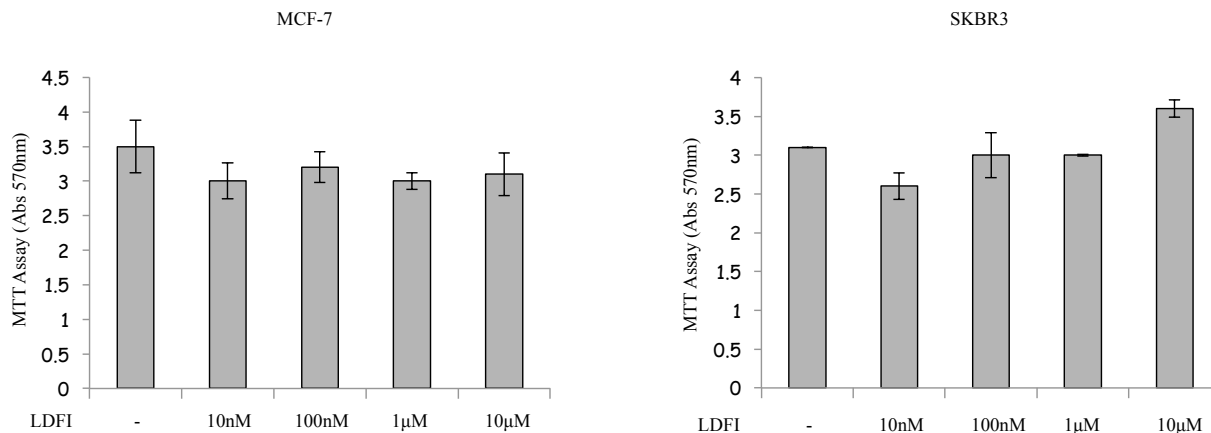


Figure 1. Molecular structure and  $^1\text{H-NMR}$  spectrum profile of peptide LDFI.

### Peptide LDFI Reduces Leptin-Induced Cell Growth and Motility.

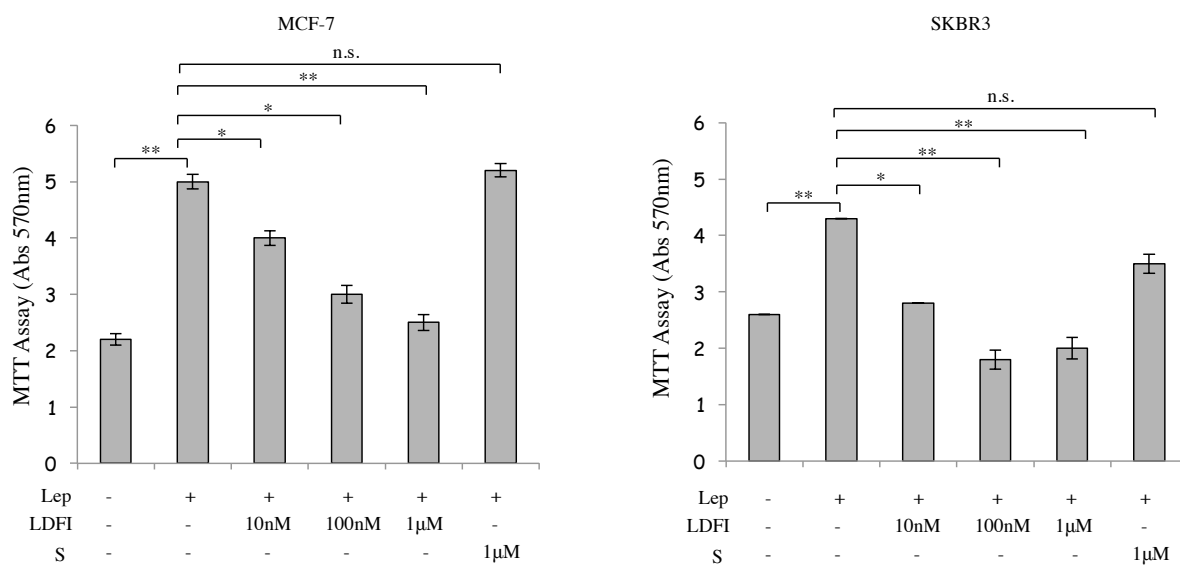
First, we tested the biological activity of the peptide on anchorage-dependent cell proliferation using as experimental models both ER-positive (MCF-7) and ER-negative (SKBR3) breast cancer cells. Either MCF-7 and SKBR-3 cells were treated with the peptide at increasing concentrations (10nM, 100nM, 1 $\mu\text{M}$  and 10  $\mu\text{M}$ ) for 96 hours. We did not observe any significant effects on cell growth at all the doses tested (Fig. 2). This is an important feature distinguishing this peptide from other potential ObR inhibitors that can act as ObR agonists in the absence of leptin, thus are not suitable for pharmaceutical development.



**Figure 2. LDFI effects on cell proliferation.** MTT growth assays in MCF-7 and SKBR3 cells treated with vehicle (-) or increasing doses of LDFI for 96 hours.

Next, we explored the ability of peptide LDFI to inhibit leptin-induced cell proliferation in MTT growth assays (Fig. 3A). Our results showed that the peptide significantly reversed the enhanced leptin cell growth in a dose-dependent manner. In contrast, a peptide "scrambled", consisting of a random sequence of amino acids, used as a negative control, showed no leptin antagonistic properties. Consistently with MTT assays, the peptide significantly reduced colonies formation in both cell lines, as revealed by soft agar growth assays (Fig. 3B). These data well correlated with a reduction of leptin induced Cyclin D1 expression in cells treated with the peptide (Fig. 3C).

A





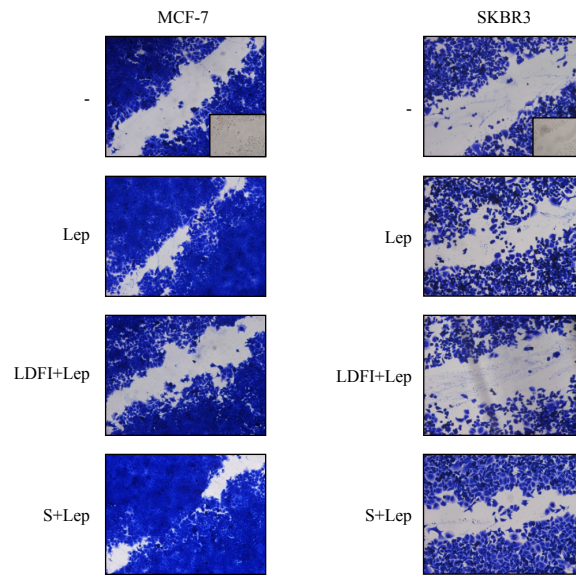


**Figure 4. LDFI reduces leptin-induced cell motility.** Cells were subjected to “in vitro” scratch assay with images captured at 0 and 24 h after incubation with with vehicle (-), leptin 500ng/ml alone or in combination with LDFI 1 $\mu$ mol/L using phase-contrast microscopy. Small squares, time 0.

### Peptide LDFI Antagonizes Leptin Signaling Pathways.

Leptin exerts its biologic function through binding to its receptors which mediate a downstream signal by activating multiple signaling pathways. Thus, we examined the effects of peptide LDFI on major leptin signaling pathways that are known to mediate proliferation and motility in breast cancer cells. In MCF-7 and SKBR3 cells, as expected, leptin treatment significantly induced phosphorylation of JAK2/STAT3, AKT and MAPK, whereas treatment with peptide LDFI completely abrogated the leptin activation of these signaling pathways (Fig. 5).

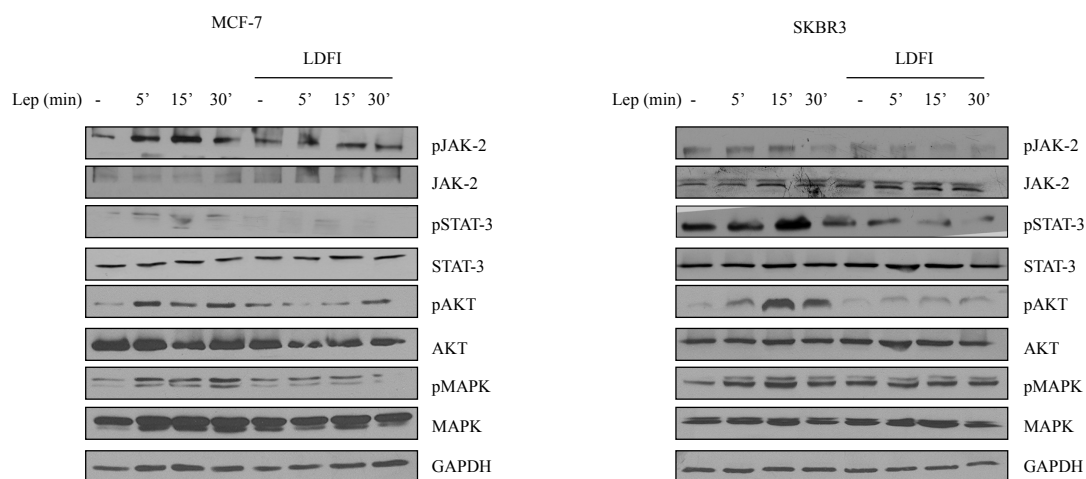


**Figure 5. Effects of LDFI on leptin signaling pathways.** MCF-7 and SKBR3 cells were treated for with vehicle (-) or leptin 500ng/ml with or without LDFI 1 $\mu$ mol/L before lysis. Equal amounts of total cellular extract were analyzed for pJAK2, JAK2, pSTAT3, STAT3, pAKT, AKT, pMAPK, MAPK levels by immunoblotting. GAPDH was used as loading control.

### Peptide LDFI Abolishes Leptin-Induced Up-regulation of the Ob gene.

Since it has been previously demonstrated that leptin was able to up-regulate its own gene expression (50), we then determined whether LDFI could also conteract this effect. RT-PCR analysis demonstrated that the Ob gene induction after leptin treatment was totally abrogated in the presence of the peptide (Fig. 6).

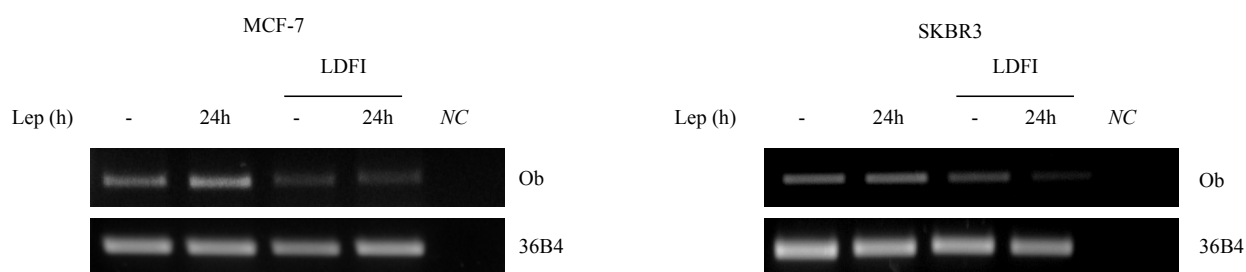


**Figure 6. Effects of Peptide LDFI on Ob gene expression.** RT-PCR for Ob gene and 36B4 (internal standard) after treatment with vehicle (-), leptin 500ng/ml alone or in combination with LDFI 1 $\mu$ mol/L for 24 hours. NC, negative control.

### Specifity of Peptide LDFI on Leptin Signaling Pathway.

To test if LDFI action was specific for leptin signaling pathway, different cell biological assays were performed in cells treated with EGF (Epidermal Growth Factor), that is well known to stimulate cell growth and differentiation through interaction with a receptor that is structurally and functionally different from the leptin receptor. We found that LDFI treatment did not reduce EGF-induced cell growth and motility (Fig. 7A and 7B). In addition, the enhanced AKT and MAPK phoshorylation observed after treatment with EGF was not affected by the peptide (Fig. 7C).

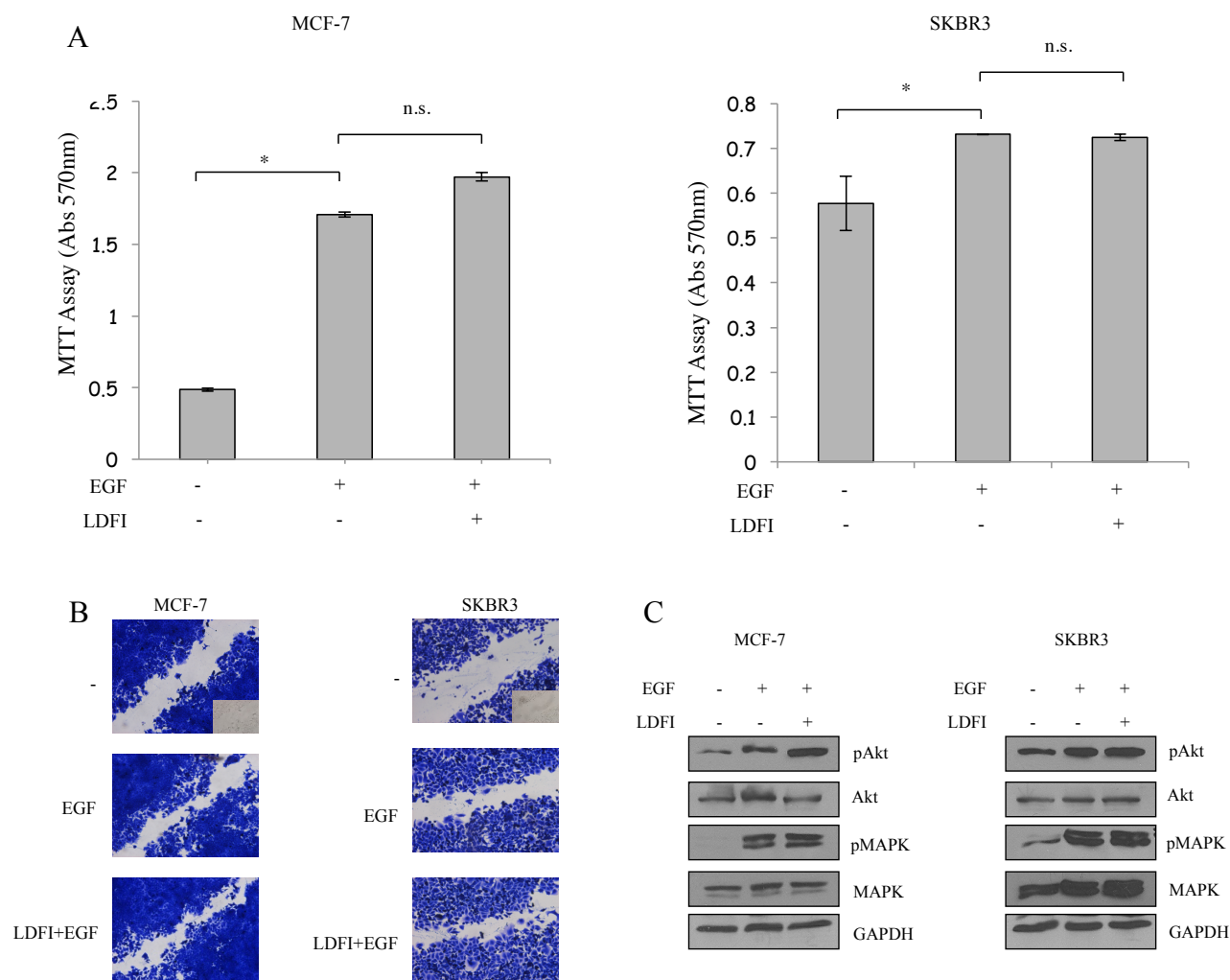


**Figure 7. LDFI effects are specific for leptin signaling pathways.** **A**, MTT growth in MCF-7 and SKBR3 cells treated with vehicle (-) or EGF 100ng/ml alone or in combination with LDFI 1 $\mu$ mol/L. ns, non significant, \*P<0.05. **B**, Cells were subjected to “in vitro” scratch assay with images captured at 0 and 24 h after incubation with with vehicle (-), EGF 100ng/ml alone or in combination with LDFI 1 $\mu$ mol/L using phase-contrast microscopy. Small squares, time 0. **C**, MCF- 7 and SKBR3 cells were treated as indicated before lysis. Equal amounts of total cellular extract were analyzed for pAKT, AKT-tot, pMAPK, MAPK-tot levels by immunoblotting. GAPDH was used as loading control.

### Efficacy of PEG-LDFI Treatment in Breast Cancer Xenografts.

As a final step of this study, we evaluated the efficacy of the peptide in *in vivo* models. However, considering the extremely short half-life of the low molecular mass peptides, we developed for our studies a pegylated leptin antagonist (PEG-LDFI). Pegylation may result in improved *in vivo* potency related to a better stability, greater protection against proteolytic degradation and lower clearance. After verifying the structure and the purity of the pegylated leptin peptide (data not shown), we tested its effects on cell proliferation and motility (Fig. 8).

We found that peptide PEG-LDFI was as effective as peptide LDFI in inhibiting leptin-induced soft agar anchorage-independent growth and migration, mimicking the same antagonistic activity of the native peptide LDFI.

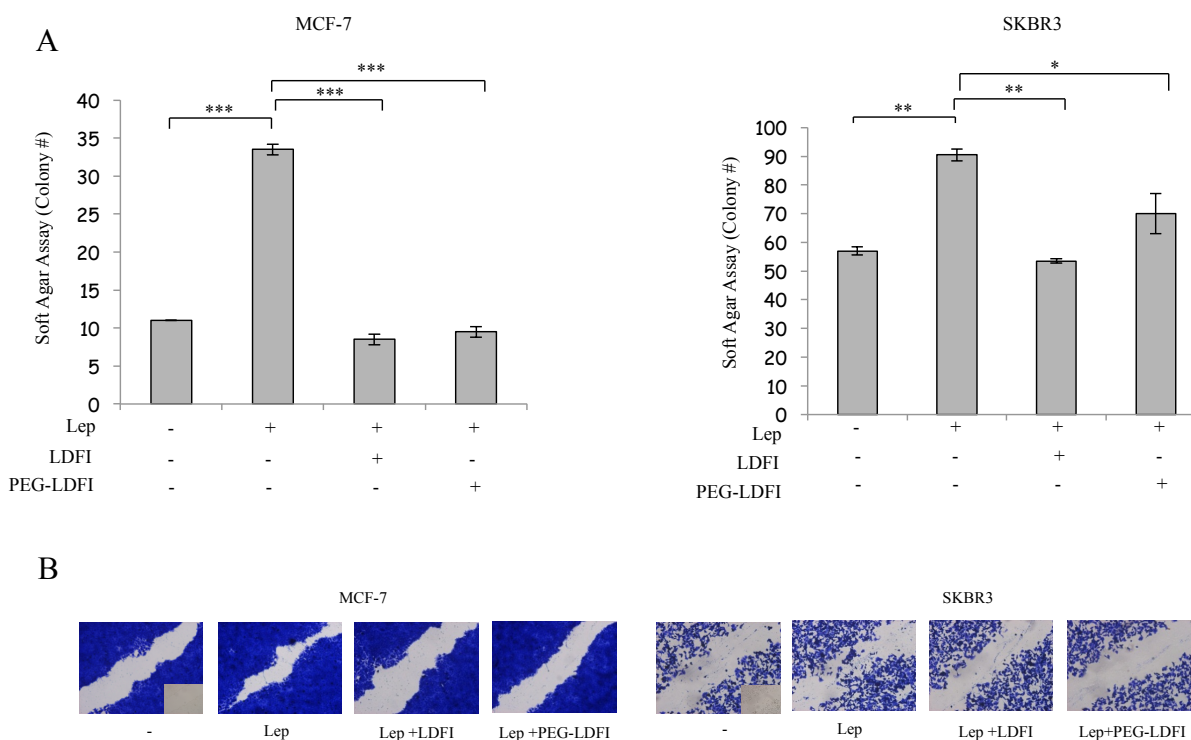


**Figure 8. PEG-LDFI effects on cell growth and motility.** **A**, MTT growth assays in MCF-7 and SKBR3 cells treated with vehicle (-), leptin 500ng/ml alone or in combination with LDFI 1 $\mu$ mol/L or PEG-LDFI 1 $\mu$ mol/L. \*P<0.05, \*\*P<0.01, \*\*\*P<0.001. **B**, cells treated as indicated were subjected to “in vitro” scratch assay with images captured at 0 and 24 h using phase-contrast microscopy. Small squares, time 0.

Therefore, we then used the SKBR3 tumor xenografts model to examine the effects of peptide PEG-LDFI on tumor growth *in vivo*. To this aim, we injected SKBR3 breast cancer cells into the intrascapular region of female nude mice and followed tumor growth after administration of PEG-LDFI at 10mg/Kg/day. As SKBR3 cells can produce endogenous leptin and can growth when xenotransplanted into mice without leptin addition, exogenous leptin was not inoculated into the mice. We found that the administration of PEG-LDFI was well tolerated because no change in body weight or in food and water consumption, was observed, highlighting how this peptide may not have any effect at the hypothalamic level. As shown in figure 9A, after PEG-LDFI treatment tumor volumes continued to reduce over control for the duration of experiment. At the time of killing (28 days), tumor size was markedly smaller in animals treated with PEG-LDFI when compared with vehicle-treated mice (data not shown).

Corresponding to their growth characteristics, phosphorylation levels of STAT3, MAPK and AKT were strongly reduced in PEG-LDFI-treated mice (Fig. 9B).

All together results from the present investigation demonstrate that peptide LDFI is able to reduce breast cancer cell growth both *in vitro* and *in vivo*, suggesting its potential use in the treatment of breast cancer.

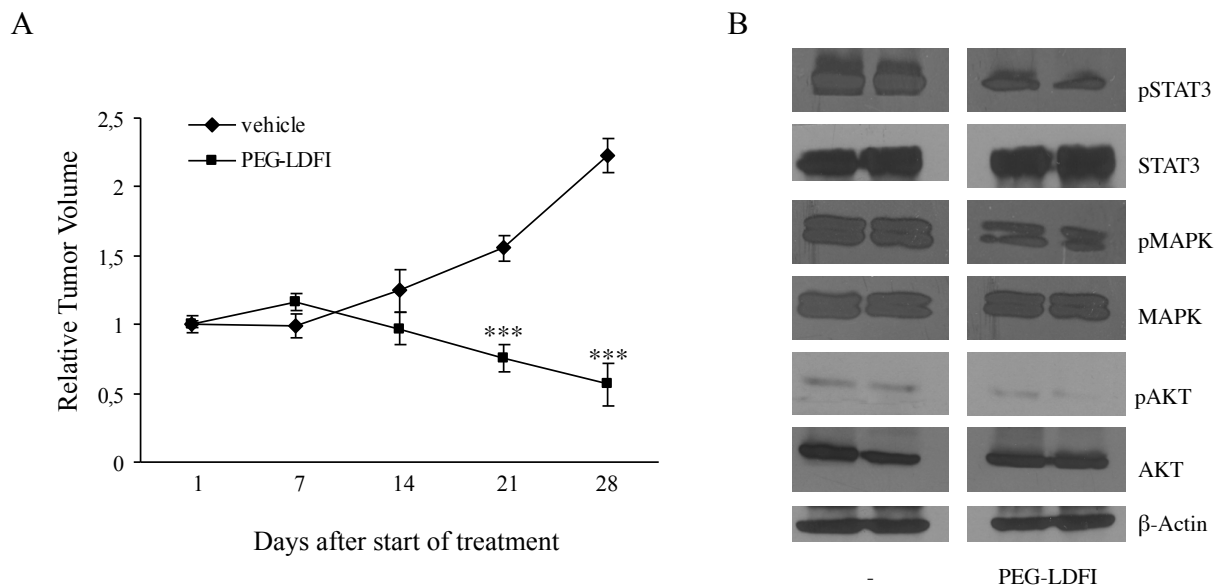


**Figure 9. Impact of PEG-LDFI treatment on tumor growth of SKBR3 xenografts.** **A**, SKBR3 cells were inoculated into the intrascapular region of female nude mice (10 mice) and then treated daily with vehicle (-) or PEG-LDFI 10mg/kg/day by intraperitoneal injection for 28 days (5 mice each group). Relative tumor volume (RTV) was calculated from the following formula:  $RTV = (V_x/V_1)$ , where  $V_x$  is the tumor volume on day X and  $V_1$  is the tumor volume at initiation of the treatment (day 1). \*\*\* $P < 0.0001$  **B**, protein extracts from xenografts excised from vehicle (-) and PEG-LDFI treated mice analyzed for pSTAT3, pMAPK and pAKT and total protein levels by immunoblotting.  $\beta$ -actin was used as loading control.

# *Discussion*

Breast cancer is a heterogeneous disease encompassing multiple subgroups with differing molecular signatures, prognoses, and responses to therapies. From the clinical view point, breast cancer is subdivided into three major subtypes: tumors expressing estrogen receptors (ERs) and/or progesterone receptors (PRs) (commonly referred to as hormone receptor–positive [HR-positive] tumors), ERBB2-amplified (also known as human epidermal receptor 2–amplified [HER2-amplified]) breast cancer, and the remaining group commonly referred to as triple-negative breast cancer (TNBC) due to lack of expression of the ERs and PRs and normal or negative HER2 expression (51). Knowing that nearly 70% of breast tumors express ER, targeting of the ER has been a reliable therapeutic modality for all stages of the disease. Indeed, ER serves as a predictive marker for responsiveness to endocrine therapy and is targeted either directly by selective estrogen receptor modulators (SERMs) and pure antagonists or indirectly by aromatase inhibitors (AIs) that block estrogen production, thus endocrine therapy has been an integral adjuvant treatment for patients with hormone-dependent breast cancers (52). Despite the documented benefits of ER-targeted therapy in breast cancer, it is known that not all patients respond to endocrine manipulation (*de novo* resistance) and a substantial number of patients who do respond will develop disease progression or recurrence while on therapy (acquired resistance). Many mechanisms have been described to be involved in the development for acquired endocrine resistance in breast cancers, and these include: activation of ER-independent pro-survival pathways; altered expression of ER co-regulators; altered regulation of downstream effectors of the ER involved in cell cycle and apoptosis; changes in ER expression; mutations in the ER gene and single nucleotide polymorphisms in cytochrome P450 2D6 (CYP2D6) (53). In addition, it has been recently proposed that tumor microenvironment could have an important role in endocrine resistance (39).

The tumor microenvironment includes the extracellular matrix (ECM), diffusible growth factor and cytokines, and a variety of known epithelial cell types including those comprising the vasculature (endothelial cells, smooth muscle cells), those that can respond to infection and injury (lymphocytes, macrophages, mast cells), and cancer associated fibroblasts (CAFs). It has long been recognized that carcinomas induce a modified stroma through expression of growth factors that promotes angiogenesis, altered ECM expression, accelerated fibroblasts proliferation and increased inflammatory cell recruitment (1-4).

Our results contributed to elucidate the complex crosstalk existing between breast cancer cells and tumor microenvironment. In particular, we identified, for the first time, leptin, a known

cytokine involved in breast cancer development, as a determinant for CAFs-tumor promoting activities in ER-positive breast cancer cells (AIM 1). Next, we demonstrated the important role of leptin in driving aromatase inhibitor resistance in the context of tumor microenvironment (AIM 2). Finally, we developed and tested a novel leptin antagonist to block leptin action in breast cancer (AIM 3).

### **Tumor Stroma Interaction Supports ER-positive Breast Cancer Progression through Leptin Signaling (Aim 1).**

ER $\alpha$  expression has important implications for breast cancer biology and therapy. Fuqua and colleagues identified a lysine to arginine transition at residue 303 of ER $\alpha$  (K303R-ER $\alpha$ ) in 30% of breast hyperplasias and in 50% of invasive breast cancers (20, 21), although using another detection method, the mutation was identified in only 6% of tumors (26); thus the frequency is still unresolved. This mutation was associated with older age, larger tumor size, lymph node positivity, and shorter time to recurrence—all features related to a more aggressive breast cancer phenotype. Because of the recently recognized importance of tumor–stroma cross-talk in promoting breast cancer progression and metastasis, it is imperative to elucidate the molecular events occurring between cancer cells and adjacent stroma at the site of primary tumors to provide new treatment options for breast cancer. Here, we elucidated the complex interactions between peritumoral tissue, locally derived factors, and neoplastic cells in dependency of ER $\alpha$  status, with a special focus on leptin effects in influencing the behavior of breast cancer cells bearing the naturally occurring K303R ER $\alpha$  mutation. We showed that the entire complement of secretory proteins released by CAFs have more profound effects on K303R ER $\alpha$ -expressing cell proliferation and migration than on WT ER $\alpha$  cells. We evidenced an important role for JAK2/STAT3 and ER $\alpha$  signaling pathways in CAFs-mediated effects. Our microarray study pointed to the regulation of several important transcriptional programs of growth factors and cytokine receptors that, acting as mediators of stromal–epithelial interactions, are potentially involved in carcinoma progression. Among them, the gene encoding for leptin receptor was the most highly induced in K303R-expressing breast cancer cells.

Leptin is primarily synthesized from adipocytes but is also produced by other cells, including fibroblasts (54–57). We revealed, for the first time, Ob mRNA expression and leptin secretion in CAFs. CAFs also expressed ObR long isoforms, implying that an autocrine feedback loop may exist. Leptin immunodepletion from CAF-derived conditioned media substantially reduced the

growth- and migration-promoting activities of CAFs suggesting that CAFs through leptin signaling may influence tumor cell behavior, especially in K303R ER $\alpha$ -expressing breast cancer cells.

Leptin, a pleiotropic molecule that regulates food intake, hematopoiesis, inflammation, cell differentiation, and proliferation, is also required for mammary gland development and tumorigenesis. Indeed, leptin and its receptor isoforms (ObRs) have been detected in mammary epithelium and breast cancer cell lines and are overexpressed in cancer tissue compared with healthy epithelium, with a positive correlation between ObR and ER $\alpha$  expression (57, 58). Real-time PCR, immunoblotting, and immunofluorescent experiments revealed an increase in mRNA and protein expressions of ObR long and short isoforms in K303R-ER $\alpha$ -expressing cells. Moreover, we showed that the mutant expression was associated with enhanced leptin signaling activation and increased sensitivity to leptin stimulation on growth, motility, and invasiveness. Besides, a significant increase in the growth of leptin-treated mutant tumors was observed *in vivo*. Leptin is a potent modulator of the estrogen signaling pathway (41, 59). On the contrary, estradiol modulates ObR expression in rat brain, through a putative estrogen-responsive element in its promoter (60, 61), and others showed that estradiol induces leptin and ObR expression in MCF-7 breast cancer cells (58). Thus, leptin and estrogen might cooperate in sustaining estrogen-dependent breast carcinoma growth. We showed an increased S167 and S118 phosphorylation of the K303R receptor, an enhanced K303R-ER $\alpha$  transactivation, and a more pronounced upregulation of classical estrogen-regulated genes in K303R-expressing cells. Indeed, the pure antiestrogen ICI182760 drastically suppressed leptin-stimulated anchorage-independent growth and motility of mutant cells. These results suggest that the mutation may potentiate the role of ER $\alpha$  as an effector of leptin intracellular signal transduction, which may enhance cell proliferation, migration, and invasiveness, contributing to the more aggressive phenotype of K303R-associated breast cancers.

In the same way as tumor microenvironment plays active roles in shaping the fate of a tumor, cancer cells actively recruit fibroblasts into the tumor mass, in particular, the subpopulation named CAFs. This cell type is defined on the basis of the morphologic characteristics or expression of markers as the FAP (1–4). Studies addressing these issues are heterogeneous in terms of cell systems used, tumor cell types, and fibroblast sources. Experimental systems have used different tumor-derived conditioned media to stimulate CAFs, and others have cocultured tumor cells with normal fibroblasts or mesenchymal stem cells and measured chemokines levels

in the resulting conditioned media. For instance, fibroblasts growth with tumor cells resulted in increased production of chemokines whose source is in CAFs themselves. Chemokines produced under these "mixed" conditions promoted tumor promalignancy activities (6, 9, 62). We showed increased leptin mRNA expression and secretion by CAFs in response to soluble K303R-ER $\alpha$  cell-secreted factors compared with WT-derived conditioned media, suggesting that K303R cells have the ability to instruct their surrounding fibroblasts to augment leptin production, thereby enhancing tumor growth. This further indicates that interactions between the two subpopulations are actually bidirectional. These interactions become more productive when tumor cells have a higher aggressiveness phenotype (62–64). CAFs exposed to K303R cell-derived conditioned media acquired a more activated phenotypic characteristic, as revealed by an altered morphology, an increased FAP mRNA expression, and enhanced proliferative and migratory capabilities. We identified the epidermal growth factor, known to affect CAFs phenotype and leptin secretion (11, 44–47), as the factor responsible of the paracrine activation of the surrounding stroma. Thus, a positive feedback loop is established which leads to the development and growth of the tumor.

In conclusion, we proposed a model in which leptin, secreted from CAFs, binds to its receptor, activates K303R-ER $\alpha$ , and promotes proliferation, migration, and invasiveness of K303R-ER $\alpha$ -expressing breast cancer cells. In turn, K303R cells release factors as EGF that "educate" CAFs to enhance secretion of leptin, which, acting back on malignant cells, may establish a positive feedback loop between cancer and stromal cells to further support breast tumor progression (Fig. 1).

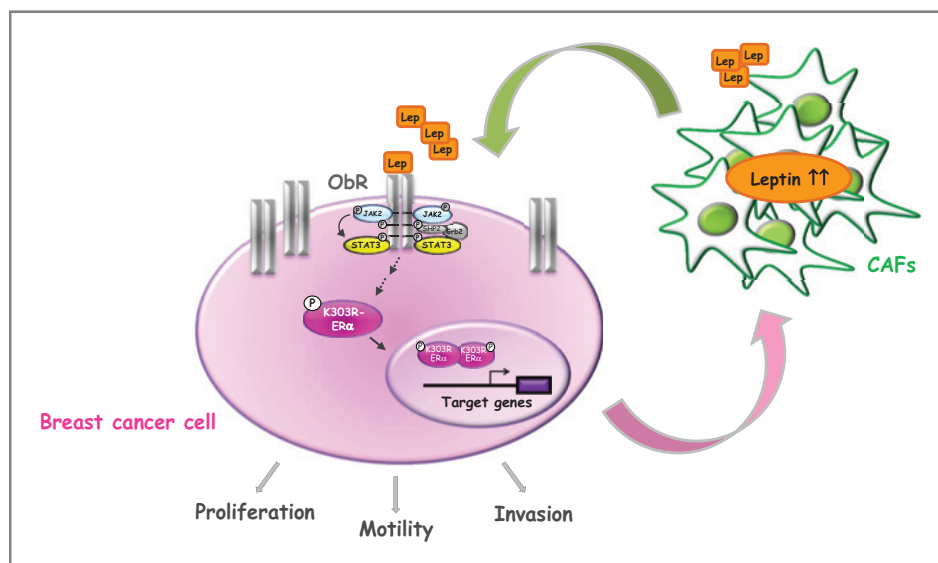


**Figure 1. Schematic illustration of tumor–stroma interactions in K303R- ER $\alpha$  breast cancer microenvironment.** CAFs secrete leptin, which, acting in a paracrine fashion, binds to its cognate receptors (ObR) overexpressed on the surface of K303R ER $\alpha$  breast cancer cells and activates K303R ER $\alpha$ . This results in increased cell proliferation, motility, and invasion. K303R ER $\alpha$ -expressing cells, in turn, secrete factors that stimulate leptin production by adjacent CAFs, thus creating a positive feedback loop between cancer and stromal cells to further promote breast tumor progression.

## **Aromatase Inhibitor Resistance in Breast Cancer: a Novel Potential Role for Leptin (Aim 2).**

Resistance to aromatase inhibitors (AIs) is frequently acquired with an associated poor prognosis. Breast cancer models revealed the importance of growth factor signals in sustaining endocrine-resistant growth; but these models do not involve an assessment of the contribution of stromal elements. Our results demonstrated that CAFs were more effective in stimulating growth and motility of AI resistant cells compared to parental sensitive cells. Inhibition of the classic leptin JAK2/STAT3 cascade suppressed CAFs-induced proliferation, especially in anastrozole resistant (AnaR) cells, suggesting a potential role for leptin in influencing the aggressive behavior of AnaR cells. Indeed, the resistant cell line expressed high mRNA levels of leptin and the long and short receptor isoforms. This is concomitant with an increased leptin signaling activation as revealed by an enhanced phosphorylation of JAK2/STAT3, AKT and MAPK pathways.

The adipocyte-derived hormone leptin has been shown to regulate the immune response in normal and pathological conditions (49). The overall leptin action in the immune system is a

proinflammatory effect, activating proinflammatory cells, promoting T-helper 1 responses, and mediating the production of the other proinflammatory cytokines, such as tumor necrosis factor- $\alpha$ , interleukin (IL)-2, or IL-6. Leptin receptor is also up-regulated by proinflammatory signals (49). Of note, molecular profiling of AI-treated breast tumors identified an increased expression of genes relating to inflammatory processes that are associated with poor anti-proliferative AI response (65, 66). In our study, we evinced that AnaR through leptin may tightly control the phenotype of macrophage, an important component of the inflammatory microenvironment within the breasts, in particular we found that AnaR cells-secreted soluble factors induced a significantly higher migration and pro-tumor activation of a macrophage cell line (RAW) than factors released from sensitive cells. These effects are strictly dependent on leptin signaling since motility of macrophages was strongly reduced when RAW cells were treated with a specific JAK2/STAT3 inhibitor or with AnaR conditioned media depleted of leptin used as chemoattractant. Finally, AnaR cells cocultured with macrophages showed enhanced growth and migration highlighting the existence of an enhanced bidirectional cross-talk between AnaR and macrophages cells.

In conclusion, AnaR cell-secreted factors induced an enhanced recruitment and activation of macrophages, which, acting back on malignant cells, established a positive feedback loop between cancer and inflammatory microenvironment to further support breast tumor progression.

### **Development of a Leptin Antagonist Peptide: Implications for Breast Cancer (Aim 3).**

The role of the obesity cytokine leptin in breast cancer progression has raised interest in interfering with leptin's action as a valuable therapeutic strategy. Indeed, several *in vitro* and *in vivo* studies have demonstrated that leptin stimulates breast cancer cell growth and invasiveness. Leptin is known to crosstalk with and transactivate several pathways that are targets for breast cancer therapy, including the estrogen, EGF receptor and HER2 pathways (43). Furthermore, our studies demonstrate a role for leptin in mediating tumor/stroma interaction in hormone-dependent and -resistant breast cancer cells. Leptin interacts with its receptor through three different binding sites: I-III. Site III is crucial for the formation of an active leptin-leptin receptor complex and its subsequent activation. Amino-acids 39-42 (LDFI) were shown to contribute to leptin site III and their mutations in alanine resulted in muteins acting as a typical antagonists (67). Antagonists to the receptor of the obesity hormone leptin are being developed both as

mutants of the full protein and peptide fragments representing single receptor-binding sites (68). We synthesized the unmodified leptin fragment LDFI and we demonstrated the ability of this peptide to inhibit the leptin-induced anchorage-dependent and –independent growth as well as migration in breast cancer cells without any agonistic activity. These results well correlated with the reduction of phosphorylation levels of leptin downstream effectors, as JAK2/STAT3/AKT/MAPK. Importantly, the LDFI fragment reversed the leptin mediated up-regulation of its own gene expression, as an additional mechanism able to enhance the peptide antagonistic activity. The described effects were specific for leptin signaling since the developed peptide was not able to antagonize the other growth factor's actions on signaling activation, proliferation and migration. Finally, we showed that the pegylated-LDFI (PEG-LDFI) markedly reduced breast cancer tumor in xenografts models. Thus, peptide LDFI acts as a full leptin antagonist both *in vitro* and *in vivo*.

### **Conclusions.**

Our study highlights the functional importance of tumor–host cross-talk in impacting malignant cell behavior and implies several clinical implications. First, because K303R mutation was identified in breast premalignant hyperplasia, it is tempting to speculate that this specific mutation hypersensitive to leptin signaling may promote or accelerate the development of cancers from premalignant breast lesions, further increasing risk in obese women. Second, understanding the key genes in tumor–stroma interactions may help to identify novel biomarkers for hormone-dependent and -resistant breast cancers. Finally, our findings support the development of new therapeutics targeting stroma signaling components (e.g., leptin) to be implemented in the adjuvant therapy for improving clinical care and reducing mortality from breast cancer.

1. Bhowmick NA, Neilson EG, Moses HL. Stromal fibroblasts in cancer initiation and progression. *Nature* 2004;432:332–7.
2. Hanahan D, Weinberg RA. The hallmarks of cancer. *Cell* 2000;100:57–70.
3. Mueller MM, Fusenig NE. Friends or foes-bipolar effects of the tumour stroma in cancer. *Nat Rev Cancer* 2004;4:839–49.
4. Orimo A, Weinberg RA. Stromal fibroblasts in cancer: a novel tumor-promoting cell type. *Cell Cycle* 2006;5:1597–601.
5. Augsten M, Hagglof C, Olsson E, Stolz C, Tsagozis P, Levchenko T, et al. CXCL14 is an autocrine growth factor for fibroblasts and acts as a multimodal stimulator of prostate tumor growth. *Proc Natl Acad Sci U S A* 2009;106:3414–9.
6. Jung DW, Che ZM, Kim J, Kim K, Kim KY, Williams D. Tumor-stromal crosstalk in invasion of oral squamous cell carcinoma: a pivotal role of CCL7. *Int J Cancer* 2009;127:332–44.
7. Matsuo Y, Ochi N, Sawai H, Yasuda A, Takahashi H, Funahashi H, et al. CXCL8/IL-8 and CXCL12/SDF-1 cooperatively promote invasiveness and angiogenesis in pancreatic cancer. *Int J Cancer* 2009;124:853–61.
8. Wolf JS, Chen Z, Dong G, Sunwoo JB, Bancroft CC, Capo DE, et al. IL (interleukin)-1 alpha promotes nuclear factor-kappaB and AP-1- induced IL-8 expression, cell survival, and proliferation in head and neck squamous cell carcinomas. *Clin Cancer Res* 2001;7:1812–20.
9. Kumar S, Kishimoto H, Chua HL, Badve S, Miller KD, Bigsby RM, et al. Interleukin-1 alpha promotes tumor growth and cachexia in MCF-7 xenograft model of breast cancer. *Am J Pathol* 2003; 163:2531–41.
10. Wu MH, Chou YC, Chou WY, Hsu GC, Chu CH, Yu CP, et al. Circulating levels of leptin, adiposity and breast cancer risk. *Br J Cancer* 2009;100: 578–82.
11. Schaffler A, Scholmerich J, Buechler C. Mechanisms of disease: adipokines and breast cancer-endocrine and paracrine mechanisms that connect adiposity and breast cancer. *Nat Clin Pract Endocrinol Metab* 2007;3:345–54.
12. Chen P, Bonaldo P. Role of macrophage polarization in tumor angiogenesis and vessel normalization: implications for new anticancer therapies. *Int Rev Cell Mol Biol.* 2013;301:1-35.
13. Tang X. Tumor-associated macrophages as potential diagnostic and prognostic biomarkers in

- breast cancer. *Cancer Letter* 2013 332 3–10
14. Catalán V, Gomez-Ambrosi J, Rodriguez A, Fruhbeck G. Adipose tissue immunity and cancer. *Front Physiol* 2013 2;4:275
  15. Ribeiro R, Monteiro C, Catalán V, Hu P, Cunha V, Rodríguez A, et al. Obesity and prostate cancer: gene expression signature of human periprostatic adipose tissue. *BMC Med* 2012; 10:108.
  16. Hursting S D, and Dunlap S M. Obesity, metabolic dys- regulation, and cancer: a growing concern and an inflammatory (and microenvironmental) issue. *Ann NY Acad Sci* 2012, 1271:82–7.
  17. Osborne CK, Schiff R. Estrogen-receptor biology: continuing progress and therapeutic implications. *J Clin Oncol* 2005;23:1616–22.
  18. Herynk MH, Fuqua SA. Estrogen receptor mutations in human disease. *Endocr Rev* 2004;25:869–98.
  19. Barone I, Brusco L, Fuqua SA. Estrogen receptor mutations and changes in downstream gene expression and signaling. *Clin Cancer Res* 2010;16:2702–8.
  20. Fuqua SA, Wiltschke C, Zhang QX, Borg A, Castles CG, Friedrichs WE, et al. A hypersensitive estrogen receptor- $\alpha$  mutation in premalignant breast lesions. *Cancer Res* 2000;60:4026–9.
  21. Herynk MH, Parra I, Cui Y, Beyer A, Wu MF, Hilsenbeck SG, et al. Association between the estrogen receptor  $\alpha$  A908G mutation and outcomes in invasive breast cancer. *Clin Cancer Res* 2007;13:3235–43.
  22. Tebbit CL, Bentley RC, Olson JA, Marks JR. Estrogen receptor  $\alpha$  (ESR1) mutant A908G is not a common feature in benign and malignant proliferation of the breast. *Genes Chromosomes Can* 2004;40:51–4.
  23. Tokunaga E, Kimura Y, Maehara Y. No hypersensitive estrogen receptor  $\alpha$  mutation (K303R) in Japanese breast carcinomas. *Breast Canc Res Treat* 2004;84:289–92. 19.
  24. Zhang Z, Yamashita H, Toyama T, Omoto Y, Sugiura H, Hara Y, et al. Estrogen receptor  $\alpha$  mutation (A-to-G transition at nucleotide 908) is not found in different types of breast lesions from Japanese women. *Breast Cancer* 2003;10:70–3.
  25. Davies MP, O'Neill PA, Innes H, Sibson DR. Hypersensitive K303R oestrogen receptor- $\alpha$  variant not found in invasive carcinomas. *Breast Cancer Res* 2005;7:R113–8.
  26. Conway K, Parrish E, Edmiston SN, Tolbert D, Tse CK, Geradts J, et al. The estrogen

- receptor- $\alpha$  A908G (K303R) mutation occurs at a low frequency in invasive breast tumors: results from a population-based study. *Breast Cancer Res* 2005;7:R871–80.
27. Cui Y, Zhang M, Pestell R, Curran EM, Welshons WV, Fuqua SA. Phosphorylation of estrogen receptor alpha blocks its acetylation and regulates estrogen sensitivity. *Cancer Res* 2004;64:9199–208.
  28. Barone I, Iacopetta D, Covington KR, Cui Y, Tsimelzon A, Beyer A, et al. Phosphorylation of the mutant K303R estrogen receptor alpha at serine 305 affects aromatase inhibitor sensitivity. *Oncogene* 2010;29: 2404–14.
  29. Herynk MH, Hopp T, Cui Y, Niu A, Corona-Rodriguez A, Fuqua SA. A hypersensitive estrogen receptor alpha mutation that alters dynamic protein interactions. *Breast Cancer Res Treat* 2010;122:381–93.
  30. Giordano C, Cui Y, Barone I, Ando S, Mancini M, Berno V, et al. Growth factor-induced resistance to tamoxifen is associated with a mutation of estrogen receptor  $\alpha$  and its phosphorylation at serine 305. *Breast Cancer Res Treat* 2010;119:71–81.
  31. Barone I, Cui Y, Herynk MH, Corona-Rodriguez A, Giordano C, Selever J, et al. Expression of the K303R estrogen receptor  $\alpha$  breast cancer mutation induces resistance to an aromatase inhibitor via addiction to the PI-3K/Akt kinase pathway. *Cancer Res* 2009;69: 4724–32.
  32. Encarnacion CA, Ciocca DR, McGuire WL, Clark GM, Fuqua SA, Osborne CK. Measurement of steroid hormone receptors in breast cancer patients on tamoxifen. *Breast Cancer Res Treat* 1993;26:237–46.
  33. Blume-Jensen P, Hunter T. Oncogenic kinase signalling. *Nature* 2001;411:355–65.
  34. Evan GI, Brown L, Whyte M, Harrington E. Apoptosis and the cell cycle. *Curr Opin Cell Biol* 1995;7:825–34.
  35. Martin LA, Farmer I, Johnston SR, Ali S, Marshall C, Dowsett M. Enhanced estrogen receptor (ER)  $\alpha$ , ERBB2, and MAPK signal transduction pathways operate during the adaptation of MCF-7 cells to long term estrogen deprivation. *J Biol Chem* 2003;278:30458–68.
  36. Schiff R, Massarweh SA, Shou J, Bharwani L, Mohsin SK, Osborne CK. Cross-talk between estrogen receptor and growth factor pathways as a molecular target for overcoming endocrine resistance. *Clin Cancer Res* 2004;10:331S–6S.;
  37. Sabnis GJ, Jelovac D, Long B, Brodie A. The role of growth factor receptor pathways in human breast cancer cells adapted to long-term estrogen deprivation. *Cancer Res*

- 2005;65:3903–10.
38. Staka CM, Nicholson RI, Gee JM. Acquired resistance to oestrogen deprivation: role for growth factor signalling kinases/oestrogen receptor cross-talk revealed in new MCF-7X model. *Endocr Relat Cancer* 2005;12:S85–97.
  39. Martinez-Outschoorn UE, Goldberg A, Lin Z, Ko YH, Flomenberg N, Wang C, et al. Anti-estrogen resistance in breast cancer is induced by the tumor microenvironment and can be overcome by inhibiting mitochondrial function in epithelial cancer cells. *Cancer Biol Ther* 2011 15;12(10):924-38
  40. Lephart ED, Simpson ER 1991 Assay of aromatase activity. *Methods Enzymol* 206:477–483
  41. Catalano S, Mauro L, Marsico S, Giordano C, Rizza P, Rago V, et al. Leptin induces, via ERK1/ERK2 signal, functional activation of estrogen receptor alpha in MCF-7 cells. *J Biol Chem* 2004;279:19908-15
  42. Mauro L, Catalano S, Bossi G, Pellegrino M, Barone I, Morales S, et al. Evidence that leptin up-regulates E-cadherin expression in breast cancer: effects on tumor growth and progression. *Cancer Res* 2007; 67:3412-21
  43. Cirillo D, Rachiglio AM, la Montagna R, Giordano A, Normanno N. Leptin signaling in breast cancer: an overview. *J Cell Biochem* 2008;105:956–64.
  44. Leroy P, Dessolin S, Villageois P, Moon BC, Friedman JM, Ailhaud G, et al. Expression of ob gene in adipose cells Regulation by insulin. *J Biol Chem* 1996;271:2365–8.
  45. Cascio S, Ferla R, D'Andrea A, Gerbino A, Bazan V, Surmacz E, et al. Expression of angiogenic regulators, VEGF and leptin, is regulated by the EGF/PI3K/STAT3 pathway in colorectal cancer cells. *J Cell Physiol* 2009;221:189–94.
  46. Trujillo ME, Sullivan S, Harten I, Schneider SH, Greenberg AS, Fried SK. Interleukin-6 regulates human adipose tissue lipid metabolism and leptin production in vitro. *J Clin Endocrinol Metab* 2004;89:5577–82.
  47. Wabu A, Smith K, Allen FD, Lauffenburger DA, Wells A. Epidermal growth factor induces fibroblast contractility and motility via a protein kinase C delta-dependent pathway. *J Biol Chem* 2004;279:14551–60.
  48. Baumgarten SC, Frasor J. Minireview: Inflammation: an instigator of more aggressive estrogen receptor (ER) positive breast cancers. *Mol Endocrinol* 2012; 26:360-71.
  49. Fernández-Riejos P, Najib S, Santos-Alvarez J, Martín-Romero C, Pérez-Pérez A, González-Yanes C, et al. Role of leptin in the activation of immune cells. *Mediat Inflamm*

- 2010;2010:568343.
50. Catalano S, Mauro L, Bonofiglio D, Pellegrino M, Qi H, Rizza P, et al. In vivo and in vitro evidence that PPAR $\gamma$  ligands are antagonists of leptin signaling in breast cancer. *Am J Pathol* 2011;179:1030-40
  51. Higgins MJ, Baselga J. Targeted therapies for breast cancer. *J Clin Invest* 2011;121:3797-803.
  52. Massarweh S, Schiff R. Resistance to endocrine therapy in breast cancer: exploiting estrogen receptor/growth factor signaling crosstalk. *Endocr Relat Cancer* 2006;13:S15-24.
  53. Williams C, Lin CY. Oestrogen receptors in breast cancer: basic mechanisms and clinical implications. *Ecancermedalscience* 2013;7:370.
  54. Glasow A, Kiess W, Anderegg U, Berthold A, Bottner A, Kratzsch J. Expression of leptin (Ob) and leptin receptor (Ob-R) in human fibroblasts: regulation of leptin secretion by insulin. *J Clin Endocrinol Metab* 2001;86:4472–9.
  55. Torday JS, Sun H, Wang L, Torres E. Leptin mediates the parathyroid hormone-related protein paracrine stimulation of fetal lung maturation. *Am J Physiol Lung Cell Mol Physiol* 2002;282:L405–10.
  56. Lin TC, Lee TC, Hsu SL, Yang CS. The molecular mechanism of leptin secretion and expression induced by aristolochic acid in kidney fibroblast. *PLoS One* 2011;6:e16654.
  57. Ishikawa M, Kitayama J, Nagawa H. Enhanced expression of leptin and leptin receptor (OB-R) in human breast cancer. *Clin Cancer Res* 2004;10:4325–31.
  58. Garofalo C, Koda M, Cascio S, Sulkowska M, Kanczuga-Koda L, Golaszewska J, et al. Increased expression of leptin and the leptin receptor as a marker of breast cancer progression: possible role of obesity-related stimuli. *Clin Cancer Res* 2006;12:1447–53.
  59. Catalano S, Marsico S, Giordano C, Mauro L, Rizza P, Panno ML, et al. Leptin enhances, via AP-1, expression of aromatase in the MCF-7 cell line. *J Biol Chem* 2003;278:28668–76.
  60. Bennett PA, Lindell K, Karlsson C, Robinson IC, Carlsson LM, Carlsson B. Differential expression and regulation of leptin receptor isoforms in the rat brain: effects of fasting and oestrogen. *Neuroendocrinology* 1998;67:29–36.
  61. Lindell K, Bennett PA, Itoh Y, Robinson IC, Carlsson LM, Carlsson B. Leptin receptor 50 untranslated regions in the rat: relative abundance, genomic organization and relation to putative response elements. *Mol Cell Endocrinol* 2001;172:37–45.
  62. Li L, Dragulev B, Zigrino P, Mauch C, Fox JW. The invasive potential of human melanoma

- cell lines correlates with their ability to alter fibroblast gene expression in vitro and the stromal microenvironment in vivo. *Int J Cancer* 2009;125:1796–804.
63. Tsujino T, Seshimo I, Yamamoto H, Ngan CY, Ezumi K, Takemasa I, et al. Stromal myofibroblasts predict disease recurrence for colorectal cancer. *Clin Cancer Res* 2007;13:2082–90.
64. Infante JR, Matsubayashi H, Sato N, Tonascia J, Klein AP, Riall TA, et al. Peritumoral fibroblast SPARC expression and patient outcome with resectable pancreatic adenocarcinoma. *J Clin Oncol* 2007;25:319–25.
65. Dunbier AK, Ghazoui Z, Anderson H, Salter J, Nerurkar A, Osin P, et al. Molecular profiling of aromatase inhibitor-treated postmenopausal breast tumors identifies immune-related correlates of resistance. *Clin Cancer Res* 2013;19:2775-86.
66. Mello-Grand M, Singh V, Ghimenti C, Scatolini M, Regolo L, Grosso E, et al. Gene expression profiling and prediction of response to hormonal neoadjuvant treatment with anastrozole in surgically resectable breast cancer. *Breast Cancer Res Treat* 2010;121:399-41.
67. Otvos L Jr, Surmacz E. Targeting the leptin receptor: a potential new mode of treatment for breast cancer. *Expert Rev Anticancer Ther* 2011;11:1147-50.
68. Otvos L Jr, Kovalszky I, Scolaro L, Sztodola A, Olah J, Cassone M, et al. Peptide-based leptin receptor antagonists for cancer treatment and appetite regulation. *Biopolymers* 2011;96:117-25.

#### AUTHORS OF 3 FULL PAPERS

1. Gu G., Barone I., **Gelsomino L.**, Giordano C., Bonofiglio D., Statti G., Menichini F., Catalano S. and Andò S. Oldenlandia Diffusa extracts exert antiproliferative and apoptotic effects on human breast cancer cells through ER $\alpha$ /Sp1-mediated p53 activation. *J Cell Physiol.* 227(10):3363-72, 2012
2. Barone I., Catalano S., **Gelsomino L.**, Marsico S., Giordano C., Panza S., Bonofiglio D., Bossi G., Covington K., Fuqua S., and Andò S. Leptin mediates tumor-stromal interactions that promote the invasive growth of breast cancer cells. *Cancer Res.* 72(6):1416-27, 2012.
3. Giordano C., Catalano S., Panza S., Vizza D., Barone I., Bonofiglio D., **Gelsomino L.**, Rizza P., Fuqua SAW and Andò S. Farnesoid X receptor inhibits Tamoxifen-resistant MCF-7 breast cancer cells growth through down-regulation of HERB2 expression, *Oncogene*, 30(39):4129-40, 2011.

#### AUTHOR OF 7 ABSTRACTS AND PRESENTATIONS

1. **Gelsomino L.**, Guowei G., Covington K.R., Babarinde T., Zhou J., Rechoum Y., <sup>1</sup>Arnoldo Corona-Rodriguez A., O'Malley B., Mangelsdorf D., Minna J., Ando' S., Fuqua S., Thyroid Hormone Receptor  $\beta$  Enhances Chemosensitivity and Induces ER $\alpha$  in Estrogen Receptor Negative Breast Cancer. From general pathology to molecular and translational medicine Young Scientist Meeting, Rome, October 23-24, 2013
2. Barone I., **Gelsomino L.**, Giordano C., Lanzino M., Bonofiglio D., Fuqua S., Catalano S., Ando' S. Aromatase inhibitor resistance in breast cancer: a potential role for cytokine signaling network. Experimental Biology 2013, Boston, MA, USA, April 20-24, 2013.
3. Barone I., **Gelsomino L.**, Leggio A., De Marco R., Giordano C., Bonofiglio D., Liguori A., Catalano S., Ando' S. Development of leptin antagonist peptide: implications for breast cancer. Joint meeting of SIPMeT and AIPaCMEM in collaboration with ASIP 2012, Udine, Italy, September 12-15, 2012. Published as supplement to the American Journal Pathology, vo.181
4. Barone I., Catalano S., **Gelsomino L.**, Panza S., Marsico S., Giordano C., Bonofiglio D., Casaburi I., Covington K.R., Fuqua S., Ando' S. Estrogen receptor-positive breast cancer cells drive CAFs to secrete leptin and support tumor invasiveness. Experimental Biology, San Diego, CA, USA, April 21-25, 2012. Published as supplement to FASEB Journal, vol. 26.
5. Barone I., **Gelsomino L.**, Panza S., Giordano C., Marsico S., Bonofiglio D., Fuqua S., Catalano S., Ando' S. May tumor microenvironment cooperate with a mutant ER $\alpha$  to promote breast cancer progression? 93rd Annual Meeting & Expo of The Endocrine Society, Boston, MA June 4-7, 2011

6. **Gelsomino L.**, Giordano C., Vizza D., Panza S., Barone I., Bonofiglio D., Fuqua S.A., Catalano S., Andò S. Activated Farnesoid X Receptor inhibits growth of tamoxifen-resistant MCF-7 breast cancer cells, through down-regulation of HER2 expression. Fondazione “Lilli Funaro”, Ricerca, tutela ambientale e prevenzione contro i tumori, Cosenza, Italia, 1-2 Aprile 2011
  
7. **Gelsomino L.**, Giordano C., Vizza D., Panza S., Barone I., Bonofiglio D., Fuqua S.A., Catalano S., Andò S. Activated Farnesoid X Receptor inhibits growth of tamoxifen-resistant MCF-7 breast cancer cells, through down-regulation of HER2 expression. Fondazione “Lilli Funaro”, Ricerca, tutela ambientale e prevenzione contro i tumori, Cosenza, Italia, 21-22 Maggio, 2010

# Oldenlandia diffusa Extracts Exert Antiproliferative and Apoptotic Effects on Human Breast Cancer Cells Through ER $\alpha$ /Sp1-Mediated p53 Activation

GUOWEI GU,<sup>1</sup> INES BARONE,<sup>2,3</sup> LUCA GELSOMINO,<sup>4</sup> CINZIA GIORDANO,<sup>2</sup> DANIELA BONOFILIO,<sup>2,4</sup> GIANCARLO STATTI,<sup>5</sup> FRANCESCO MENICHINI,<sup>5</sup> STEFANIA CATALANO,<sup>2,4\*</sup> AND SEBASTIANO ANDÒ<sup>2,3\*\*</sup>

<sup>1</sup>Lester and Sue Smith Breast Center and Department of Molecular and Cellular Biology, Baylor College of Medicine, One Baylor Plaza, Houston, Texas

<sup>2</sup>Centro Sanitario, University of Calabria, Arcavacata di Rende, Cosenza, Italy

<sup>3</sup>Department of Cellular Biology, University of Calabria, Arcavacata di Rende, Cosenza, Italy

<sup>4</sup>Department of Pharmaco-Biology, University of Calabria, Arcavacata di Rende, Cosenza, Italy

<sup>5</sup>Department of Pharmaceutical Sciences, University of Calabria, Arcavacata di Rende, Cosenza, Italy

Breast cancer is the most frequent tumor and a major cause of death among women. Estrogens play a crucial role in breast tumor growth, which is the rationale for the use of hormonal antiestrogen therapies. Unfortunately, not all therapeutic modalities are efficacious and it is imperative to develop new effective antitumoral drugs. *Oldenlandia diffusa* (OD) is a well-known medicinal plant used to prevent and treat many disorders, especially cancers. The aim of this study was to investigate the effects of OD extracts on breast cancer cell proliferation. We observed that OD extracts strongly inhibited anchorage-dependent and -independent cell growth and induced apoptosis in estrogen receptor alpha (ER $\alpha$ )-positive breast cancer cells, whereas proliferation and apoptotic responses of MCF-10A normal breast epithelial cells were unaffected. Mechanistically, OD extracts enhance the tumor suppressor p53 expression as a result of an increased binding of ER $\alpha$ /Sp1 complex to the p53 promoter region. Finally, we isolated ursolic and oleanolic acids as the bioactive compounds able to upregulate p53 expression and inhibit breast cancer cell growth. These acids were greatly effective in reducing tamoxifen-resistant growth of a derivative MCF-7 breast cancer cell line resistant to the antiestrogen treatment. Our results evidence how OD, and its bioactive compounds, exert antiproliferative and apoptotic effects selectively in ER $\alpha$ -positive breast cancer cells, highlighting the potential use of these herbal extracts as breast cancer preventive and/or therapeutic agents.

J. Cell. Physiol. 227: 3363–3372, 2012. © 2011 Wiley Periodicals, Inc.

Breast cancer is the most common malignancy among women in industrialized countries and is a significant cause of morbidity and mortality (Parkin et al., 2005). Development and progression of many human breast cancers are strongly dependent on estrogens, via interaction with specific estrogen receptors (ERs). Binding of hormone to ER $\alpha$  facilitates “classical” genomic activities of the receptor, and its direct interaction with estrogen response elements (ERE) in target genes function to either activate or repress gene expression. However, it has been demonstrated that estrogen actions are also mediated by ERE-independent mechanisms through which ER $\alpha$ , via protein–protein interactions with other transcription factors such as c-Fos/c-Jun B (AP-1), Sp1, and nuclear factor- $\kappa$ B (NF- $\kappa$ B), modulates key genes involved in cell cycle regulation (Katzenellenbogen and Katzenellenbogen, 2000; Osborne and Schiff, 2005; Barone et al., 2010). Recently, nonclassical actions of estrogens have been reported through binding to membrane-associated ER, which resides in or near the cell membrane and cross talks with the signal transduction pathways, including the c-Src/Ras/MAPK and cAMP pathway. Therefore, hormonal endocrine therapy directed at inhibiting the action of ER $\alpha$  by using selective estrogen receptor modulator such as tamoxifen, is a major therapeutic option in the management of all stage of breast cancer. Unfortunately, not all patients who have ER-positive tumors respond to this

**Conflicts of interest:** We confirm that all authors fulfill all conditions required for authorship. We also confirm that there is no potential conflict of interest as described in the instruction for authors. All authors have read and approved the manuscript.

Guowei Gu, Ines Barone, Stefania Catalano and Sebastiano Andò are contributed equally to this work.

Additional Supporting Information may be found in the online version of this article.

Contract grant sponsor: Reintegration AIRC/Marie Curie International Fellowship.

Contract grant sponsor: Lilli Funaro Foundation.

Contract grant sponsor: European Commission/FSE/Regione Calabria.

Contract grant sponsor: AIRC Grant IGI482.

\*Correspondence to: Stefania Catalano, Department of Pharmaco-Biology, University of Calabria, 87036 Arcavacata di Rende (CS), Italy. E-mail: stefcatalano@libero.it

\*\*Correspondence to: Sebastiano Andò, Department of Cell Biology, University of Calabria, 87036 Arcavacata di Rende (CS), Italy. E-mail: sebastiano.ando@unical.it

Manuscript Received: 9 August 2011

Manuscript Accepted: 9 December 2011

Accepted manuscript online in Wiley Online Library

(wileyonlinelibrary.com): 29 December 2011.

DOI: 10.1002/jcp.24035

therapy, developing local and/or regional recurrence, frequently with distant metastasis (Normanno et al., 2005). Chemotherapy remains the treatment of choice for metastasis, but is associated with severe adverse effects. Thus, looking for new antitumoral drugs with low toxicity to approach breast cancer treatment is required.

Natural dietary agents including fruits, vegetables, and spices have drawn a great deal of attention from both the scientific and general community, as a less intensive and more "natural" approach to achieving health or improving quality of life. They consist of a wide variety of biological active compounds that are ubiquitous in plants and are believed to suppress the inflammatory processes that lead to transformation, hyperproliferation and initiation of carcinogenesis (Richardson et al., 2000; Reddy et al., 2003). However, definitive literature in this area is scant and therefore has not been integrated into the mainstream medical community.

*Oldenlandia diffusa* (Willd.) Roxb. (OD), a member of the Rubiaceae Family, is a well-known medicinal plant commonly used in Southern China for the treatment of hepatitis, tonsillitis, sore throat, appendicitis, urethral infection, rheumatism, arthritis, autoimmune disease, and malignant tumors of the liver, lung, and stomach. Several studies have demonstrated multiple biological activities of the different fractions of OD, including antitumor, chemopreventive, anti-angiogenic, anti-inflammatory, anti-oxidant, and proapoptotic effects (Gupta et al., 2004; Ovesna et al., 2004). It has been shown that the aqueous extract of OD exhibits immunomodulating activity in murine spleen cells and mouse peritoneal macrophages, and it may stimulate the immune system to eliminate tumor cells (Yoshida et al., 1997; Chung et al., 2002). The aqueous extract has also been proven effective in inhibiting the growth of different cancer cell lines and inducing selectively apoptosis in the leukemic cell line HL60 but not human lymphocytes (Sadava et al., 2002; Gupta et al., 2004; Willimott et al., 2007). In addition, ursolic acid, a main component of the methanol extract not found in the aqueous extract of OD, exhibits significant anti-tumor effects in lung, ovary, skin, brain, and colon cancer cells (Bagiin et al., 2003). Moreover, ursolic acid isolated also from *Salvia officinalis* triggers apoptosis and bcl-2 downregulation in MCF-7 breast cancer cells (Kassi et al., 2009). Recently, Wu et al. (2009) have demonstrated that oleanolic acid isolated from OD exhibits growth inhibitory effects against ras-transformed fibroblasts. Both oleanolic acid (3  $\beta$ -hydroxy-olea-12-en-28-oic acid) and its isomer ursolic acid (3  $\beta$ -hydroxy-urs-12-en-28-oic acid) are triterpenoid compounds which exist widely in natural plants like prunes, plums, basil, salvia, rosemary etc., in the form of free acid or aglycones for triterpenoid saponins (Liu, 1995; Aggarwal and Shishodia, 2006).

Herein, we have explored the biological effects of OD extracts and the OD-derived different fractions on normal (MCF-10A) and several tumoral breast cell lines (MCF-7, T47-D, SKBR3, and MCF-7 TRI). We have demonstrated that OD extracts inhibit growth and induce apoptosis selectively in ER $\alpha$ -positive breast cancer cells. This occurs through an ER $\alpha$ /Sp1-mediated activation of the p53 gene. Two compounds, ursolic and oleanolic acids, isolated from OD extracts in our laboratory, are responsible for the OD-induced anticancer activity.

## Materials and Methods

### Preparation of *Oldenlandia diffusa* (OD) extracts

The herbal sample of OD was kindly provided by China Pharmaceutical University of Nanjing (China). The dried whole plant (200 g) of OD was extracted with 70% ethanol at room temperature for 2 days and repeated for three times. The extract was vacuum dried and gave 16.3 g hydro-alcoholic extract.

## Plasmids

The p53 promoter-luciferase reporters (p53-1, -6, and -13), kindly provided by Dr. Stephen H. Safe (Texas A&M University, College Station, TX), were generated from the human p53 gene promoter as follows: p53-1 (containing the -1,800 to +12 region), p53-6 (containing the -106 to +12 region), p53-13 (containing the -106 to -40 region) (Qin et al., 2002). The Sp1 expression vector was from Addgene, Cambridge, MA.

## Cell culture

MCF-10A and MCF-7 cells were cultured in DMEM/F-12 medium supplemented with 5% Horse Serum or 5% Newborn Calf Serum (Eurobio, Les Ullis, Cedex, France), respectively, and 0.1 nmol/L nonessential amino acid, 2 mmol/L L-glutamine, and 50 units/ml penicillin/streptomycin. T47-D and SKBR3 cells were cultured in DMEM (high glucose) and McCoy's 5A medium, respectively, supplemented with 10% fetal bovine serum (FBS) (Eurobio). Tamoxifen-resistant MCF-7 cells were generated as described previously by Knowlden et al. (2003) and Herman and Katzenellenbogen (1996). Briefly, we cultured parental MCF-7 cells in phenol red-containing MEM medium supplemented with 5% FBS, and  $10^{-6}$  M 4-hydroxy-tamoxifen. Cells were continuously exposed to 4-hydroxy-tamoxifen for 6 months during which time the medium was replaced every 4–5 days. Initially cell growth was slow, but gradually increased, at which time the cells were designated MCF-7 TRI. MCF-7 TRI cells were continuously maintained in  $10^{-6}$  M tamoxifen for longer than 1 year.

Subconfluent cell cultures, synchronized for 48 h in DMEM without phenol red and serum (SFM), were used for all experiments.

## Cell proliferation assays

**MTT anchorage-dependent growth assay.** Cell viability was determined by using the 3-(4,5-dimethylthiazol-2-yl)-2,5-diphenyltetrazolium (MTT, Sigma, Milan, Italy) assay. Cells ( $2 \times 10^4$  cells/ml) were plated in 24-well plates and treated as indicated. The MTT assay was performed as the following: 100  $\mu$ l MTT stock solution in PBS (2 mg/ml) was added into each well and incubated at 37°C for 2 h followed by media removal and solubilization in 500  $\mu$ l dimethyl sulphoxide (DMSO). After shaking the plates for 15 min, the absorbance in each well, including the blanks at 570 nm in Beckman Coulter, was measured. A minimum of three experiments, contained three different doses of OD, ursolic, and oleanolic acids in triplicate, was combined for IC<sub>50</sub> calculations. The absorbance readings were used to determine the IC<sub>50</sub> using GraphPad Prism 4 (GraphPad Software). Briefly, values were log-transformed, normalized, and nonlinear regression analysis was used to generate a sigmoidal dose-response curve to calculate IC<sub>50</sub> values.

### Soft agar anchorage-independent growth assays.

Cells ( $10^4$ /well) were plated in 4 ml of 0.35% agarose with 5% charcoal stripped-FBS in phenol red-free media, with a 0.7% agarose base in six-well plates. Two days after plating, media containing vehicle or treatments as indicated were added to the top layer, and replaced every 2 days. After 14 days, 300  $\mu$ l of MTT was added to each well and allowed to incubate at 37°C for 4 h. Plates were then placed at 4°C overnight and colonies >50  $\mu$ m diameter from triplicate assays were counted. The data are representative of three independent experiments, each performed in triplicate.

## Immunoblotting analysis

Total protein lysates were subjected to SDS-PAGE as described (Catalano et al., 2009). Briefly, cells were harvested in cold PBS and resuspended in lysis buffer containing 20 mmol/L HEPES (pH 8), 0.1 mmol/L EGTA, 5 mmol/L MgCl<sub>2</sub>, 0.5 M NaCl, 20% glycerol, 1% Triton, and inhibitors (0.1 mmol/L sodium orthovanadate, 1% phenylmethylsulfonylfluoride, and 20 mg/ml aprotinin). Nuclear extracts were obtained using the buffer containing 20 mM HEPES pH 8, 0.1 mM EDTA, 5 mM MgCl<sub>2</sub>, 0.5 M NaCl, 20% glycerol, 1% NP-40, inhibitors (as above). Equal amounts of protein lysates were

resolved on a 10% SDS–polyacrylamide gel, transferred to a nitrocellulose membrane, and probed with antibodies directed against p53 and p21<sup>WAF1/Cip1</sup>, PARP, Sp1, laminin B, and  $\beta$ -actin (Santa Cruz Biotechnology, Santa Cruz, CA). The antigen–antibody complex was detected by incubation of the membranes for 1 h at room temperature with peroxidase-coupled anti-mouse, anti-rabbit or anti-goat IgG and revealed using the enhanced chemiluminescence system (Amersham Pharmacia, Buckinghamshire, UK). The intensity of bands representing relevant proteins was measured by Scion Image laser densitometry scanning program.

#### Reverse transcription–PCR assays

Cells were grown in 10 cm dishes to 70–80% confluence and exposed to treatments in SFM as indicated. Total cellular RNA was extracted using TRIZOL reagent (Invitrogen, Carlsbad, CA) as suggested by the manufacturer. The purity and integrity were checked spectroscopically and by gel electrophoresis before carrying out the analytical procedures. Two microgram of total RNA were reverse transcribed in a final volume of 20  $\mu$ l using a RETROscript kit as suggested by the manufacturer (Promega, Madison, WI). The cDNAs obtained were amplified by PCR using the following primers: 5'-GTGGAAGGAAATTTGCGTGT-3' (p53 forward) and 5'-CCAGTGTGATGATGGTGAGG-3' (p53 reverse), 5'-GCTTCATGCCAGCTACTTCC-3' (p21 forward) and 5'-CTGTGCTCACTTCAGGGTCA-3' (p21 reverse), 5'-CTCAACATCTCCCCCTTCTC-3' (36B4 forward) and 5'-CAAATCCCATATCCTCGTCC-3' (36B4 reverse) to yield, respectively, products of 190 bp with 18 cycles, 270 bp with 18 cycles, and 408 bp with 12 cycles.

#### Transfection assays

MCF-7 cells were plated into 24-well plates in regular growth medium the day before transfection. The medium was replaced with SFM on the day of transfection, which was performed using the FuGENE 6 (Roche Diagnostic, Indianapolis, IN) reagent as recommended by the manufacturer with the mixture containing 0.5  $\mu$ g/well p53-1, p53-6, and p53-13 plasmids. Twenty-four hours after transfection, the medium was changed and the cells were treated in the presence of vehicle or OD extracts for 24 h with or without 1  $\mu$ M of the pure anti-estrogen ICI 182,780 (Tocris Bioscience, Bristol, UK) and 100 nM of Mithramycin (Tocris Bioscience). Another set of experiments was performed cotransfecting 0.5  $\mu$ g/well p53-1 plasmid and 0.5  $\mu$ g/well Sp1 expression vector. TK Renilla luciferase plasmid (25 ng/well) was used to normalize the efficiency of the transfection. Firefly and Renilla luciferase activities of triplicate samples were measured using a Dual Luciferase kit (Promega).

#### DNA fragmentation

DNA fragmentation was determined as described (Bonfiglio et al., 2009). Briefly, cells were collected and washed with PBS and pelleted at 1,800 rpm for 5 min. The samples were resuspended in 0.5 ml of extraction buffer (50 mmol/L Tris–HCl, pH 8; 10 mmol/L EDTA, 0.5% SDS) for 20 min in rotation at 4°C. DNA was extracted three times with phenol–chloroform and one time with chloroform. The aqueous phase was used to precipitate nucleic acids with 0.1 volumes of 3 M sodium acetate and 2.5 volumes cold ethanol overnight at –20°C. The DNA pellet was resuspended in 15  $\mu$ l H<sub>2</sub>O treated with RNase A for 30 min at 37°C. The extracted DNA was subjected to electrophoresis on 1.5% agarose gels, stained with ethidium bromide and then photographed.

#### Chromatin immunoprecipitation (ChIP) and Re-ChIP assays

MCF-7 cells were treated with 100  $\mu$ g/ml of OD extracts for 3 h and then crosslinked with 1% formaldehyde and sonicated. Supernatants were immunocleared with salmon sperm DNA/protein A-agarose for 1 h at 4°C. The precleared chromatin was

immunoprecipitated with specific anti-Sp1, anti-ER $\alpha$ , or anti-polymerase II antibodies. The anti-Sp1 immunoprecipitated samples were re-immunoprecipitated with an anti-ER $\alpha$  antibody. A normal mouse serum IgG was used as a negative control. Pellets were washed, eluted with elution buffer (1% SDS, 0.1 M NaHCO<sub>3</sub>), and digested with proteinase K. DNA was obtained by phenol/chloroform/isoamyl alcohol extractions and precipitated with ethanol; 5  $\mu$ l of each sample and input were used for real-time PCR. Real-time PCR was performed in the iCycler iQ Detection System (BioRad), using SYBR Green Universal PCR Master Mix (BioRad, Milan, Italy) with the dissociation protocol used for gene amplification. The primers flanking the Sp1 sequence present in the p53 promoter region were the following: 5'-TTCCCCTCCCATGTGCTCAAG-3' and 5'-CCAATCCAGGGAACGTGTCA-3'. Final results were calculated using the DDC<sub>t</sub> method as previously reported (Siriani et al., 2007), using input C<sub>t</sub> values instead of the 18S. The basal sample was used as calibrator.

#### Identification of bioactive fractions of OD

Hydroalcoholic extract (EtOH/H<sub>2</sub>O) of OD was subjected to bioguided fractionation. The powdered whole plant 70% ethanol OD extract (15 g) was dissolved in 500 ml 90% ethanol solution. This solution was subsequently portioned with *n*-hexane, chloroform, ethyl acetate, and *n*-butanol to give 3.92, 4.2, 0.52, and 1.717 g, respectively. Each fraction was re-dissolved in ethanol or DMSO to make the stocking solution for use.

The chloroformic fraction was subjected to column chromatography over silica gel (CH<sub>2</sub>Cl<sub>2</sub>/MeOH 95:5, 90:10, 80:20, 70:30). Column fractions were assayed according to their TLC (thin layer chromatography) profile on silica gel (70–230 mesh, VWR International, Milan, Italy) (CH<sub>2</sub>Cl<sub>2</sub>/MeOH 90:10, 85:15) by detection on UV light at 254 and 365 nm and sulphuric vanillin. A total of 17 fractions were collected.

Fraction 9 was further purified by repeated silica gel column chromatography (CH<sub>2</sub>Cl<sub>2</sub>/MeOH from 98:2 to 30:70) and preparative TLC on silica gel 60 (CH<sub>2</sub>Cl<sub>2</sub>/MeOH 90:10, 80:20), resulting in two compounds, whose structures were elucidated using <sup>1</sup>H and <sup>13</sup>C NMR. <sup>1</sup>H and <sup>13</sup>C NMR were recorded on a Bruker 300 MHz spectrophotometer in deuterio-methanol (Aldrich–Steinheim, Steinheim, Germany).

#### Statistical analysis

Data were analyzed for statistical significance ( $P < 0.05$ ) using a two-tailed Student's Test, performed by Graph Pad Prism 4. Standard deviations (SD) are shown.

## Results

### OD extracts inhibit breast cancer cell growth

First, we aimed to evaluate the effects of increasing concentrations of OD extracts on proliferation of MCF-10A normal breast epithelial cells and ER $\alpha$ -positive MCF-7 breast cancer cells by using MTT assays (Fig. 1A). We observed that OD treatment for 48 h strongly reduced cell viability in MCF-7 cells at all the doses tested (10, 100, 200  $\mu$ g/ml), while OD did not elicit any significant inhibitory effects in MCF-10A cells. The prolonged treatments up to 96 h showed greater antiproliferative responses, with IC<sub>50</sub> values of 53.9  $\mu$ g/ml in MCF-7 cells (Table 1). A second approach we employed was to evaluate the antiproliferative effects mediated by OD extracts using anchorage-independent soft agar growth assays (Fig. 1B). Consistently with MTT assays, OD treatment significantly reduced colony formation in MCF-7 cells. To extend our results we also investigated the effects of OD extracts in affecting growth of ER-positive T47-D and ER-negative SKBR3 breast cancer cell lines (Supplementary Fig. 1). We demonstrated that OD treatment inhibited cell proliferation only in T47-D cells.

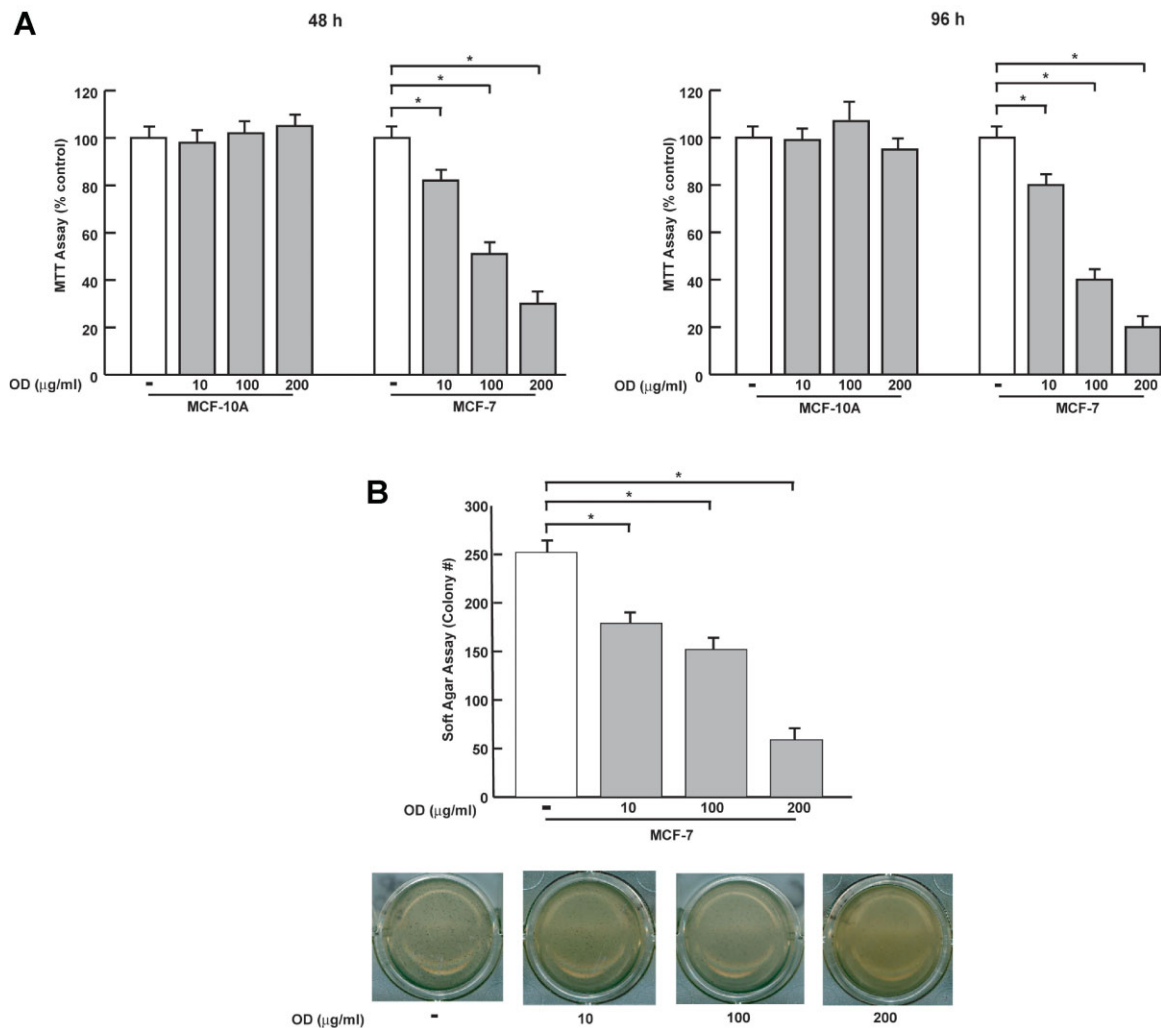


**Fig. 1.** Effects of OD extracts on breast cancer cell growth. **A:** MTT assays in MCF-10A and MCF-7 cells treated with vehicle (–), or OD at 10, 100, and 200  $\mu\text{g/ml}$  of concentrations for 48 or 96 h. Cell proliferation is expressed as % of control (vehicle-treated cells). The values represent the means  $\pm$  SD of three different experiments, each performed with triplicate samples. \* $P < 0.05$ . **B: Upper panel,** MCF-7 cells were plated in soft agar and then treated with vehicle (–) or increasing concentrations of OD (10, 100, and 200  $\mu\text{g/ml}$ ). Cells were allowed to grow for 14 days and the number of colonies  $>50 \mu\text{m}$  were quantified and the results were graphed. Data are the mean colony number  $\pm$  SD of three plates of three independent experiments. \* $P < 0.05$ . **Bottom panel,** a typical well for each condition is shown. [Color figure can be seen in the online version of this article, available at <http://wileyonlinelibrary.com/journal/jcp>]

Taken together, these results showed that OD extracts induced a growth inhibition in ER $\alpha$ -positive breast cancer cells, while no effects were observed in ER $\alpha$ -negative SKBR3 breast cancer cells as well as in normal MCF-10A breast epithelial cells.

#### OD extracts increase p53 and p21<sup>WAF1/Cip1</sup> expression in breast cancer cells

Since the tumor suppressor gene p53 has been mainly implicated in cell growth arrest promoted by different factors,

**TABLE 1.** IC<sub>50</sub> of Oldenlandia diffusa extracts (OD), oleanolic acid (OA) and ursolic acid (UA) in MCF-7 cells from MTT growth assay

Compounds	IC <sub>50</sub> ( $\mu\text{g/ml}$ )	95% CI
OD	53.9	45.5–63.7
OA	6.4	5.6–7.3
UA	7.1	6.1–8.3

IC<sub>50</sub>, half-maximal inhibitory concentration.

we examined the potential ability of OD extracts to modulate the expression of p53 along with its natural target gene p21<sup>WAF1/Cip1</sup>. Cells were treated with OD at 10 and 100  $\mu\text{g/ml}$  concentrations for 48 h and whole cell lysates were then analyzed using immunoblotting analysis. As shown in Figure 2A, we did not find any significant variations in the levels of p53 and p21<sup>WAF1/Cip1</sup> in MCF-10A cells. In contrast, OD treatment increased p53 and p21<sup>WAF1/Cip1</sup> protein expression in MCF-7 cells. In the same experimental conditions, we observed an up-regulation of both p53 and p21<sup>WAF1/Cip1</sup> mRNA levels only in MCF-7 cells after treatment with OD at the higher dose of 100  $\mu\text{g/ml}$  (Fig. 2B).

#### OD extracts transactivate p53 gene promoter via ER $\alpha$ /Sp1

The results we obtained prompted us to investigate whether OD extracts are able to transactivate the p53 promoter gene. Thus, MCF-7 cells were transiently transfected with a luciferase reporter construct (named p53-l) containing the upstream

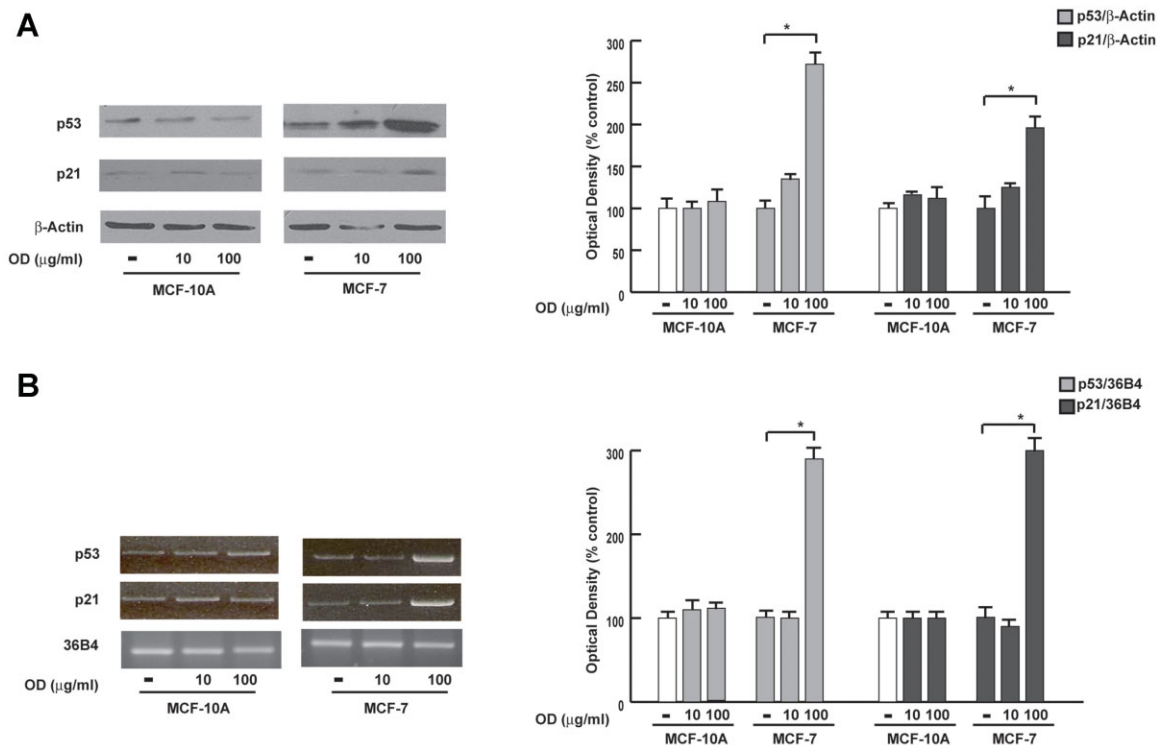


**Fig. 2.** Up-regulation of p53 and p21 expression by OD extracts in breast cancer cells. **A:** Left panel, immunoblots of p53, and p21<sup>WAF1/Cip1</sup> from extracts of MCF-10A and MCF-7 cells treated with vehicle (–) or OD at 10, and 100 µg/ml of concentrations for 48 h. β-Actin was used as control for equal loading and transfer. Right panel, the histograms represent the mean ± SD of three separate experiments in which band intensities were evaluated in terms of optical density arbitrary units and expressed as percentage of control which was assumed to be 100%. \**P* < 0.05. **B:** Left panel, MCF-10A and MCF-7 cells were treated with vehicle (–) or OD (10 or 100 µg/ml) for 48 h. Total RNA was isolated from cells and reverse transcribed. cDNA was subjected to PCR using primers specific for p53, p21<sup>WAF1/Cip1</sup> and 36B4 (internal standard). Right panel, the histograms represent the mean ± SD of three separate experiments in which band intensities were evaluated in terms of optical density arbitrary units and expressed as percentage of control which was assumed to be 100%. \**P* < 0.05.

region of the p53 gene spanning from –1,800 to +12 (Fig. 3A) and treated with increasing concentrations of OD for 24 h. We found a significant dose-dependent activation of p53-l after treatment with OD extracts (Fig. 3B). To identify the region within the p53 promoter responsible for this transactivation, we used deletion constructs containing putative binding sites for CTF-1/YY1, nuclear factor-Y (NF-Y), nuclear factor-κB (NF-κB) and Sp1-like proteins (GC) (Fig. 3A). Using the p53-6 plasmid encoding the region from –106 to +12, the responsiveness to OD extracts was still observed, whereas in the presence of the p53-13 construct encoding the sequence from –106 to –40 we did not detect any increase in p53 luciferase activity (Fig. 3B). Consequently, the region from –40 to +12, which contains the GC-rich/Sp1 motifs, was required for OD-induced transactivation of the p53 promoter. The importance of Sp1 site in p53 promoter modulation was strengthened by the observations that the expression of additional Sp1 protein in MCF-7 cells was able to reproduce the activation of OD extracts in luciferase assay experiments (Fig. 3C). In addition, functional experiments were performed using mithramycin (Mit) that binds to GC boxes and prevents sequential Sp1 binding to its consensus sequence. Luciferase assays revealed that the induction by OD on p53 promoter was significantly reduced after the addition of mithramycin (Fig. 3D), demonstrating that the up-regulatory effects of OD extracts on p53 expression require Sp1 sequence motif.

Several studies have demonstrated that GC-rich binding sites are potential targets for ER-mediated transactivation in different model systems. Thus, we investigated the involvement

of estrogen receptor (ERα) in mediating the stimulatory effects of OD on p53 transactivation. Cells were transiently transfected with the p53-luciferase reporter construct and treated with OD extracts with or without the pure antiestrogen ICI 182,780 (ICI). Remarkably, ICI efficiently antagonized the p53-luciferase activity induced by OD extracts in MCF-7 cells (Fig. 3D).

To better define the involvement of ERα/Sp1 in OD-mediated p53-upregulation at the promoter level, ChIP assays were performed. Using specific antibodies against Sp1, ERα and RNA-polymerase II, protein–chromatin complexes were immunoprecipitated from cells treated with vehicle or OD for 3 h. The resulting precipitated DNA was then quantified using real-time PCR with primers spanning the Sp1-binding element in the p53 promoter region. Sp1 and ERα recruitment was significantly increased upon OD treatment (Fig. 4A,B). Moreover, re-ChIP assay demonstrated that OD extracts induced Sp1/ERα occupancy of the Sp1 containing promoter region (Fig. 4C). These results were well correlated with an enhanced association of RNA-polymerase II to the p53 regulatory region (Fig. 4D).

Our findings confirmed the ability of OD extracts to stimulate the transcription of p53 in an ERα/Sp1-dependent manner.

#### OD extracts induce apoptosis in MCF-7 cells

Since p53 induces apoptotic cascade, acting as a tumor suppressor gene, we then investigated whether OD treatment

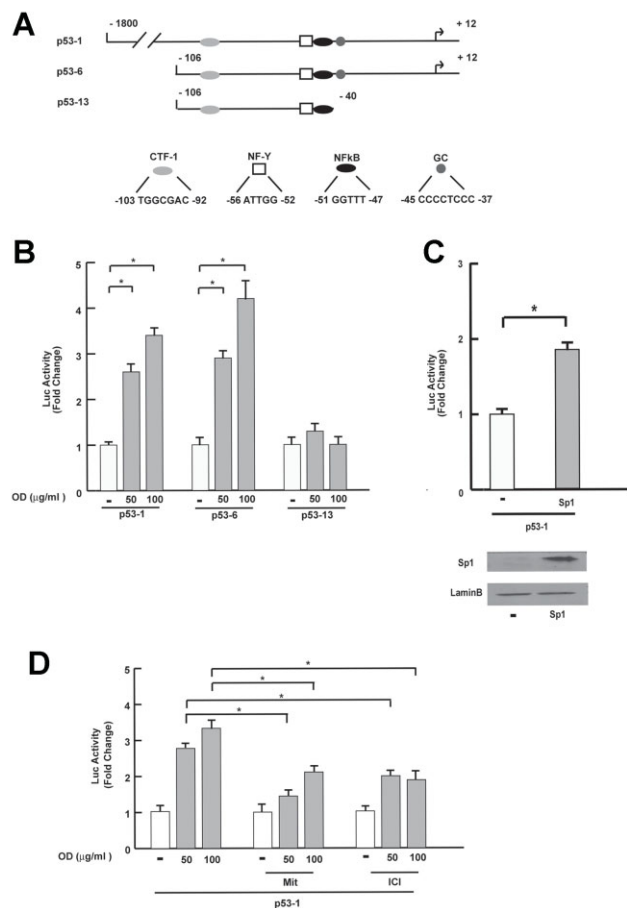


**Fig. 3.** Effects of OD extracts on p53 gene promoter luciferase reporter constructs. **A:** Schematic map of the p53 promoter fragments used in this study. CTF-1, CCAAT-binding transcription factor-1; NF-Y, nuclear factor-Y; NFkB, nuclear factor- $\kappa$ B, GC, GC-rich motif. **B:** MCF-7 cells were transiently transfected with p53 gene promoter luciferase reporter constructs (p53-1, p53-6, p53-13) and treated for 24 h with vehicle (–) or OD at 50, and 100  $\mu$ g/ml of concentrations. **C:** *Upper panel*, MCF-7 cells were transiently transfected with p53 gene promoter luciferase reporter construct p53-1 and Sp1 expression vector for 24 h. *Lower panel*, immunoblots of Sp1 from nuclear extracts of MCF-7 cells transfected with Sp1 expression vector. Lamin B was used as control for equal loading and transfer. **D:** MCF-7 cells were transiently transfected with p53 gene promoter luciferase reporter construct p53-1 and treated for 24 h with vehicle (–) or OD (50 and 100  $\mu$ g/ml) alone or in combination with 100 nM of Mithramycin (Mit) or 1  $\mu$ M of ICI 182,760 (ICI). The luciferase activities were normalized to the Renilla luciferase as internal transfection control and data were reported as fold change. Columns are the means  $\pm$  SD of three independent experiments performed in triplicate. \* $P < 0.05$ .

may induce cell death by apoptosis in our model system, by using two different approaches. First, we evaluated the proteolysis of poly (ADP-ribose) polymerase (PARP), a known substrate of effector caspases, by immunoblotting analysis (Fig. 5A). We found an increase in the levels of the proteolytic form of PARP (86 kDa) in MCF-7 breast cancer cells under OD treatment in a dose-dependent fashion, while PARP-cleavage levels were unchanged in MCF-10A cells. The second approach we employed was to determine whether OD treatment may induce changes in the internucleosomal fragmentation profile of genomic DNA, a diagnostic hallmark of cells undergoing apoptosis (Fig. 5B). Marked DNA fragmentation in MCF-7 cells was evidenced after 48 h exposure with OD. Again, no

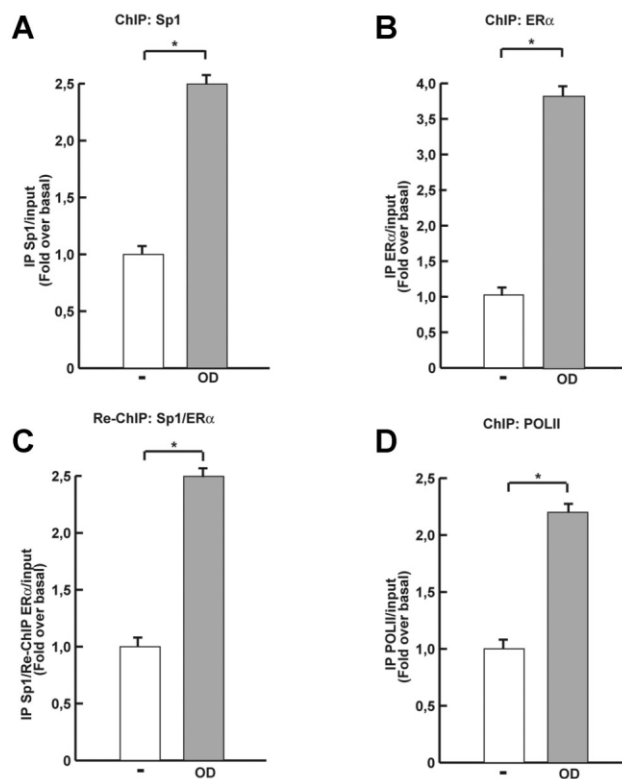


**Fig. 4.** OD extracts enhance ER $\alpha$ /Sp1 recruitment to p53 promoter region. MCF-7 cells were treated with vehicle (–) or OD 100  $\mu$ g/ml for 3 h, then crosslinked with formaldehyde, and lysed. The precleared chromatin was immunoprecipitated with anti-Sp1 (A), anti-ER $\alpha$  (B), and anti-RNA polymerase II (D) antibodies. Chromatin immunoprecipitated with anti-Sp1 antibody was re-immunoprecipitated with anti-ER $\alpha$  antibody (C). A 5  $\mu$ l volume of each sample and input were analyzed by real-time PCR using specific primers to amplify p53 promoter sequence, including the GC-rich motif. Similar results were obtained in multiple independent experiments. \* $P < 0.05$ .

modifications in apoptotic response were observed in the normal breast cell line.

All these data evidenced two separate actions of OD extracts on normal and malignant cells, leading us to investigate the specific bioactive fractions of this herbal medicinal plant responsible for all the described effects.

#### Identification of OD bioactive fractions

The hydroalcoholic extract of OD was submitted at bioguided fractionation and partitioned into four fractions with *n*-hexane (3.9 g), chloroform (4.2 g), ethyl-acetate (0.5 g), and *n*-butanol (1.7 g). The growth inhibitory effects of each of these fractions were then tested on cell proliferation of MCF-10A and MCF-7 cells for 48 h by using MTT assays (Fig. 6A). As expected, growth of MCF-10A cells was not affected by treatment with all of these fractions, confirming our previous results. The *n*-hexane and the *n*-butanol extracts had no effects on breast cancer cell growth. The ethyl-acetate extract induced only a slight growth inhibitory effects, while treatment with 100  $\mu$ g/ml of the chloroform extract resulted in a strong reduction of MCF-7 breast cancer cell proliferation.

Since the chloroformic fraction was the most active fraction we tested, it was subjected to column chromatography over

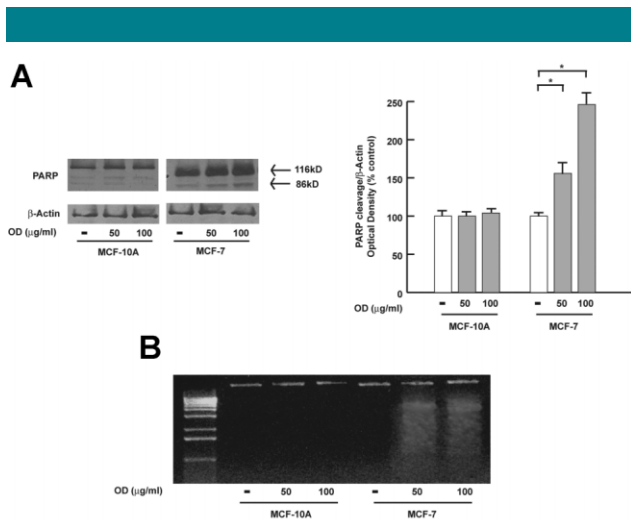


**Fig. 5.** Induction of apoptosis by OD extracts in breast cancer cells. **A:** Left panel, immunoblots of PARP protein from extracts of MCF-10A and MCF-7 cells treated with vehicle (–) or OD at 50 and 100  $\mu\text{g/ml}$  of concentrations for 48 h.  $\beta$ -Actin was used as control for equal loading and transfer. Right panel, the histograms represent the means  $\pm$  SD of three separate experiments in which band intensities were evaluated in terms of optical density arbitrary units and expressed as percentage of control which was assumed to be 100%. \* $P < 0.05$ . **B:** DNA laddering performed in MCF-10A and MCF-7 cells treated with vehicle (–) or OD (50 and 100  $\mu\text{g/ml}$ ) for 48 h. One of three similar experiments is presented.

silica gel and column fractions were then assayed according to their TLC profile on silica gel by detection on UV light at 254 and 365 nm and sulphuric vanillin. Seventeen fractions were collected and subsequently tested on cell survival over a period of 48 h by using MTT assay (data not shown). None of these 17 fractions affected MCF-10A cell proliferation, while only fraction 9 (F.9) had a significant inhibitory growth effect on MCF-7 cells (Fig. 6B).

Further analysis of the fraction 9 by repeated silica gel column chromatography and preparative TLC on silica gel resulted in the isolation of two compounds: oleanolic acid (OA) and ursolic acid (UA) (Fig. 6C).

### Effects of oleanolic and ursolic acids on breast cancer cell survival

Finally, we tested the effects of the two isolated compounds from OD fraction 9 on MCF-7 cell proliferation by using MTT assays (Fig. 7A). MCF-7 cells were treated for 96 h with either OA and UA at the doses of 5, 7.5, and 10  $\mu\text{g/ml}$ . We observed that both pentacyclic triterpenoids inhibited cell survival in a dose-dependent fashion with  $\text{IC}_{50}$  values of 6.4 and 7.1  $\mu\text{g/ml}$  for OA and UA, respectively (Table 1). As expected, no inhibitory effects were detectable in MCF-10A breast cells (data not shown). Moreover, we performed immunoblotting analysis of whole cell lysates treated with either OA or UA to evaluate p53 and p21<sup>WAF1/Cip1</sup> protein levels. As shown in Figure 7B, both OA and UA increased p53 and p21<sup>WAF1/Cip1</sup> protein expression in MCF-7 breast cancer cells.

Of note, the ursolic and oleanolic acids strongly reduced 17- $\beta$  estradiol ( $\text{E}_2$ )-induced breast cancer cell proliferation (Fig. 7C).

Finally, we assessed the capability of OA and UA to affect growth of tamoxifen-resistant malignant breast cells (MCF-7 TR1, Fig. 7D). We observed that tamoxifen (Tam) treatment reduced cell vitality of parental MCF-7 cells and the combined treatment of Tam with both OA and UA did not augment the

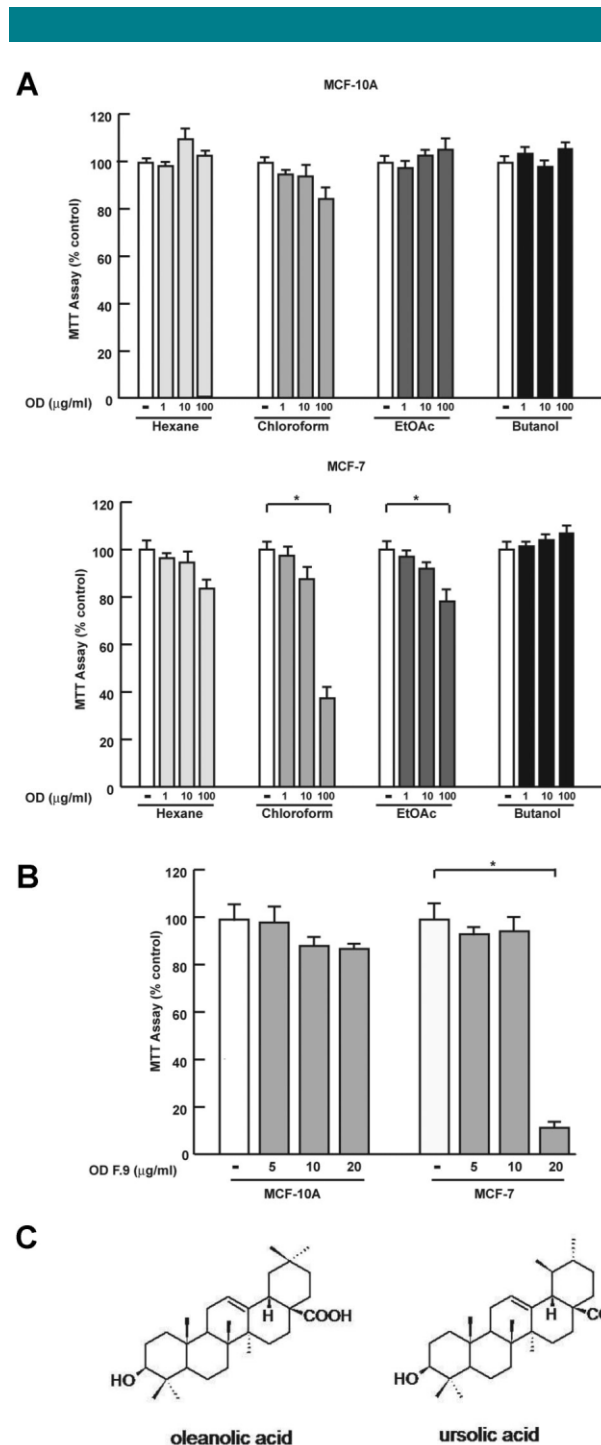


**Fig. 6.** Effects of different OD fractions on breast cancer cell growth. **A:** MTT assays performed in MCF-10A (upper panel) and MCF-7 (lower panel) cells treated with vehicle (–), 1, 10, or 100  $\mu\text{g/ml}$  of four OD fractions with *n*-hexane, chloroform, ethyl acetate (EtOAc) and *n*-butanol for 48 h. **B:** MTT assays performed in MCF-10A and MCF-7 cells treated with vehicle (–) or F.9 chloroformic OD fraction at 5, 10, or 20  $\mu\text{g/ml}$  of concentrations for 48 h. Cell proliferation is expressed as % of control (vehicle-treated cells). The values represent the means  $\pm$  SD of three different experiments, each performed with triplicate samples. \* $P < 0.05$ . **C:** Chemical structures of the two compounds (oleanolic and ursolic acids) obtained from the F.9 chloroformic OD fraction purified by preparative TLC and elucidated using  $^1\text{H}$  and  $^{13}\text{C}$  NMR.

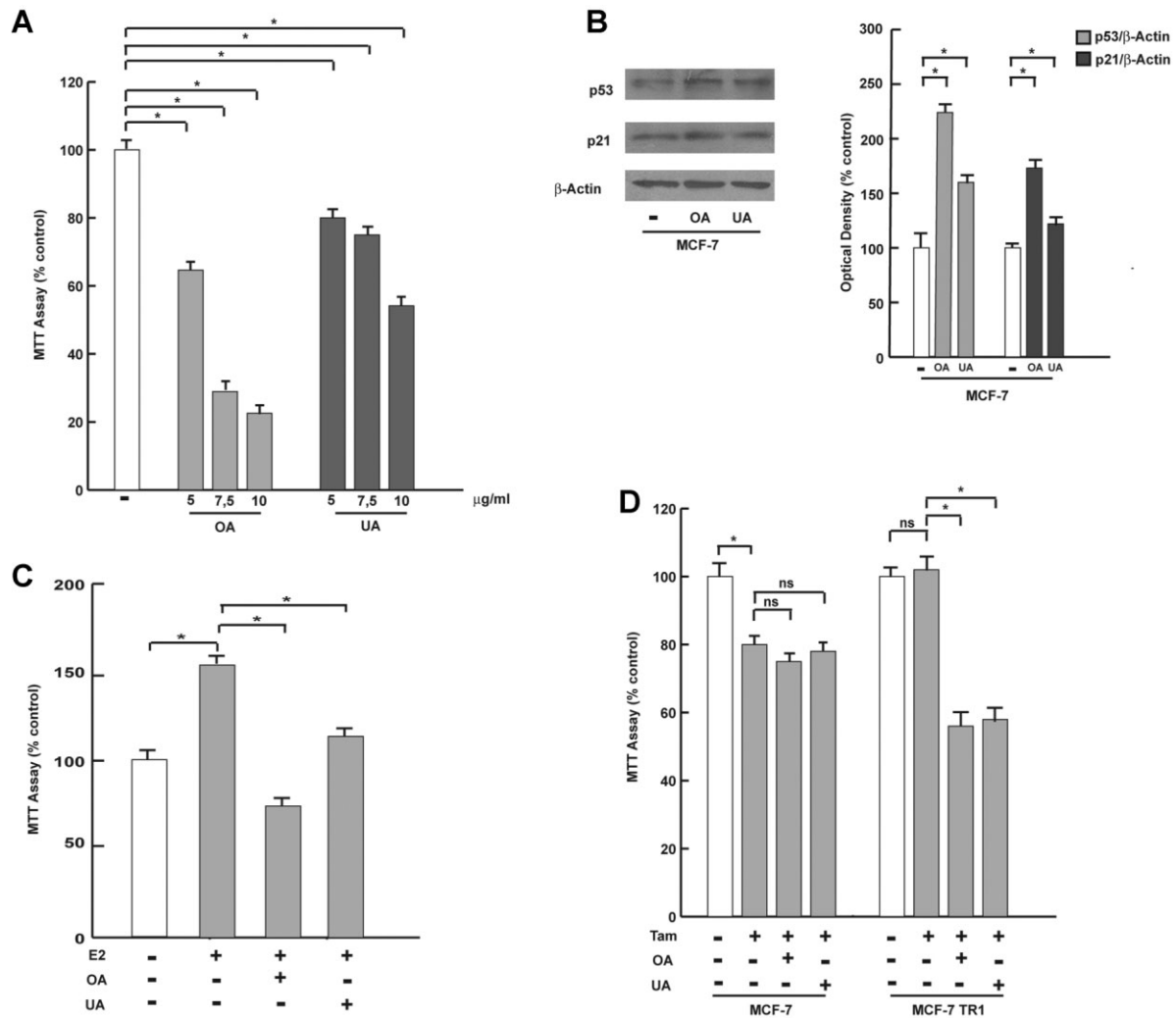


**Fig. 7.** Oleanoic acid (OA) and Ursolic acid (UA) effects on breast cancer cell growth. **A:** MTT assays performed in MCF-7 cells treated with vehicle (-), 5, 7.5, or 10 µg/ml of each compound (OA and UA) for 96 h. Cell proliferation is expressed as % of control (vehicle-treated cells). The values represent the means  $\pm$  SD of three different experiments, each performed with triplicate samples. \* $P < 0.05$ . **B:** Left panel, immunoblots of p53, and p21<sup>WAF1/Cip1</sup> from extracts of MCF-7 cells treated with OA and UA 10 µg/ml for 48 h.  $\beta$ -Actin was used as control for equal loading and transfer. Right panel, the histograms represent the means  $\pm$  SD of three separate experiments in which band intensities were evaluated in terms of optical density arbitrary units and expressed as percentage of control which was assumed to be 100%. \* $P < 0.05$ . **C:** MTT assays performed in MCF-7 cells treated with vehicle (-), 17 $\beta$ -estradiol (E<sub>2</sub> 10 nM) and 10 µg/ml of OA or UA for 48 h. **D:** MTT assays performed in parental MCF-7 cells and its derivatives tamoxifen-resistant MCF-7 TR1 cells treated with vehicle (-), Tamoxifen (Tam, 1 µM) alone or in combination with 10 µg/ml of each compound (OA and UA) for 48 h. Cell proliferation is expressed as % of control (vehicle-treated cells). The values represent the means  $\pm$  SD of three different experiments, each performed with triplicate samples. ns, nonsignificant; \* $P < 0.05$ .

inhibitory effects of Tam alone. As expected, growth of MCF-7 TR1 cells was completely unaffected after Tam exposure, but in the presence of OA and UA cell viability was strongly reduced.

All these results demonstrate that OA and UA compounds effectively inhibit breast cancer cell growth, however, this effect assumes a great importance in tamoxifen-resistant breast cancer cells, since resistance to endocrine therapy still remains a major clinical concern.

## Discussion

In the present study, we have shown that OD extracts exert significant antiproliferative effects and apoptotic responses by inducing p53 gene expression in ER $\alpha$ -positive MCF-7 breast cancer cells.

*Oldenlandia diffusa*, a traditional Chinese medicinal plant, is known for its anticancer activities. Indeed, OD treatment has long been investigated for its effects on tissue culture and animal models, and it has been demonstrated to induce cell cycle arrest in different cancer systems (Sadava et al., 2002; Gupta et al., 2004; Willimott et al., 2007). However, the molecular mechanisms underlying the anticancer activities of this herb need to be better elucidated. Herein, we have shown that OD treatment inhibits anchorage-dependent and -independent cell growth in ER $\alpha$ -positive breast cancer cells in a dose-related manner, whereas it does not affect growth of ER $\alpha$ -negative SKBR3 breast cancer cells as well as normal MCF-10A breast epithelial cells.

It has been reported that induction of apoptosis is one of the mechanisms for the anticancer activities of OD (Gupta et al., 2004; Willimott et al., 2007). Apoptosis occurs as result of the

initiation of a proteolytic cascade mechanism that leads to the irreversible fragmentation of DNA. We have found that OD extracts significantly increase cell apoptosis as evidenced by a marked DNA fragmentation in breast cancer cells. According to these findings, immunoblotting analysis for PARP protein, a crucial target that signals the presence of DNA damage and facilitates DNA repair, reveals an increase in the levels of the proteolytic form of PARP only in MCF-7 breast cancer cells under OD treatment. All these results suggest that the induction of apoptosis may be the main mechanism responsible for the antiproliferative activities exerted by OD extracts in our cell model system.

A large body of evidence has suggested the straightforward role of p53 signaling in the apoptotic cascades (Schuler and Green, 2001; Haupt et al., 2003; Yu and Zhang, 2005). p53 acts as a tumor suppressor depending on its physical and functional interaction with diverse cellular proteins, like some nuclear receptors that, in turn, exert an inhibitory activity on p53 biological outcomes. Activation of p53 by UV damage or other agents/signals results in p53-mediated transcription or up-regulation of genes such as the cyclin-dependent kinase inhibitor p21<sup>WAF1/Cip1</sup> to induce apoptotic process, inhibiting the growth of cells with damaged DNA or cancer cells (Oren et al., 2002; Sengupta and Wasylyk, 2004). Our results provide new insights into the inhibitory action exerted by OD extracts in ER $\alpha$ -positive breast cancer cells. We have shown that OD exposure up-regulates both p53 mRNA and protein levels with a concomitant increase of p21<sup>WAF1/Cip1</sup> expression in MCF-7 cells. Functional studies evidence the ability of OD extracts to up-regulate p53 promoter gene in a dose-dependent manner. Using different deletion mutants of p53 promoter gene, we have found that the OD-mediated p53 transactivation involves the region spanning from -40 to +12, which contains the GC-rich/Sp1 motifs. Moreover, treatment with Mithramycin, a specific inhibitor of Sp1, completely reverses the OD induction on p53 transcriptional activity, confirming that Sp1 sequence motif is essential for the responsiveness to this medicinal herb.

It is well known that ERs can transactivate gene promoters without directly binding to DNA but instead through interaction with other DNA-bound factors in promoter regions lacking TATA box. This has been most extensively investigated in relationship to protein complexes involving Sp1 and ER $\alpha$  at GC boxes, which are classic binding sites for members of the Sp1 family of transcription factors (Krishnan et al., 1994; Porter et al., 1997; Sisci et al., 2010). The role of ER $\alpha$  in inducing OD-mediated transcription of p53 in MCF-7 cells was evidenced by the ability of the pure antiestrogen ICI 182,760 to reverse OD-induced p53 promoter activity. ChIP experiments further demonstrated that OD extracts induce Sp1/ER $\alpha$  occupancy of the Sp1 motif in the p53 promoter region specifying the molecular mechanism by which OD extracts up-regulate p53 expression in ER $\alpha$ -positive breast cancer cells.

Previous phytochemical studies of OD have demonstrated that *Herba oldenlandiae* contains a majority of iridoid glucosides, triterpenoids, flavonoids, and polysaccharides (Liang et al., 2006). In the present study, we have isolated and identified from the most effective chloroformic extract of OD two bioactive compounds able to selectively affect breast cancer cells growth. As elucidated by using <sup>1</sup>H and <sup>13</sup>C NMR these compounds are ursolic (UA) and oleanolic (OA) acids.

UA and OA, present in OD at high abundance, are pentacyclic triterpenoids that exist widely in plants (Liu, 1995; Aggarwal and Shishodia, 2006). OA and UA share a similar chemical structure and the only difference between the two compounds is the position of the methyl group; UA is methylated on C19 while OA is methylated on C20 of the E loop. It has been largely reported that these two pentacyclic triterpenoids have different potency in terms of their

anticancer and chemopreventive activities (Novotny et al., 2001; Li et al., 2002; Cipak et al., 2006; Ikeda et al., 2007; Yeh et al., 2010). Our results evidenced that both pentacyclic triterpenoids can inhibit cell survival of MCF-7 breast cancer cells, and increase p53 and p21<sup>WAF1/Cip1</sup> expression. In addition, OA and UA exert a significant inhibitory effect in tamoxifen-resistant cells, suggesting a potential role for these compounds in breast cancers developing hormone resistance.

In summary, we have demonstrated that OD treatment is effective in inhibiting the growth of ER $\alpha$ -positive and tamoxifen-resistant breast cancer cell lines, while it exhibits no effects in normal epithelial breast cells as well as in ER $\alpha$ -negative SKBR3 breast cancer cells. Furthermore, our results have evidenced ursolic and oleanolic acids, derived from OD extracts, as the bioactive components of the herb in inhibiting ER $\alpha$ -positive breast cancer cell growth.

Understanding the mechanism of action of dietary components such as traditionally used spices and herbs having preventive and therapeutic effects on cancer is one of the main challenges for modern science. Our data emphasize the importance of validating traditional medicinal herbs as new pharmacological tools to be perspective implemented in the adjuvant therapy for breast cancer treatment.

### Acknowledgments

This work was supported by Reintegration AIRC/Marie Curie International Fellowship in Cancer Research to IB, Lilli Funaro Fondation to IB and LG, European Commission/FSE/Regione Calabria to LG, AIRC Grant (IG1482) to SC, DB, and SA. We are grateful to Prof. S. Fuqua (Baylor College of Medicine, Houston, TX) for providing MCF-7 TR1 cells.

### Literature Cited

- Aggarwal BB, Shishodia S. 2006. Molecular targets of dietary agents for prevention and therapy of cancer. *Biochem Pharmacol* 71:1397–1421.
- Baglin I, Mitaine-Offer AC, Nour M, Tan K, Cavé C, Lacaillle-Dubois MA. 2003. A review of natural and modified betulinic, ursolic and echinocystic acid derivatives as potential antitumor and anti-HIV agents. *Mini Rev Med Chem* 3:525–539.
- Barone I, Brusco L, Fuqua SA. 2010. Estrogen receptor mutations and changes in downstream gene expression and signaling. *Clin Cancer Res* 16:2702–2708.
- Bonofiglio D, Cione E, Qi H, Pingitore A, Perri M, Catalano S, Vizza D, Panno ML, Genchi G, Fuqua SA, Andò S. 2009. Combined low doses of PPAR $\gamma$  and RXR ligands trigger an intrinsic apoptotic pathway in human breast cancer cells. *Am J Pathol* 175:1270–1280.
- Catalano S, Giordano C, Rizza P, Gu G, Barone I, Bonofiglio D, Giordano F, Malivindi R, Gaccione D, Lanzino M, De Amicis F, Andò S. 2009. Evidence that leptin through STAT and CREB signaling enhances cyclin D1 expression and promotes human endometrial cancer proliferation. *J Cell Physiol* 218:490–500.
- Chung HS, Jeong HJ, Hong SH, Kim MS, Kim SJ, Song BK, Jeong IS, Lee EJ, Ahn JW, Baek SH, Kim HM. 2002. Induction of nitric oxide synthase by *Oldenlandia diffusa* in mouse peritoneal macrophages. *Biol Pharm Bull* 25:1142–1146.
- Cipak L, Grausova L, Miadokova E, Novotny L, Rauko P. 2006. Dual activity of triterpenoids: Apoptotic versus antidifferentiation effects. *Arch Toxicol* 80:429–435.
- Gupta S, Zhang D, Yi J, Shao J. 2004. Anticancer activities of *Oldenlandia diffusa*. *J Herb Pharmacother* 4:21–33.
- Haupt S, Berger M, Goldberg Z, Haupt Y. 2003. Apoptosis—The p53 network. *J Cell Sci* 116:4077–4085.
- Herman ME, Katzenellenbogen BS. 1996. Response-specific antiestrogen resistance in a newly characterized MCF-7 human breast cancer cell line resulting from long-term exposure to trans-hydroxytamoxifen. *J Steroid Biochem Mol Biol* 59:121–134.
- Ikeda Y, Murakami A, Fujimura Y, Tachibana H, Yamada K, Masuda D, Hirano K, Yamashita S, Ohigashi H. 2007. Aggregated ursolic acid, a natural triterpenoid, induces IL-1 $\beta$  release from murine peritoneal macrophages: Role of CD36. *J Immunol* 178:4854–4864.
- Kassi E, Sourlingas TG, Spiliotaki M, Papoutsis Z, Pratsinis H, Aligiannis N, Moutsatsou P. 2009. Ursolic acid triggers apoptosis and Bcl-2 downregulation in MCF-7 breast cancer cells. *Cancer Invest* 27:723–733.
- Katzenellenbogen BS, Katzenellenbogen JA. 2000. Estrogen receptor transcription and transactivation: Estrogen receptor alpha and estrogen receptor beta: Regulation by selective estrogen receptor modulators and importance in breast cancer. *Breast Cancer Res* 2:335–344.
- Knowlden JM, Hutcheson IR, Jones HE, Madden T, Gee JM, Harper ME, Barrow D, Wakeling AE, Nicholson RI. 2003. Elevated levels of epidermal growth factor receptor/c-erbB2 heterodimers mediate an autocrine growth regulatory pathway in tamoxifen-resistant MCF-7 cells. *Endocrinology* 144:1032–1044.
- Krishnan V, Wang X, Safe S. 1994. Estrogen receptor-Sp1 complexes mediate estrogen-induced cathepsin D gene expression in MCF-7 human breast cancer cells. *J Biol Chem* 269:15912–15917.
- Li J, Guo WJ, Yang QY. 2002. Effects of ursolic acid and oleanolic acid on human colon carcinoma cell line HCT15. *World J Gastroenterol* 8:493–495.

- Liang ZT, Jiang ZH, Leung KS, Zhao ZZ. 2006. Determination of iridoid glucosides for quality assessment of *Herba oldenlandiae* by high-performance liquid chromatography. *Chem Pharm Bull (Tokyo)* 54:1131–1137.
- Liu J. 1995. Pharmacology of oleanolic acid and ursolic acid. *J Ethnopharmacol* 49:57–68.
- Normanno N, Di Maio M, De Maio E, De Luca A, de Matteis A, Giordano A, Perrone F. 2005. Mechanisms of endocrine resistance and novel therapeutic strategies in breast cancer. *Endocr Relat Cancer* 12:721–747.
- Novotny L, Vachalkova A, Biggs D. 2001. Ursolic acid: An anti-tumorigenic and chemopreventive activity. Minireview. *Neoplasma* 48:241–246.
- Oren M, Damalas A, Gottlieb T, Michael D, Taplick J, Leal JF, Maya R, Moas M, Seger R, Taya Y, Ben-Ze'Ev A. 2002. Regulation of p53: Intricate loops and delicate balances. *Ann N Y Acad Sci* 973:374–383.
- Osborne CK, Schiff R. 2005. Estrogen-receptor biology: Continuing progress and therapeutic implications. *J Clin Oncol* 23:1616–1622.
- Ovesna Z, Vachalkova A, Horvathova K, Tothova D. 2004. Pentacyclic triterpenoid acids: New chemoprotective compounds. Minireview. *Neoplasma* 51:327–333.
- Parkin DM, Bray F, Ferlay J, Pisani P. 2005. Global cancer statistics, 2002. *CA Cancer J Clin* 55:74–108.
- Porter W, Saville B, Hoivik D, Safe S. 1997. Functional synergy between the transcription factor Sp1 and the estrogen receptor. *Mol Endocrinol* 11:1569–1580.
- Qin C, Nguyen T, Stewart J, Samudio I, Burghardt R, Safe S. 2002. Estrogen up-regulation of p53 gene expression in MCF-7 breast cancer cells is mediated by calmodulin kinase IV-dependent activation of a nuclear factor kappaB/CCAAT-binding transcription factor-1 complex. *Mol Endocrinol* 16:1793–1809.
- Reddy L, Odhav B, Bhoola KD. 2003. Natural products for cancer prevention: A global perspective. *Pharmacol Ther* 99:1–13.
- Richardson MA, Sanders T, Palmer JL, Greisinger A, Singletary SE. 2000. Complementary/alternative medicine use in a comprehensive cancer center and the implications for oncology. *J Clin Oncol* 18:2505–2514.
- Sadava D, Ahn J, Zhan M, Pang ML, Ding J, Kane SE. 2002. Effects of four Chinese herbal extracts on drug-sensitive and multidrug-resistant small-cell lung carcinoma cells. *Cancer Chemother Pharmacol* 49:261–266.
- Schuler M, Green DR. 2001. Mechanisms of p53-dependent apoptosis. *Biochem Soc Trans* 29:684–688.
- Sengupta S, Wasylyk B. 2004. Physiological and pathological consequences of the interactions of the p53 tumor suppressor with the glucocorticoid, androgen, and estrogen receptors. *Ann N Y Acad Sci* 1024:54–71.
- Sirianni R, Chimento A, Malivindi R, Mazzitelli I, Ando S, Pezzi V. 2007. Insulin-like growth factor-1, regulating aromatase expression through steroidogenic factor 1, supports estrogen-dependent tumor Leydig cell proliferation. *Cancer Res* 67:8368–8377.
- Sisci D, Middea E, Morelli C, Lanzino M, Aquila S, Rizza P, Catalano S, Casaburi I, Maggiolini M, Ando S. 2010. 17beta-estradiol enhances alpha(5) integrin subunit gene expression through ERalpha-Sp1 interaction and reduces cell motility and invasion of ERalpha-positive breast cancer cells. *Breast Cancer Res Treat* 124:63–77.
- Willimott S, Barker J, Jones LA, Opara EI. 2007. Apoptotic effect of *Oldenlandia diffusa* on the leukaemic cell line HL60 and human lymphocytes. *J Ethnopharmacol* 114:290–299.
- Wu PK, Chi Shing Tai W, Liang ZT, Zhao ZZ, Hsiao WL. 2009. Oleanolic acid isolated from *Oldenlandia diffusa* exhibits a unique growth inhibitory effect against ras-transformed fibroblasts. *Life Sci* 85:113–121.
- Yeh CT, Wu CH, Yen GC. 2010. Ursolic acid, a naturally occurring triterpenoid, suppresses migration and invasion of human breast cancer cells by modulating c-Jun N-terminal kinase, Akt and mammalian target of rapamycin signaling. *Mol Nutr Food Res* 54:1285–1295.
- Yoshida Y, Wang MQ, Liu JN, Shan BE, Yamashita U. 1997. Immunomodulating activity of Chinese medicinal herbs and *Oldenlandia diffusa* in particular. *Int J Immunopharmacol* 19:359–370.
- Yu J, Zhang L. 2005. The transcriptional targets of p53 in apoptosis control. *Biochem Biophys Res Commun* 331:851–858.



# Cancer Research

## Leptin Mediates Tumor–Stromal Interactions That Promote the Invasive Growth of Breast Cancer Cells

Ines Barone, Stefania Catalano, Luca Gelsomino, et al.

*Cancer Res* 2012;72:1416-1427. Published OnlineFirst January 26, 2012.

### Updated Version

Access the most recent version of this article at:  
doi:[10.1158/0008-5472.CAN-11-2558](https://doi.org/10.1158/0008-5472.CAN-11-2558)

### Supplementary Material

Access the most recent supplemental material at:  
<http://cancerres.aacrjournals.org/content/suppl/2012/01/26/0008-5472.CAN-11-2558.DC1.html>

### Cited Articles

This article cites 49 articles, 25 of which you can access for free at:  
<http://cancerres.aacrjournals.org/content/72/6/1416.full.html#ref-list-1>

### E-mail alerts

[Sign up to receive free email-alerts](#) related to this article or journal.

### Reprints and Subscriptions

To order reprints of this article or to subscribe to the journal, contact the AACR Publications Department at [pubs@aacr.org](mailto:pubs@aacr.org).

### Permissions

To request permission to re-use all or part of this article, contact the AACR Publications Department at [permissions@aacr.org](mailto:permissions@aacr.org).

## Leptin Mediates Tumor–Stromal Interactions That Promote the Invasive Growth of Breast Cancer Cells

Ines Barone<sup>1,2</sup>, Stefania Catalano<sup>1,3</sup>, Luca Gelsomino<sup>3</sup>, Stefania Marsico<sup>1,3</sup>, Cinzia Giordano<sup>1</sup>, Salvatore Panza<sup>3</sup>, Daniela Bonofiglio<sup>1,3</sup>, Gianluca Bossi<sup>4</sup>, Kyle R. Covington<sup>5</sup>, Suzanne A.W. Fuqua<sup>5</sup>, and Sebastiano Andò<sup>1,2</sup>

### Abstract

Obesity confers risks to cancer development and progression but the mechanisms underlying these risks remain unclear. In this study, we identify a role for the obesity cytokine leptin, which has been implicated previously in breast cancer development, as a determinant for the tumor-promoting activity of cancer-associated fibroblasts (CAF) in both wild-type (WT) and K303R mutant estrogen receptor- $\alpha$  (ER $\alpha$ )-expressing breast cancer cells. Human CAFs stimulated a greater increase in the proliferation and migration of breast cancer cells expressing the K303R-ER $\alpha$  hyperactive receptor than WT-ER $\alpha$ -expressing cells. A concomitant increase was seen in leptin receptor isoform expression and activation of the leptin signaling pathway in cells expressing K303R-ER $\alpha$  compared with WT-ER $\alpha$ , correlating with leptin effects on cell growth, motility, and invasiveness in mutant cells. Epidermal growth factor and other factors secreted by K303R-ER $\alpha$  cells stimulated CAF proliferation, migration, and subsequent leptin secretion. Moreover, K303R-ER $\alpha$  expression generated a leptin hypersensitive phenotype *in vivo*. Together, our results reveal a bidirectional cross-talk between breast cancer cells and "educated" CAFs that drives tumor progression via leptin signaling. In elucidating a mechanism that connects obesity and cancer, these findings reinforce the concept that blocking cancer–stromal cell communication may represent an effective strategy for targeted therapy of breast cancer. *Cancer Res*; 72(6); 1416–27. ©2012 AACR.

### Introduction

For the past 3 decades, cancer research focused predominantly on the characteristics of breast cancer cells. Recently, clinical and experimental studies revealed that both tumor initiation and progression are related to the complex interactions that transpire within the tumor microenvironment. The stromal compartment is composed of mesenchymal cells (fibroblasts, adipocytes, blood cells) and extracellular matrix (ECM; lamin, fibronectin, collagen, proteoglycans, and so on), and signals from these cells come as soluble secreted factors, ECM components, or direct cell–cell contacts. Growth factors, cytokines, adipokines, proteases, and vascular-stimulating factors are involved in stroma-mediated procarcinogenic activities (1–4). The chemokines CXCL12, CXCL14, and CCL7

stimulated tumor cell proliferation and invasion *in vitro* and *in vivo* and increased tumor angiogenesis and macrophage presence at tumor sites (5–7). The interleukins (IL)-1 and -8 induced cancer progression by enhancing metastasis and cachexia (8, 9). As important adipocyte-derived endocrine and paracrine mediator, the adipokine leptin has been correlated with breast cancer occurrence. Indeed, leptin synthesis and plasma levels increase with obesity, a pandemic condition that influences both risk and prognosis of breast cancers (10).

The processes of heterotypic signaling involve a constant bidirectional cross-talk between stromal cells and malignant cells. Stromal cells influence tumor invasiveness and malignancy, whereas at the onset and during breast cancer progression, the microenvironment is reorganized by cancer cells (11). Tumors recruit stromal fibroblasts in a process referred to as the desmoplastic reaction, and these carcinoma-associated fibroblasts (CAF) are reprogrammed to produce growth factors, cytokines, and ECM-remodeling proteins, that acting in autocrine and paracrine fashion support tumor proliferation and invasion into surrounding tissues (4). Moreover, a variety of these factors may activate estrogen receptor- $\alpha$  (ER $\alpha$ ; ref. 12).

Estrogens and its receptor play a crucial role in regulating breast cancer growth and differentiation. Variant forms of ER $\alpha$  due to alternative splicing or gene mutation have been reported, but their clinical significance is still unresolved (13, 14). A naturally occurring mutation at nucleotide 908, introducing a lysine to arginine transition at residue 303 within the hinge domain of the receptor (K303R-ER $\alpha$ ), was identified in one third of premalignant breast hyperplasias and one half of

**Authors' Affiliations:** <sup>1</sup>Centro Sanitario and Departments of <sup>2</sup>Cellular Biology and <sup>3</sup>Pharmacology-Biology, University of Calabria, Rende, Italy; <sup>4</sup>Regina Elena Cancer Institute, Rome, Italy; and <sup>5</sup>Lester and Sue Smith Breast Center and Department of Molecular and Cellular Biology, Baylor College of Medicine, Houston, Texas

**Note:** Supplementary data for this article are available at Cancer Research Online (<http://cancerres.aacrjournals.org/>).

I. Barone and S. Catalano contributed equally to this work.

**Corresponding Author:** Sebastiano Andò, Department of Cellular Biology, Faculty of Pharmacy, Nutritional and Health Sciences, University of Calabria, Via P. Bucci, Arcavacata di Rende (CS) 87036, Italy. Phone: 39-098-449-6201; Fax: 39-098-449-6203; E-mail: [sebastiano.ando@unical.it](mailto:sebastiano.ando@unical.it)

doi: 10.1158/0008-5472.CAN-11-2558

©2012 American Association for Cancer Research.

invasive breast tumors. This mutation correlated with poor outcomes, older age, larger tumor size, and lymph node-positive disease (15, 16). Other studies did not detect the mutation in invasive cancers (17–20), but our studies suggest that the detection method used might be insensitive. However, K303R expression was found at low frequency in invasive breast tumors by Conway and colleagues (21). K303R mutation allows ER $\alpha$  to be more highly phosphorylated by different kinases, and it alters the dynamic recruitment of coactivators and corepressors (22–24). Mutant overexpression in MCF-7 breast cancer cells increased sensitivity to subphysiologic levels of estrogen and decreased tamoxifen responsiveness when elevated growth factor signaling was present (15, 25). K303R-ER $\alpha$  mutation also conferred resistance to the aromatase inhibitor anastrozole (23, 26), suggesting a pivotal role for this mutation in more aggressive breast cancers.

The aim of this study was to elucidate the mechanisms underlying tumor–stroma interaction in ER $\alpha$ -positive breast cancer cells. First, we investigated how tumoral microenvironment pressure, exerted by CAFs, impacts breast cancer cell proliferation, migration, and invasiveness in relation to the expression of wild-type (WT) or the K303R-ER $\alpha$ . We then defined the effect that a single factor leptin has on stroma-mediated breast cancer progression. Finally, we examined the bidirectional interactions between CAFs and breast cancer cells, leading to increased malignancy.

## Materials and Methods

### Reagents and antibodies

The following reagents and antibodies were used: leptin, 17 $\beta$ -estradiol, and epidermal growth factor (EGF) from Sigma; ICI182780 from Tocris Bioscience; AG490, AG1478, PD98059, and LY294002 from Calbiochem; ER $\alpha$ , ER $\beta$ , glyceraldehyde-3-phosphate dehydrogenase (GAPDH), ObRl, ObRs, Ob, Akt, and pAkt<sup>Ser437</sup> antibodies from Santa Cruz Biotechnology; and mitogen-activated protein kinase (MAPK), Janus-activated kinase (JAK)2, STAT3, pMAPK<sup>Thr202/Tyr204</sup>, pJAK2<sup>Tyr1007/1008</sup>, pSTAT3<sup>Tyr705</sup>/pER $\alpha$ <sup>Ser118</sup>, and pER $\alpha$ <sup>Ser167</sup> from Cell Signaling Technology.

### Plasmids

Generation of yellow fluorescent protein (YFP)-tagged expression constructs, YFP-WT and YFP-K303R-ER $\alpha$ , was done as described in the work of Cui and colleagues (22). XETL plasmid, containing an estrogen-responsive element, was provided by Dr. Picard, University of Geneva, Geneva, Switzerland.

### Cell culture

MCF-7 and SKBR3 cells were acquired in 2010 from American Type Culture Collection where they were authenticated, stored according to supplier's instructions, and used within 4 months after frozen aliquots resuscitations. YFP-WT and YFP-K303R-ER $\alpha$  stably expressing MCF-7 cells, MCF-7 and SKBR3 pools stably transfected with YFP-WT and YFP-K303R-ER $\alpha$  were generated as described earlier (23, 26). Immortalized normal human foreskin fibroblasts BJ1-hTERT were provided

by Dr Lisanti, Jefferson University, Philadelphia, PA. Every 4 months, cells were authenticated by single tandem repeat analysis at our Sequencing Core; morphology, doubling times, estrogen sensitivity, and mycoplasma negativity were tested (MycoAlert, Lonza).

### CAF isolation

Human breast cancer specimens were collected in 2011 from primary tumors of patients who signed informed consent. Following tumor excision, small pieces were digested (500 IU collagenase in Hank's balanced salt solution; Sigma; 37°C for 2 hours). After differential centrifugation (90  $\times$  *g* for 2 minutes), the supernatant containing CAFs was centrifuged (500  $\times$  *g* for 8 minutes), resuspended, and cultured in RPMI-1640 medium supplemented with 15% FBS and antibiotics. CAFs between 4 and 10 passages were used, tested by mycoplasma presence, and authenticated by morphology and fibroblast activation protein (FAP) expression.

### Conditioned medium systems

CAF were incubated with regular full media (48–72 hours). Conditioned media were collected, centrifuged to remove cellular debris, and used in respective experiments. Alternatively, conditioned media were collected from WT- and K303R-ER $\alpha$ -expressing MCF-7 cells incubated in 5% charcoal-stripped FBS (72 hours).

### Expression microarray analysis

Expression profiles were determined with Affymetrix GeneChip Human Genome U133 plus 2.0 arrays. Data quality and statistical analyses were conducted as described in the work of Barone and colleagues (23). Microarray study followed MIAME (Minimum Information About a Microarray Experiment) guidelines. All data are available in our previous publication (23).

### Immunoblot analysis

Protein extracts were subjected to SDS-PAGE as described (27). Immunoblots show a single representative of 3 separate experiments.

### Immunofluorescence

Cells were fixed with 4% paraformaldehyde, permeabilized with PBS + 0.2% Triton X-100 followed by blocking with 5% bovine serum albumin (1 hour at room temperature), and incubated with anti-ObR antibody (4°C, overnight) and with fluorescein isothiocyanate-conjugated secondary antibody (30 minutes at room temperature). IgG primary antibody was used as negative control. 4',6-Diamidino-2-phenylindole (DAPI; Sigma) staining was used for nuclei detection. Fluorescence was photographed with OLYMPUS BX51 microscope, 100 $\times$  objective.

### Reverse transcription and real-time reverse transcriptase PCR assays

The gene expression of FAP, Ob, cyclin D1, pS2, cathepsin D, and 36B4 was evaluated by reverse transcription PCR (RT-PCR) method as described in the work of Catalano and

colleagues (27). The gene expression of ObRl, ObRs, CXCR4, insulin receptor (IR), IL-2RB, IL-6R, EGF receptor (EGFR), insulin-like growth factor-1 receptor (IGF1R), fibroblast growth factor receptor 3 (FGFR3), ER $\alpha$ , EGF, IL-6, and insulin was assessed by real-time RT-PCR, using SYBR Green Universal PCR Master Mix (Bio-Rad). Each sample was normalized on 18S mRNA content. Relative gene expression levels were calculated as described (28). Primers are listed in Supplementary Table S1.

#### ER $\alpha$ transactivation assays

ER $\alpha$  transactivation assays were conducted as described in the work of Catalano and colleagues (29).

#### Cell proliferation assays

**MTT assays.** After 4 days of treatments, cell proliferation was assessed by MTT (Sigma) and expressed as fold change relative to vehicle-treated cells.

**Trypan blue cell count assays.** After 4 days of treatment, cell numbers were evaluated by trypsin suspension of samples followed by microscopic evaluation using a hemocytometer.

**Soft agar growth assays.** Anchorage-independent growth assays were conducted as described in the work of Barone and colleagues (26).

Data represent 3 independent experiments carried out in triplicate.

#### Wound-healing scratch assays

Cell monolayers were scraped and treated as indicated. Wound closure was monitored over 24 hours; cells were fixed and stained with Coomassie brilliant blue. Images represent 1 of 3 independent experiments (10 $\times$  magnification, phase contrast microscopy).

#### Transmigration assays

Cells treated with or without leptin were placed in the upper compartments of Boyden chamber (8- $\mu$ m membranes; Corning Costar). Bottom well contained regular full media. After 24 hours, migrated cells were fixed and stained with Coomassie brilliant blue. Migration was quantified by viewing 5 separate fields per membrane at 20 $\times$  magnification and expressed as the mean number of migrated cells. Data represent 3 independent experiments, assayed in triplicate.

#### Invasion assays

Matrigel-based invasion assay was conducted in invasion chambers (8- $\mu$ m membranes) coated with Matrigel (BD Biosciences; 0.4  $\mu$ g/mL). Cells treated with or without leptin were seeded into top Transwell chambers, whereas regular full medium was used as chemoattractant in lower chambers. After 24 hours, invaded cells were evaluated as described for transmigration assays. Data represent 3 independent experiments, assayed in triplicate.

#### Tumor xenografts

*In vivo* studies were conducted as described in the work of Mauro and colleagues (30).

#### Leptin measurement by radioimmunoassay

Leptin was measured by a competitive in-house immunoassay (Chematil) following manufacturer's protocol. Results are presented as nanograms per cell.

#### Leptin-immunodepleted conditioned media

Protein G-agarose beads were incubated with anti-leptin or IgG antibodies. Antibody-beads complexes were incubated with CAF conditioned media and centrifuged. Leptin immunodepletion was verified by radioimmunoassay (RIA).

#### Statistical analysis

Data were analyzed for statistical significance with 2-tailed Student *t* test using GraphPad Prism 4. SDs are shown. Survival curves were computed by Kaplan–Meier method and compared using 2-sided log-rank tests.

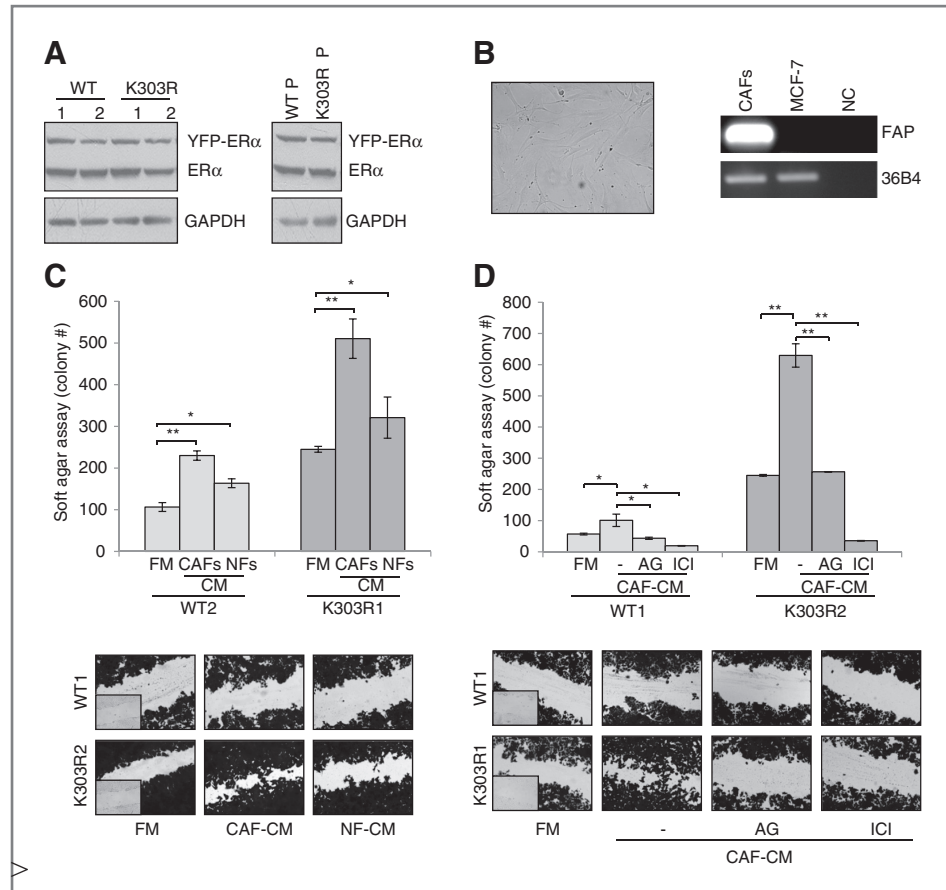
## Results

### Tumor–stroma interactions stimulate cell proliferation and motility

Epithelial–stromal interactions support tumor cell proliferation and invasion. Thus, we first investigated the role of tumoral microenvironment in influencing breast cancer phenotype in relation to the expression of WT- or K303R-ER $\alpha$  mutant receptor.

We used ER $\alpha$ -positive MCF-7 cells stably transfected with YFP-WT or YFP-K303R-ER $\alpha$  expression vectors as experimental models for breast cancer. We chose this approach because wild-type receptor was present along with K303R-ER $\alpha$  in invasive breast tumors (16). Stable clones were screened for ER $\alpha$  expression using immunoblot analysis (Fig. 1A). Two clones stably expressing YFP-WT (WT1-2) or YFP-K303R-ER $\alpha$  (K303R1-2) are shown along with wild-type or mutant receptor stable pools (WT P and K303R P). As stromal cells, we used CAFs isolated from biopsies of primary breast tumors. CAFs possessed the basic fibroblast characteristics with long and spindle-shaped morphology and highly expressed the FAP (Fig. 1B). To create *in vitro* conditions that can mimic the complex *in vivo* microenvironment, we used coculture experiments. Breast cancer cells were incubated with regular full media, CAF-derived conditioned media, or normal fibroblasts conditioned media, and growth was evaluated by soft agar assays (Fig. 1C). As previously shown (23, 26), control basal growth of mutant-expressing cells was elevated compared with wild-type-expressing cells. CAF-derived conditioned media significantly increased colony numbers in both WT- and K303R-ER $\alpha$ -expressing cells; however, CAF-derived conditioned media enhanced K303R-expressing cell growth at a higher extent than wild-type-expressing cells. We then examined the ability of CAF-derived conditioned media to promote WT- and K303R-expressing cell movement in wound-healing scratch assays (Fig. 1C). The mutant cells moved the farthest in either direction to close the gap compared with wild-type-expressing cells. CAF-derived conditioned media promoted net movement of wild-type-expressing cells compared with full media, but K303R-expressing cells exposed to CAF-derived conditioned media moved at higher rate to close the

**Figure 1.** CAF-induced breast cancer cell growth and motility. A, immunoblotting for ER $\alpha$  expression in YFP-WT and YFP-K303R-ER $\alpha$  stably expressing MCF-7 cells and WT P and K303R P stable pools. GAPDH (glyceraldehyde-3-phosphate dehydrogenase) was used as a loading control. B, CAF morphology in monolayer growth using phase contrast microscopy. RT-PCR for FAP and 36B4 (internal standard). NC, negative control. C, soft agar and scratch assays in cells treated with regular full media (FM), CAF-derived conditioned media (CAF-CM), or normal fibroblasts-derived conditioned media (NF-CM). D, soft agar and scratch assays in cells treated with FM, CAF-CM with or without AG490 (AG, 10  $\mu$ mol/L) or ICI182760 (ICI, 1  $\mu$ mol/L). \*,  $P < 0.05$ ; \*\*,  $P < 0.005$ . Small squares, time 0.



gap in the cell bed. As expected, CAFs possessed a higher ability to enhance both proliferation and motility of breast cancer cells than normal fibroblasts (Fig. 1C). CAF-derived conditioned media-induced cell growth and migratory potential was blocked by inhibition of the classic cytokine JAK2/STAT3 signaling cascade (AG490) and the ER $\alpha$  signaling inhibitor (ICI182780), although to a higher extent in K303R clones (Fig. 1D). All functional effects described so far are the results of exposure to the total complement of CAF-secreted proteins. However, it is desirable, albeit experimentally difficult, to define the contribution of a single factor. Thus, we addressed which CAF-secreted factor may promote breast cancer cell growth and motility.

#### Gene transcription patterns of WT- and K303R-ER $\alpha$ -overexpressing cells

Diffusible growth factors, interleukins, chemokines, and adipokines implicated as mediators of stromal-epithelial interactions are involved in breast carcinoma initiation and progression. To determine changes in gene expression for the different receptors of CAF-secreted factors that may be responsible for the different sensitivity of wild-type and mutant clones to CAF-derived conditioned media exposure, we conducted microarray analysis. Gene expression profile comparing RNA isolated from K303R-expressing with WT-expressing cells are shown in Table 1 and Supplementary Table S2. K303R-ER $\alpha$

expression induced several genes potentially involved into tumor-stroma interactions; however, the leptin receptor (ObR) gene was the most highly induced (2.4-fold; Table 1). We also observed increased expression of different leptin signaling downstream effectors such as JAK2, the transcription factors fos, and STAT, as well as the suppressor of cytokine signaling 3 (Supplementary Table S3). To validate the microarray study, YFP-WT and YFP-K303R-ER $\alpha$ -expressing cells were evaluated for a panel of genes using real-time PCR (Fig. 2A). K303R-associated induction could be confirmed for all of them, and again, the gene encoding the long and short leptin receptor isoforms (ObRl/ObRs) was the most highly upregulated in mutant-expressing cells. However, we did not detect any differences in IGF1R mRNA expression levels between the 2 cells, although microarray analysis showed a significant decrease of IGF1R. ER $\alpha$  RNA levels were similar between WT- and K303R-ER $\alpha$ -expressing cells.

The increase in both ObRl and ObRs was then confirmed by evaluating protein levels using immunoblotting (Fig. 2B) and immunofluorescent staining of WT- and K303R-ER $\alpha$ -expressing cells (Fig. 2C, red).

#### K303R-ER $\alpha$ -overexpressing cells exhibit increased leptin signaling activation

Given the gene expression profile identified in the microarray study, we defined the impact that a single factor leptin

**Table 1.** Gene expression profile of the different receptors of CAF-secreted factors among WT- and K303R-ER $\alpha$ -expressing MCF-7 breast cancer cells

Gene name	Gene symbol	Parametric <i>P</i>	Fold change in K303R clones
Leptin receptor	<i>ObR/LepR</i>	<1e-07	2.4
Interleukin 28 receptor $\alpha$	<i>IL28RA</i>	<1e-07	1.9
Chemokine (C-X-C motif) receptor 4	<i>CXCR4</i>	<1e-07	1.9
Insulin receptor	<i>IR</i>	1.7e-06	1.68
Interleukin 17 receptor C	<i>IL17RC</i>	7e-07	1.6
Insulin-like growth factor 2 receptor	<i>IGF2R</i>	1e-07	1.57
Interleukin 15 receptor $\alpha$	<i>IL15RA</i>	3e-07	1.5
Macrophage stimulating receptor 1	<i>MSR1</i>	9.2e-06	1.44
Hepatocyte growth factor receptor	<i>MET</i>	1.69e-05	1.39
Interleukin 1 receptor, type I	<i>IL1R1</i>	0.0004	1.38
Chemokine (C-C motif) receptor 7	<i>CCR7</i>	0.0001	1.3
Chemokine (C-X3-C motif) receptor 1	<i>CX3CR1</i>	7.9e-05	1.32
Interleukin 2 receptor $\beta$	<i>IL2RB</i>	3.57e-05	1.25
Interleukin 9 receptor	<i>IL9R</i>	0.0002	1.23
Interleukin 10 receptor $\beta$	<i>IL10RB</i>	0.0003	1.21
Interleukin 6 receptor	<i>IL6R</i>	0.01	1.2
Interleukin 21 receptor	<i>IL21R</i>	0.0006	0.8
Interleukin 4 receptor	<i>IL4R</i>	0.0007	0.7
Epidermal growth factor receptor	<i>EGFR</i>	7.6e-06	0.7
Insulin-like growth factor 1 receptor	<i>IGF1R</i>	0.0006	0.7
Fibroblast growth factor receptor 3	<i>FGFR3</i>	0.0005	0.7

NOTE: Representative probe sets from pathway analysis showing gene expression changes in the receptor family of CAF-secreted factors along with the *P* value and the fold change of K303R-expressing cells compared with wild-type cells studied by microarray analysis. In cases in which the same genes were deemed significant across multiple probe sets, only one is shown.

may have on K303R-ER $\alpha$  breast cancer cell progression. First, time course–response studies were conducted to analyze phosphorylation of leptin downstream effectors using immunoblot analysis (Fig. 2D). WT-expressing cells exhibited low basal levels of phosphorylated JAK2, STAT3, Akt, and MAPK that were increased in a time-dependent manner after leptin treatment. In contrast, K303R-expressing cells showed elevated constitutive phosphorylation of these signaling molecules in control vehicle conditions, that was slightly increased after leptin treatment. Thus, the mutant ER $\alpha$  expression was associated with increased leptin signaling activation.

Leptin directly activates ER $\alpha$  in the absence of its own ligand in MCF-7 breast cancer cells (29). As a consequence of the enhanced leptin signaling, we found increased ER $\alpha$  transcriptional activity and upregulated mRNA levels of the classical ER $\alpha$  target genes cyclin D1, pS2, and cathepsin D in both control and leptin-treated conditions in K303R-ER $\alpha$ -expressing cells. In addition, the mutant exhibited elevated pS118 and pS167 YFP-K303R-ER $\alpha$  levels (Supplementary Fig. S1).

#### K303R-ER $\alpha$ mutation and leptin hypersensitivity

We next used these stably transfected clones as model systems to study leptin sensitivity, in relation to mutant receptor expression. First, we evaluated leptin effects on growth using anchorage-dependent growth assays (Supple-

mentary Fig. S2). As expected, in both WT- and K303R-expressing cells, treatment with leptin (100 ng/mL) increased cell proliferation. However, low leptin treatment (10 ng/mL) significantly enhanced cell viability only in K303R-expressing clones. We also evaluated leptin-mediated proliferative effects in anchorage-independent growth assays (Fig. 3A). Leptin treatments at 100 and 1,000 ng/mL concentrations enhanced colony numbers in all 4 clones tested, although to a higher extent in mutant-expressing cells. Again, leptin at 10 ng/mL increased anchorage-independent growth only in K303R cells. The increase in colony numbers induced by leptin was reversed by the JAK2/STAT3 inhibitor AG490 (Fig. 3B). We also used the antiestrogen ICI182780 and found that this treatment suppressed anchorage-independent growth of both cell lines, indicating that ER expression remains important in growth regulation of these cells (Fig. 3B).

We next evaluated the ability of increasing doses of leptin to influence cell migration in wound-healing scratch assays (Fig. 3C). Again, the mutant cells moved the farthest in either direction to close the gap compared with WT-expressing cells. Leptin treatments at 100 and 1,000 ng/mL promoted cell motility in both WT- and K303R-expressing cells, although to a higher extent in mutant cells. Interestingly, leptin at 10 ng/mL stimulated migration only in K303R-expressing cells. Then, the capacity of cells to migrate across uncoated membrane in

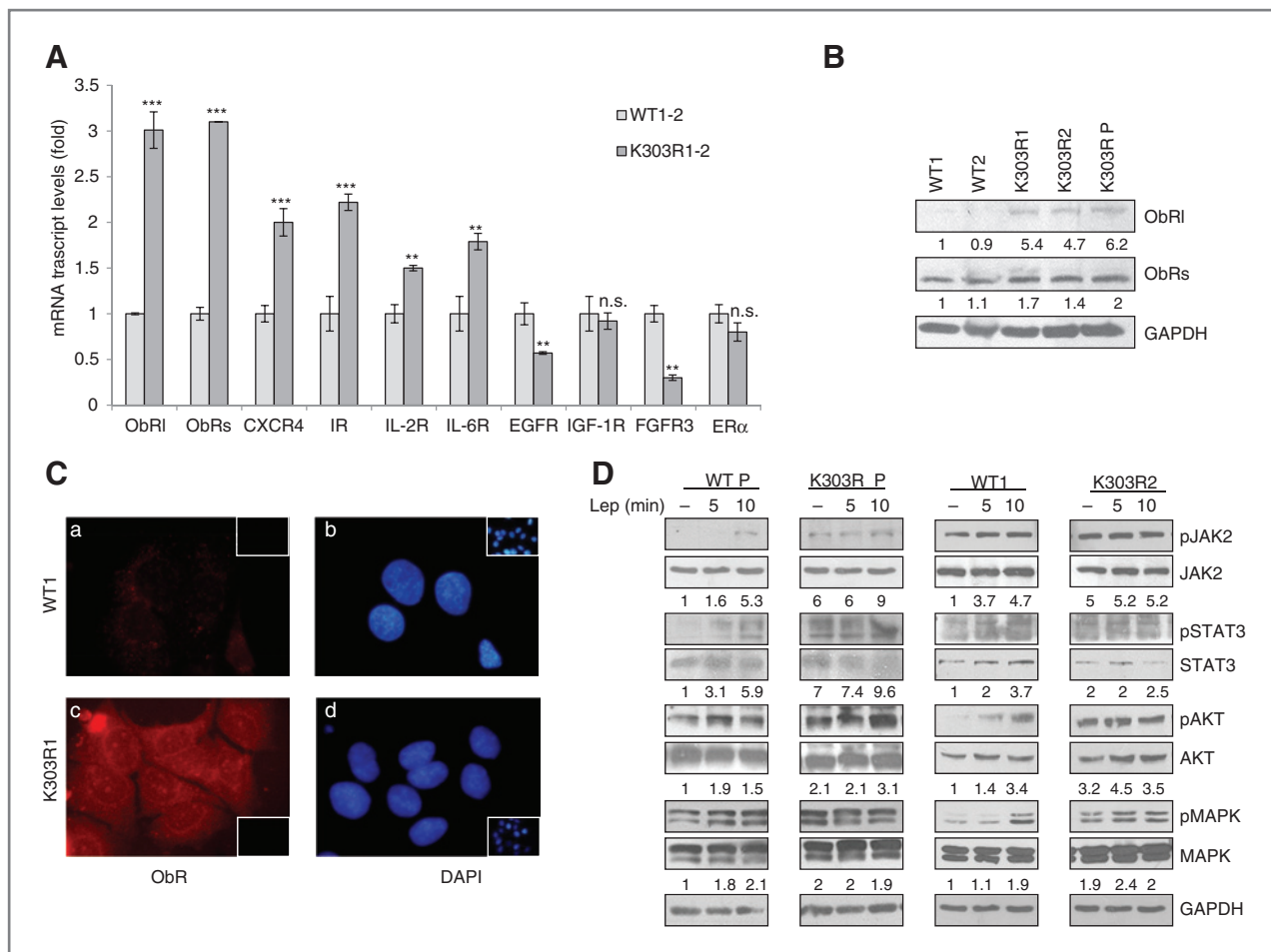


**Figure 2.** Leptin signaling activation in mutant cells. A, real-time RT-PCR for different receptors of CAF-secreted factors. n.s., nonsignificant; \*\*,  $P < 0.01$ ; \*\*\*,  $P < 0.005$ . B, immunoblotting showing leptin receptor long and short isoforms (ObRl/ObRs). GAPDH, loading control. Numbers represent the average fold change in ObRl and GAPDH and ObRs and GAPDH levels. C, immunofluorescence of ObR (a and c) and DAPI (b and d). Small squares, negative controls. D, immunoblotting of phosphorylated pJAK2/pSTAT3/pAKT/pMAPK and total proteins from cells treated with vehicle (–) or leptin (Lep; 100 ng/mL, 5 and 10 minutes). GAPDH, loading control. Numbers represent the average fold change between phospho-, total, and GAPDH levels. GAPDH, glyceraldehyde-3-phosphate dehydrogenase.

transmigration assays or to invade an artificial basement membrane Matrigel in invasion assays was tested in the presence of leptin (Fig. 3D). Although wild-type cells exhibited little motile and no invasive behavior *in vitro*, our data clearly showed that mutant receptor expression increased both motility and invasion of cells. High doses of leptin increased the number of migrated and invaded cells in both clones and again low doses of leptin stimulated motility and invasion only of cells expressing the K303R receptor. As expected, treatment with AG490 and ICI182780 resulted in a clear reduction of both control-untreated and leptin-induced cell motility in wound-healing scratch assays, especially in K303R-expressing cells (Fig. 3E). We recently published that K303R-ER $\alpha$  MCF-7 xenograft tumors grew faster than WT-ER $\alpha$  tumors (26). In addition, MCF-7 xenograft tumors doubled control value after 13 weeks of leptin exposure (30). Thus, we determined whether the mutant receptor-expressing breast cancer cells might exhibit an increased sensitivity to leptin stimulation also *in vivo*. We found that in mice treated with leptin, all xenografts derived

from cells with K303R-ER $\alpha$  expression doubled in size within 6 weeks of treatment, whereas none of xenografts from WT-ER $\alpha$ -expressing cells doubled in size during this experiment (Fig. 3F). Thus, expression of the mutant generated a leptin hypersensitive phenotype *in vitro* and *in vivo*.

#### Leptin is responsible for CAF-induced cell growth and motility

We next assessed the role of leptin in the context of heterotypic signaling working in tumor–stroma interactions. First, RIA measurement in CAF-derived conditioned media showed that leptin secretion varied from  $10 \pm 4.5$  ng per 200,000 cells. RT-PCR evidenced Ob mRNA expression in CAFs; CAFs also expressed ObR long isoform, but they did not express ObR short isoform, ER $\alpha$ , or ER $\beta$  (Supplementary Fig. S3). Leptin was then immunodepleted from CAF-derived conditioned media by leptin-specific antibodies, and resulting media were tested for the ability to induce anchorage-independent growth and migration of breast cancer cells. Leptin depletion (conditioned media +

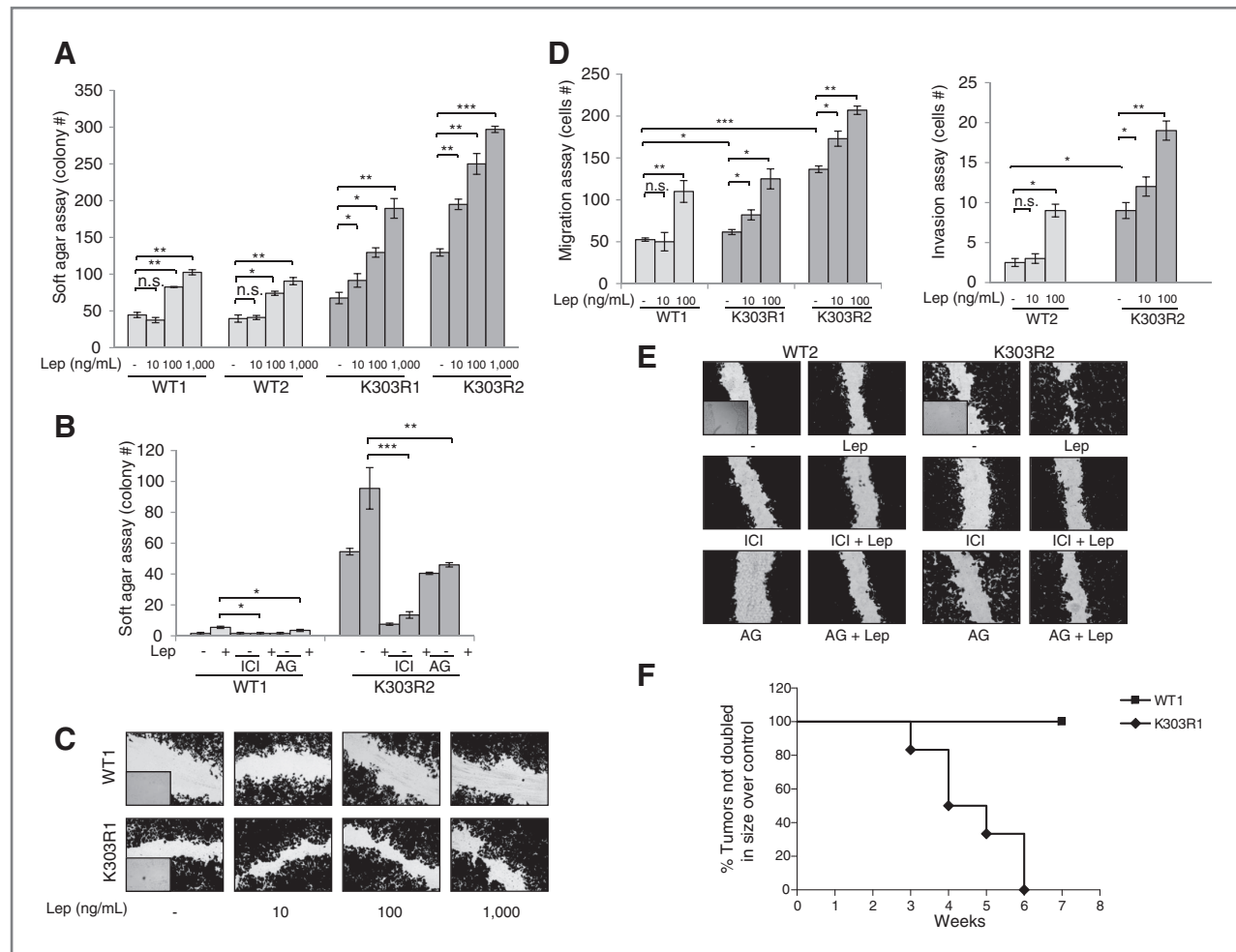


**Figure 3.** The K303R-ER $\alpha$  mutation generates a leptin hypersensitive phenotype. **A**, soft agar assay in cells treated with vehicle (–) or leptin (Lep; 10, 100, and 1,000 ng/mL). **B**, soft agar assay in cells treated with vehicle (–) or leptin (Lep; 100 ng/mL), with or without ICI182760 (ICI, 1  $\mu$ mol/L) or AG490 (AG, 10  $\mu$ mol/L). **C**, scratch assay in cells treated with vehicle (–) or 100 ng/mL leptin, with or without ICI182760 or AG490. **D**, WT- and K303R-ER $\alpha$ -expressing cells were injected into mice ( $n = 6$  per group) supplemented with E<sub>2</sub> (0.72 mg per pellet per 90-day release) and 230  $\mu$ g/kg leptin or vehicle (control). Survival curves [shown as percentage (%) of mice in which tumors had not doubled in size] are graphed as the time in weeks from treatment to a 2-fold increase in total tumor volume over baseline (time to tumor doubling).

LepAb) significantly decreased growth- and migration-promoting activities of CAF-derived conditioned media, particularly in K303R-expressing cells (Fig. 4A). Conditioned media treated with a nonspecific mouse IgG had no effects, suggesting that the neutralizing effects of leptin antibodies were specific. Our results identify leptin as a main molecular player that mediates CAF effects on tumor cell growth and migration.

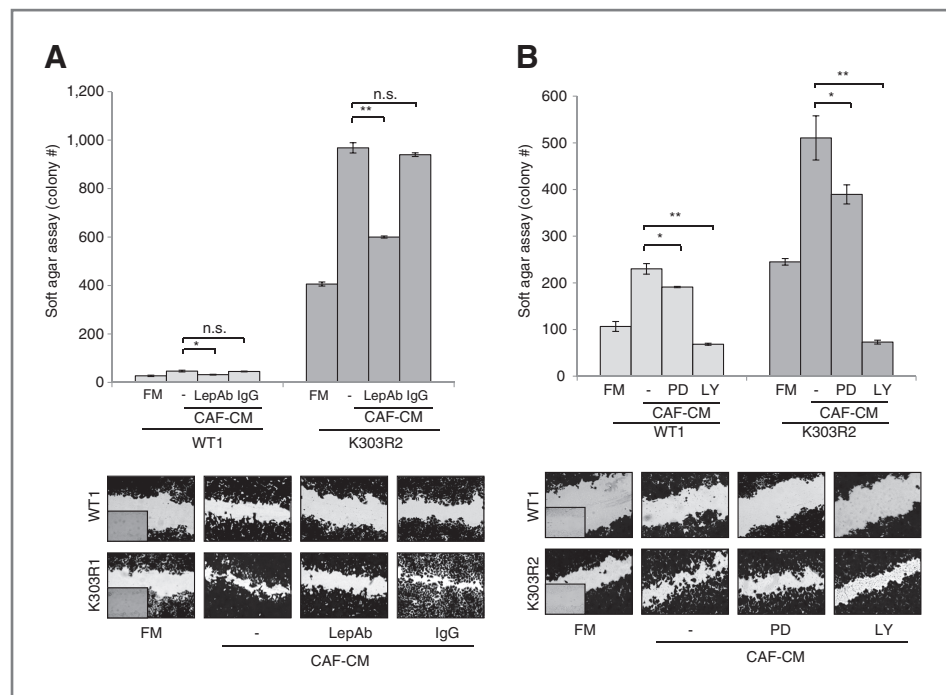
Leptin activates via JAK2 the MAPK and phosphoinositide 3-kinase (PI3K)/Akt pathways (31). Thus, we investigated the specific signaling involved in the CAF–breast cancer cells interaction and found that the PI3K/Akt inhibitor LY294002 was more effective in inhibiting CAF-induced proliferation and migration than the MEK1 inhibitor PD98059 (Fig. 4B).

#### Tumor–stroma interactions in SKBR3 breast cancer cells

To extend the results obtained, we generated pools of YFP-WT and YFP-K303R-ER $\alpha$  stable transfectants in ER $\alpha$ -

negative SKBR3 breast cancer cells (Supplementary Fig. S4). As previously shown for MCF-7 cells, we found a significant increase in both long and short leptin receptor isoforms mRNA in mutant-expressing cells. Again, treatment with leptin at 100 and 1,000 ng/mL significantly increased colony numbers of wild-type clones and to a higher extent of K303R-expressing cells; however, 10 ng/mL of leptin enhanced anchorage-independent growth only in K303R-expressing clones. Similarly, low leptin promoted migration only in mutant cells. Finally, we tested CAF-derived conditioned media for its effects on cell growth and migration. We found a great induction of anchorage-independent growth and motility after treatment with conditioned media, especially in K303R-expressing SKBR3 pools. Leptin-immunodepleted conditioned media strongly reduced conditioned media proliferative and migratory promoting activities on K303R cells, confirming that leptin hypersensitive phenotype

**Figure 4.** Leptin immunodepletion reduces CAF-induced cell growth and migration. **A**, soft agar and scratch assays in cells treated with full media (FM), CAF-derived conditioned media (CAF-CM), or leptin-depleted conditioned media (CM + LepAb). Conditioned media treated with a nonspecific IgG as a control (CM + IgG). **B**, soft agar and scratch assays in cells treated with FM, CAF-CM with or without PD98059 (PD, 10  $\mu$ mol/L) or LY294002 (LY, 10  $\mu$ mol/L). n.s., nonsignificant; \*,  $P < 0.05$ ; \*\*,  $P < 0.005$ . Small squares, time 0.



was associated with K303R-ER $\alpha$  expression in different cellular backgrounds.

#### Effects of breast cancer cell–secreted factors on CAF phenotype

CAFs and tumor cells cross-talk via different soluble factors, where the effects on both subpopulations determine the final outcome of the tumorigenic process. Thus, as a final step of this study, we defined the effects of conditioned media from WT- and K303R-ER $\alpha$ -expressing breast cancer cells on CAF phenotype. Treatment with K303R-derived conditioned media elicited a dramatic alteration in the shape of CAFs *in vitro*, accompanied by an increased FAP mRNA expression (Fig. 5A). K303R-derived conditioned media also stimulated CAF viability and motility compared with WT-derived conditioned media effects (Fig. 5B), suggesting that how soluble K303R-ER $\alpha$  cell–secreted factors may generate a more activated CAF phenotype. Because leptin synthesis is influenced by different humoral factors (32–34), we evaluated the effects of breast cancer–derived conditioned media in modulating leptin secretion from CAFs. Incubation of CAFs with K303R-derived conditioned media increased leptin mRNA expression and leptin release compared with WT-derived conditioned media, whereas no differences were detected in leptin levels among WT- and K303R-derived conditioned media (Fig. 5C). Finally, to investigate the paracrine factor by which breast cancer cells may affect CAF phenotype, we used microarray analyses to measure the expression of different genes known to be associated with CAFs and/or leptin secretion (11, 32–35). Our results showed that the genes encoding for EGF (2.8-fold), IL-6 (1.2-fold), and insulin (1.2-fold) were induced in mutant cells, and real-time PCR confirmed that the *EGF* gene was most highly upregulated (Fig. 5D). Thus, we evaluated the role of

EGF. First, addition of EGF in WT-derived conditioned media mimicked the induction of K303R-derived conditioned media on CAF motility, and the EGFR signaling inhibitor (AG1478) reduced K303R-derived conditioned media effects (Fig. 5E). Second, treatment with AG1478 reversed K303R-derived conditioned media stimulated FAP mRNA expression (Fig. 5F). Third, Ob mRNA expression and leptin secretion from CAFs cocultured with K303R-derived conditioned media were significantly decreased in the presence of AG1478 (Fig. 5F).

Our data show that K303R-ER $\alpha$ -expressing breast cancer cells through their soluble secreted factors may take advantage of the plastic nature of reactive surrounding cell populations, as CAFs, to generate a tumor-enhancing microenvironment.

#### Discussion

ER $\alpha$  expression has important implications for breast cancer biology and therapy. Fuqua and colleagues identified a lysine to arginine transition at residue 303 of ER $\alpha$  (K303R-ER $\alpha$ ) in 30% of breast hyperplasias and in 50% of invasive breast cancers (15, 16), although using another detection method, the mutation was identified in only 6% of tumors (21); thus the frequency is still unresolved. This mutation was associated with older age, larger tumor size, lymph node positivity, and shorter time to recurrence—all features related to a more aggressive breast cancer phenotype. Because of the recently recognized importance of tumor–stroma cross-talk in promoting breast cancer progression and metastasis, it is imperative to elucidate the molecular events occurring between cancer cells and adjacent stroma at the site of primary tumors to provide new treatment options for breast cancer.

Here, we elucidated the complex interactions between peritumoral tissue, locally derived factors, and neoplastic cells in dependency of ER $\alpha$  status, with a special focus on leptin effects

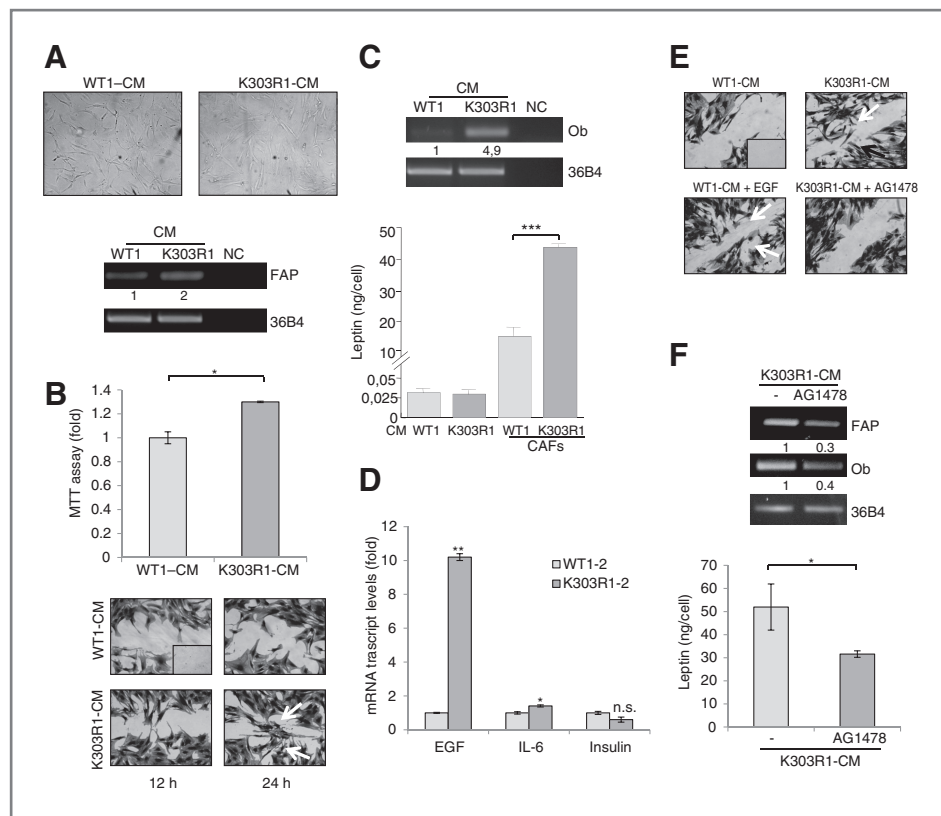


**Figure 5.** CAFs activated phenotype after K303R-ER $\alpha$  cell-derived conditioned media exposure. A, phase contrast microscopy for CAF morphology and RT-PCR for FAP and 36B4 (internal standard) after treatment with conditioned media from WT- or K303R-ER $\alpha$ -expressing cells. NC, negative control. B, MTT growth and scratch assays in CAFs treated with WT-derived conditioned media and K303R-derived conditioned media. C, RT-PCR for leptin/Ob and 36B4 and leptin release by RIA. D, real-time RT-PCR for EGF, IL-6, and insulin. E, scratch assays in CAFs treated with WT-derived conditioned media with or without 100 ng/mL EGF or K303R-derived conditioned media with or without AG1478 10  $\mu$ mol/L. F, RT-PCR for FAP, leptin/Ob, and 36B4, and leptin release from CAFs by RIA. Numbers represent the average fold change of FAP/36B4 and Ob/36B4 levels. n.s., nonsignificant; \*,  $P < 0.05$ ; \*\*,  $P < 0.005$ ; \*\*\*,  $P < 0.0001$ . Small squares, time 0.

in influencing the behavior of breast cancer cells bearing the naturally occurring K303R-ER $\alpha$  mutation. We proposed a model in which leptin, secreted from CAFs, binds to its receptor, activates K303R-ER $\alpha$ , and promotes proliferation, migration, and invasiveness of K303R-ER $\alpha$ -expressing breast cancer cells. In turn, K303R cells release factors as EGF that "educate" CAFs to enhance secretion of leptin, which, acting back on malignant cells, may establish a positive feedback loop between cancer and stromal cells to further support breast tumor progression (Fig. 6).

#### CAF $\alpha$ s promote breast cancer cell malignancy through leptin signaling

The phenotype of malignant cells appears regulated not only by cell autonomous signals but also is dependent on heterotypic signals coming from surrounding stromal cells, able to create a specific local microenvironment to tightly control breast cancer proliferation and differentiation (36–38).

We defined the molecular interactions between stromal fibroblasts isolated from biopsies of primary breast tumors (CAF $\alpha$ s), WT-, and K303R-ER $\alpha$ -expressing MCF-7 breast cancer cells. The initial conditioned media experiments showed that the entire complement of secretory proteins released by CAF $\alpha$ s have more profound effects on K303R-ER $\alpha$ -expressing cell proliferation and migration than on WT-ER $\alpha$  cells. We evidenced an important role for JAK2/STAT3 and ER $\alpha$  signaling pathways in conditioned media-mediated effects. Our microarray study pointed to the regulation of several important

transcriptional programs of growth factors and cytokines receptors that, acting as mediators of stromal-epithelial interactions, are potentially involved in carcinoma progression. Among them, the gene encoding for leptin receptor was the most highly induced in K303R-expressing breast cancer cells.

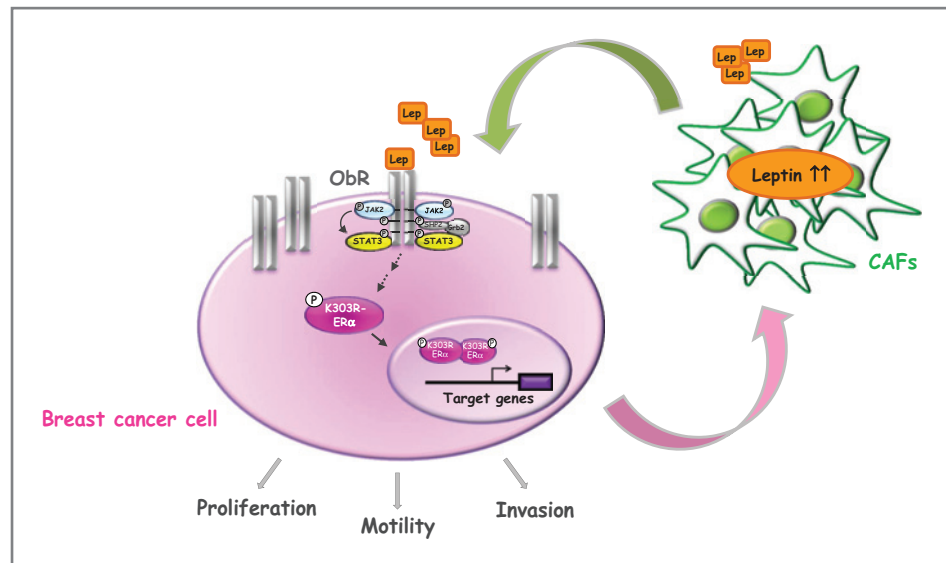
Leptin is primarily synthesized from adipocytes but is also produced by other cells, including fibroblasts (39–41). We showed, for the first time, Ob mRNA expression and leptin secretion in CAF $\alpha$ s. CAF $\alpha$ s expressed ObR long isoforms, implying that an autocrine feedback loop may exist. Leptin immunodepletion from CAF-derived conditioned media substantially reduced the growth- and migration-promoting activities of CAF $\alpha$ s. As one of the leptin downstream effectors (31), we found that the PI3K/Akt inhibitor LY294002 was effective in inhibiting CAF-induced effects.

Because fibroblasts are the principal cellular component of the stroma, our results suggest that in the breast microenvironment CAF $\alpha$ s through leptin signaling may become the main actor in influencing tumor cell behavior, especially in K303R-ER $\alpha$ -expressing breast cancer cells.

#### Cross-talk between leptin and K303R-ER $\alpha$ signaling pathways in breast cancer

Leptin, a pleiotropic molecule that regulates food intake, hematopoiesis, inflammation, cell differentiation, and proliferation, is also required for mammary gland development and tumorigenesis. Indeed, leptin and its receptor isoforms (ObRs) have been detected in mammary epithelium and breast cancer

**Figure 6.** Schematic illustration of tumor–stroma interactions in K303R-ER $\alpha$  breast cancer microenvironment. CAFs secrete leptin, which, acting in a paracrine fashion, binds to its cognate receptors (ObR) overexpressed on the surface of K303R-ER $\alpha$  breast cancer cells and activates K303R-ER $\alpha$ . This results in increased cell proliferation, motility, and invasion. K303R-ER $\alpha$ -expressing cells, in turn, secrete factors that stimulate leptin production by adjacent CAFs, thus creating a positive feedback loop between cancer and stromal cells to further promote breast tumor progression.



cell lines and are overexpressed in cancer tissue compared with healthy epithelium, with a positive correlation between ObR and ER $\alpha$  expression (42, 43). Real-time PCR, immunoblotting, and immunofluorescent experiments revealed an increase in mRNA and protein expressions of ObR long and short isoforms in K303R-ER $\alpha$ -expressing cells. We also showed that the mutant expression was associated with enhanced leptin signaling activation and increased sensitivity to leptin stimulation on growth, motility, and invasiveness. Moreover, a significant increase in the growth of leptin-treated mutant tumors was observed *in vivo*.

Leptin is a potent modulator of the estrogen signaling pathway (29, 44). On the contrary, estradiol modulates ObR expression in rat brain, through a putative estrogen-responsive element in its promoter (45, 46), and others showed that estradiol induces leptin and ObR expression in MCF-7 breast cancer cells (43). Thus, leptin and estrogen might cooperate in sustaining estrogen-dependent breast carcinoma growth. We showed an increased S167 and S118 phosphorylation of the K303R receptor, an enhanced K303R-ER $\alpha$  transactivation, and a more pronounced upregulation of classical estrogen-regulated genes in K303R-expressing cells. Indeed, the pure antiestrogen ICI182760 drastically suppressed leptin-stimulated anchorage-independent growth and motility of mutant cells.

These results suggest that the mutation may potentiate the role of ER $\alpha$  as an effector of leptin intracellular signal transduction, which may enhance cell proliferation, migration, and invasiveness, contributing to the more aggressive phenotype of K303R-associated breast cancers.

#### **K303R-ER $\alpha$ cell-derived factors contribute to CAF tumor-promoting activities**

In the same way as tumor microenvironment plays active roles in shaping the fate of a tumor, cancer cells actively recruit fibroblasts into the tumor mass, in particular, the subpopulation named CAFs. This cell type is defined on the basis of the

morphologic characteristics or expression of markers as the FAP (1–4).

Studies addressing these issues are heterogeneous in terms of cell systems used, tumor cell types, and fibroblast sources. Experimental systems have used different tumor-derived conditioned media to stimulate CAFs, and others have cocultured tumor cells with normal fibroblasts or mesenchymal stem cells and measured chemokines levels in the resulting conditioned media. For instance, fibroblasts growth with tumor cells resulted in increased production of chemokines whose source is in CAFs themselves. Chemokines produced under these "mixed" conditions promoted tumor promalignancy activities (6, 9, 47). We showed increased leptin mRNA expression and secretion by CAFs in response to soluble K303R-ER $\alpha$  cell-secreted factors compared with WT-derived conditioned media, suggesting that K303R cells have the ability to instruct their surrounding fibroblasts to augment leptin production, thereby enhancing tumor growth. This further indicates that interactions between the 2 subpopulations are actually bidirectional.

These interactions become more productive when tumor cells have a higher aggressiveness phenotype (47–49). CAFs exposed to K303R cell-derived conditioned media acquired a more activated phenotypic characteristic, as revealed by an altered morphology, an increased FAP mRNA expression, and enhanced proliferative and migratory capabilities. We identified the epidermal growth factor, known to affect CAFs phenotype and leptin secretion (11, 32–35), as the factor responsible of the paracrine activation of the surrounding stroma.

Thus, a positive feedback loop is established which leads to the development and growth of the tumor.

#### **Conclusions**

Our study highlights the functional importance of tumor–host cross-talk in impacting malignant cell behavior and implies several clinical implications. First, because K303R

mutation was identified in breast premalignant hyperplasia, it is tempting to speculate that this specific mutation hypersensitive to leptin signaling may promote or accelerate the development of cancers from premalignant breast lesions, further increasing risk in obese women. Second, understanding the key genes involved differently in relation to ER $\alpha$  status in tumor-stroma interactions may help to identify novel biomarkers for breast cancer. Finally, our findings support the development of new therapeutics targeting stroma signaling components (e.g., leptin) to be implemented in the adjuvant therapy for improving clinical care and reducing mortality from breast cancer.

#### Disclosure of Potential Conflicts of Interest

No potential conflicts of interest were disclosed.

#### References

- Bhowmick NA, Neilson EG, Moses HL. Stromal fibroblasts in cancer initiation and progression. *Nature* 2004;432:332–7.
- Hanahan D, Weinberg RA. The hallmarks of cancer. *Cell* 2000;100:57–70.
- Mueller MM, Fusenig NE. Friends or foes - bipolar effects of the tumour stroma in cancer. *Nat Rev Cancer* 2004;4:839–49.
- Orimo A, Weinberg RA. Stromal fibroblasts in cancer: a novel tumor-promoting cell type. *Cell Cycle* 2006;5:1597–601.
- Augsten M, Hagglof C, Olsson E, Stolz C, Tsagozis P, Levchenko T, et al. CXCL14 is an autocrine growth factor for fibroblasts and acts as a multimodal stimulator of prostate tumor growth. *Proc Natl Acad Sci U S A* 2009;106:3414–9.
- Jung DW, Che ZM, Kim J, Kim K, Kim KY, Williams D. Tumor-stromal crosstalk in invasion of oral squamous cell carcinoma: a pivotal role of CCL7. *Int J Cancer* 2009;127:332–44.
- Matsuo Y, Ochi N, Sawai H, Yasuda A, Takahashi H, Funahashi H, et al. CXCL8/L-8 and CXCL12/SDF-1 co-operatively promote invasiveness and angiogenesis in pancreatic cancer. *Int J Cancer* 2009;124:853–61.
- Wolf JS, Chen Z, Dong G, Sunwoo JB, Bancroft CC, Capo DE, et al. IL (interleukin)-1  $\alpha$  promotes nuclear factor- $\kappa$ B and AP-1-induced IL-8 expression, cell survival, and proliferation in head and neck squamous cell carcinomas. *Clin Cancer Res* 2001;7:1812–20.
- Kumar S, Kishimoto H, Chua HL, Badve S, Miller KD, Bigsby RM, et al. Interleukin-1  $\alpha$  promotes tumor growth and cachexia in MCF-7 xenograft model of breast cancer. *Am J Pathol* 2003;163:2531–41.
- Wu MH, Chou YC, Chou WY, Hsu GC, Chu CH, Yu CP, et al. Circulating levels of leptin, adiposity and breast cancer risk. *Br J Cancer* 2009;100:578–82.
- Schäffler A, Schömlerich J, Buechler C. Mechanisms of disease: adipokines and breast cancer-endocrine and paracrine mechanisms that connect adiposity and breast cancer. *Nat Clin Pract Endocrinol Metab* 2007;3:345–54.
- Osborne CK, Schiff R. Estrogen-receptor biology: continuing progress and therapeutic implications. *J Clin Oncol* 2005;23:1616–22.
- Herynk MH, Fuqua SA. Estrogen receptor mutations in human disease. *Endocr Rev* 2004;25:869–98.
- Barone I, Brusco L, Fuqua SA. Estrogen receptor mutations and changes in downstream gene expression and signaling. *Clin Cancer Res* 2010;16:2702–8.
- Fuqua SA, Wiltschke C, Zhang QX, Borg A, Castles CG, Friedrichs WE, et al. A hypersensitive estrogen receptor- $\alpha$  mutation in premalignant breast lesions. *Cancer Res* 2000;60:4026–9.
- Herynk MH, Parra I, Cui Y, Beyer A, Wu MF, Hilsenbeck SG, et al. Association between the estrogen receptor  $\alpha$  A908G mutation and outcomes in invasive breast cancer. *Clin Cancer Res* 2007;13:3235–43.
- Tebbit CL, Bentley RC, Olson JA, Marks JR. Estrogen receptor  $\alpha$  (ESR1) mutant A908G is not a common feature in benign and malignant

#### Acknowledgments

The authors thank Dr. F. Romeo for providing the breast cancer specimens.

#### Grant Support

This work was supported by Reintegration AIRC/Marie Curie International Fellowship in Cancer Research to I. Barone; Lilli Funaro Foundation to I. Barone and L. Gelsomino; European Commission/FSE/Regione Calabria to L. Gelsomino; AIRC grant (IG11595) to S. Catalano, D. Bonofiglio, C. Giordano, and S. Andò; AIRC grant (IG8804) to G. Bossi; and NCI RO1 CA72038 to S.A.W. Fuqua.

The costs of publication of this article were defrayed in part by the payment of page charges. This article must therefore be hereby marked *advertisement* in accordance with 18 U.S.C. Section 1734 solely to indicate this fact.

Received August 1, 2011; revised December 7, 2011; accepted January 2, 2012; published OnlineFirst January 26, 2012.

- proliferations of the breast. *Genes Chromosomes Cancer* 2004;40:51–4.
- Tokunaga E, Kimura Y, Maehara Y. No hypersensitive estrogen receptor- $\alpha$  mutation (K303R) in Japanese breast carcinomas. *Breast Cancer Res Treat* 2004;84:289–92.
- Davies MP, O'Neill PA, Innes H, Sibson DR. Hypersensitive K303R oestrogen receptor- $\alpha$  variant not found in invasive carcinomas. *Breast Cancer Res* 2005;7:R113–8.
- Zhang Z, Yamashita H, Toyama T, Omoto Y, Sugiura H, Hara Y, et al. Estrogen receptor  $\alpha$  mutation (A-to-G transition at nucleotide 908) is not found in different types of breast lesions from Japanese women. *Breast Cancer* 2003;10:70–3.
- Conway K, Parrish E, Edmiston SN, Tolbert D, Tse CK, Geradts J, et al. The estrogen receptor- $\alpha$  A908G (K303R) mutation occurs at a low frequency in invasive breast tumors: results from a population-based study. *Breast Cancer Res* 2005;7:R871–80.
- Cui Y, Zhang M, Pestell R, Curran EM, Welshons WV, Fuqua SA. Phosphorylation of estrogen receptor  $\alpha$  blocks its acetylation and regulates estrogen sensitivity. *Cancer Res* 2004;64:9199–208.
- Barone I, Iacopetta D, Covington KR, Cui Y, Tsimelzon A, Beyer A, et al. Phosphorylation of the mutant K303R estrogen receptor  $\alpha$  at serine 305 affects aromatase inhibitor sensitivity. *Oncogene* 2010;29:2404–14.
- Herynk MH, Hopp T, Cui Y, Niu A, Corona-Rodriguez A, Fuqua SA. A hypersensitive estrogen receptor  $\alpha$  mutation that alters dynamic protein interactions. *Breast Cancer Res Treat* 2010;122:381–93.
- Giordano C, Cui Y, Barone I, Andò S, Mancini M, Berno V, et al. Growth factor-induced resistance to tamoxifen is associated with a mutation of estrogen receptor  $\alpha$  and its phosphorylation at serine 305. *Breast Cancer Res Treat* 2010;119:71–81.
- Barone I, Cui Y, Herynk MH, Corona-Rodriguez A, Giordano C, Selever J, et al. Expression of the K303R estrogen receptor  $\alpha$  breast cancer mutation induces resistance to an aromatase inhibitor via addition to the PI-3K/Akt kinase pathway. *Cancer Res* 2009;69:4724–32.
- Catalano S, Malivindi R, Giordano C, Gu G, Panza S, Bonofiglio D, et al. Farnesoid X receptor, through the binding with steroidogenic factor 1-responsive element, inhibits aromatase expression in tumor Leydig cells. *J Biol Chem* 2010;285:5581–93.
- Sirianni R, Chimento A, Malivindi R, Mazzitelli I, Andò S, Pezzi V. Insulin-like growth factor-1, regulating aromatase expression through steroidogenic factor 1, supports estrogen-dependent tumor Leydig cell proliferation. *Cancer Res* 2007;67:8368–77.
- Catalano S, Mauro L, Marsico S, Giordano C, Rizza P, Rago V, et al. Leptin induces, via ERK1/ERK2 signal, functional activation of estrogen receptor  $\alpha$  in MCF-7 cells. *J Biol Chem* 2004;279:19908–15.
- Mauro L, Catalano S, Bossi G, Pellegrino M, Barone I, Morales S, et al. Evidences that leptin up-regulates E-cadherin expression in breast

- cancer: effects on tumor growth and progression. *Cancer Res* 2007;67:3412–21.
31. Cirillo D, Rachiglio AM, la Montagna R, Giordano A, Normanno N. Leptin signaling in breast cancer: an overview. *J Cell Biochem* 2008;105:956–64.
  32. Leroy P, Dessolin S, Villageois P, Moon BC, Friedman JM, Ailhaud G, et al. Expression of ob gene in adipose cells Regulation by insulin. *J Biol Chem* 1996;271:2365–8.
  33. Cascio S, Ferla R, D'Andrea A, Gerbino A, Bazan V, Surmacz E, et al. Expression of angiogenic regulators, VEGF and leptin, is regulated by the EGF/PI3K/STAT3 pathway in colorectal cancer cells. *J Cell Physiol* 2009;221:189–94.
  34. Trujillo ME, Sullivan S, Harten I, Schneider SH, Greenberg AS, Fried SK. Interleukin-6 regulates human adipose tissue lipid metabolism and leptin production *in vitro*. *J Clin Endocrinol Metab* 2004;89:5577–82.
  35. Iwabu A, Smith K, Allen FD, Lauffenburger DA, Wells A. Epidermal growth factor induces fibroblast contractility and motility via a protein kinase C delta-dependent pathway. *J Biol Chem* 2004;279:14551–60.
  36. Fidler IJ. The pathogenesis of cancer metastasis: the "seed and soil" hypothesis revisited. *Nat Rev Cancer* 2003;3:453–8.
  37. Witz IP. Yin-yang activities and vicious cycles in the tumor microenvironment. *Cancer Res* 2008;68:9–13.
  38. Wiseman BS, Werb Z. Stromal effects on mammary gland development and breast cancer. *Science* 2002;296:1046–9.
  39. Glasow A, Kiess W, Anderegg U, Berthold A, Bottner A, Kratzsch J. Expression of leptin (Ob) and leptin receptor (Ob-R) in human fibroblasts: regulation of leptin secretion by insulin. *J Clin Endocrinol Metab* 2001;86:4472–9.
  40. Torday JS, Sun H, Wang L, Torres E. Leptin mediates the parathyroid hormone-related protein paracrine stimulation of fetal lung maturation. *Am J Physiol Lung Cell Mol Physiol* 2002;282:L405–10.
  41. Lin TC, Lee TC, Hsu SL, Yang CS. The molecular mechanism of leptin secretion and expression induced by aristolochic acid in kidney fibroblast. *PLoS One* 2011;6:e16654.
  42. Ishikawa M, Kitayama J, Nagawa H. Enhanced expression of leptin and leptin receptor (OB-R) in human breast cancer. *Clin Cancer Res* 2004;10:4325–31.
  43. Garofalo C, Koda M, Cascio S, Sulkowska M, Kanczuga-Koda L, Golaszewska J, et al. Increased expression of leptin and the leptin receptor as a marker of breast cancer progression: possible role of obesity-related stimuli. *Clin Cancer Res* 2006;12:1447–53.
  44. Catalano S, Marsico S, Giordano C, Mauro L, Rizza P, Panno ML, et al. Leptin enhances, via AP-1, expression of aromatase in the MCF-7 cell line. *J Biol Chem* 2003;278:28668–76.
  45. Bennett PA, Lindell K, Karlsson C, Robinson IC, Carlsson LM, Carlsson B. Differential expression and regulation of leptin receptor isoforms in the rat brain: effects of fasting and oestrogen. *Neuroendocrinology* 1998;67:29–36.
  46. Lindell K, Bennett PA, Itoh Y, Robinson IC, Carlsson LM, Carlsson B. Leptin receptor 5' untranslated regions in the rat: relative abundance, genomic organization and relation to putative response elements. *Mol Cell Endocrinol* 2001;172:37–45.
  47. Li L, Dragulev B, Zigrino P, Mauch C, Fox JW. The invasive potential of human melanoma cell lines correlates with their ability to alter fibroblast gene expression *in vitro* and the stromal microenvironment *in vivo*. *Int J Cancer* 2009;125:1796–804.
  48. Tsujino T, Seshimo I, Yamamoto H, Ngan CY, Ezumi K, Takemasa I, et al. Stromal myofibroblasts predict disease recurrence for colorectal cancer. *Clin Cancer Res* 2007;13:2082–90.
  49. Infante JR, Matsubayashi H, Sato N, Tonascia J, Klein AP, Riall TA, et al. Peritumoral fibroblast SPARC expression and patient outcome with resectable pancreatic adenocarcinoma. *J Clin Oncol* 2007;25:319–25.

ORIGINAL ARTICLE

# Farnesoid X receptor inhibits tamoxifen-resistant MCF-7 breast cancer cell growth through downregulation of HER2 expression

C Giordano<sup>1,5</sup>, S Catalano<sup>1,2,5</sup>, S Panza<sup>2</sup>, D Vizza<sup>2</sup>, I Barone<sup>1,3</sup>, D Bonofiglio<sup>1,2</sup>, L Gelsomino<sup>2</sup>, P Rizza<sup>3</sup>, SAW Fuqua<sup>4</sup> and S Andò<sup>1,3</sup>

<sup>1</sup>Centro Sanitario, University of Calabria, Arcavacata di Rende, Italy; <sup>2</sup>Department of Pharmaco-Biology, University of Calabria, Arcavacata di Rende, Italy; <sup>3</sup>Department of Cellular Biology, University of Calabria, Arcavacata di Rende, Italy and <sup>4</sup>Lester and Sue Smith Breast Center and Department of Molecular and Cellular Biology, Baylor College of Medicine, One Baylor Plaza, Houston, TX, USA

Tamoxifen (Tam) treatment is a first-line endocrine therapy for estrogen receptor- $\alpha$ -positive breast cancer patients. Unfortunately, resistance frequently occurs and is often related with overexpression of the membrane tyrosine kinase receptor HER2. This is the rationale behind combined treatments with endocrine therapy and novel inhibitors that reduce HER2 expression and signaling and thus inhibit Tam-resistant breast cancer cell growth. In this study, we show that activation of farnesoid X receptor (FXR), by the primary bile acid chenodeoxycholic acid (CDCA) or the synthetic agonist GW4064, inhibited growth of Tam-resistant breast cancer cells (termed MCF-7 TR1), which was used as an *in vitro* model of acquired Tam resistance. Our results demonstrate that CDCA treatment significantly reduced both anchorage-dependent and anchorage-independent epidermal growth factor (EGF)-induced growth in MCF-7 TR1 cells. Furthermore, results from western blot analysis and real-time reverse transcription-PCR revealed that CDCA treatment reduced HER2 expression and inhibited EGF-mediated HER2 and p42/44 mitogen-activated protein kinase (MAPK) phosphorylation in these Tam-resistant breast cancer cells. Transient transfection experiments, using a vector containing the human HER2 promoter region, showed that CDCA treatment downregulated basal HER2 promoter activity. This occurred through an inhibition of nuclear factor- $\kappa$ B transcription factor binding to its specific responsive element located in the HER2 promoter region as revealed by mutagenesis studies, electrophoretic mobility shift assay and chromatin immunoprecipitation analysis. Collectively, these data suggest that FXR ligand-dependent activity, blocking HER2/MAPK signaling, may overcome anti-estrogen resistance in human breast cancer cells and could represent a new therapeutic tool to treat breast cancer patients that develop resistance.

Oncogene (2011) 30, 4129–4140; doi:10.1038/onc.2011.124; published online 18 April 2011

**Keywords:** FXR; breast cancer; tamoxifen resistance; HER2; NF- $\kappa$ B

## Introduction

Administration of the selective estrogen receptor (ER) modulator tamoxifen (Tam), to block ER $\alpha$  activity, is still a first-line endocrine therapy for the management of all stages of ER $\alpha$ -positive breast cancer (Fisher *et al.*, 1998; Gradishar, 2004). Unfortunately, not all patients who have ER $\alpha$ -positive tumors respond to Tam (*de novo* resistance), and a large number of patients who do respond will eventually develop disease progression or recurrence while on therapy (acquired resistance), limiting the efficacy of the treatment.

Multiple mechanisms are responsible for the development of endocrine resistance. Among these are the loss of ER $\alpha$  expression or function (Encarnacion *et al.*, 1993), alterations in the balance of regulatory cofactors, increased oncogenic kinase signaling (Blume-Jensen and Hunter, 2001), and altered expression of growth factor signaling pathways (Arpino *et al.*, 2004; Schiff *et al.*, 2004; Sabnis *et al.*, 2005; Staka *et al.*, 2005). For instance, several preclinical and clinical studies suggest that both *de novo* and acquired resistance to Tam in breast cancers can be associated with elevated levels of the membrane tyrosine kinase HER2 (c-ErbB2, Her2/neu) (Chung *et al.*, 2002; Meng *et al.*, 2004; Shou *et al.*, 2004; Gutierrez *et al.*, 2005).

The *HER2* gene codes for a 185 kDa receptor, a member of the epidermal growth factor receptor (EGFR) family of transmembrane tyrosine kinases, which also includes HER3 and HER4, mainly involved in signal transduction pathways that regulate cell growth and differentiation. This receptor has no ligand of its own, but is activated by hetero-oligomerization with other ligand-activated receptors (Yarden, 2001). The *HER2* gene is amplified and/or overexpressed in 20–25% of ER $\alpha$ -positive breast cancers (Slamon *et al.*, 1989), and

Correspondence: Professor S Andò, Department of Cell Biology and Faculty of Pharmacy, Nutritional and Health Sciences, University of Calabria, Via P. Bucci, Arcavacata di Rende (CS) 87036, Italy.  
E-mail: sebastiano.ando@unical.it

<sup>5</sup>These authors contributed equally to this work.

Received 15 November 2010; revised 8 March 2011; accepted 15 March 2011; published online 18 April 2011

clinical observations indicate that tumors with high levels of HER2 have poor outcome when treated with Tam (Osborne *et al.*, 2003; Kirkegaard *et al.*, 2007).

The mechanisms by which HER2 overexpression mediates Tam resistance result from an intimate cross-talk between ER $\alpha$  and growth factor receptors kinase cascades, such as Ras/mitogen-activated protein kinase (MAPK) signaling, that in turn can promote growth and progression in breast cancer cells, negating the inhibitory effects of Tam on nuclear ER $\alpha$  activity (Arpino *et al.*, 2008). HER2 overexpression is not attributed solely to amplification of the *HER2* gene copy number, but can also occur from a single-copy gene due to deregulation events at the transcriptional level (Hurst, 2001).

Thus, an analysis of new mechanisms controlling HER2/neu receptor gene expression could be important to enhance strategies to reverse Tam resistance in breast cancer patients.

Farnesoid X receptor (FXR), a member of the nuclear receptor superfamily of ligand-dependent transcription factors, is mainly expressed in the liver and the gastrointestinal tract, where it regulates expression of genes involved in bile acids, cholesterol and triglyceride metabolism (Forman *et al.*, 1995; Makishima *et al.*, 1999; Parks *et al.*, 1999). Recently, this receptor was also detected in different non-enterohepatic compartments, including breast cancer tissue and breast cancer cell lines (Bishop-Bailey, 2004; Swales *et al.*, 2006; Journe *et al.*, 2008; Catalano *et al.*, 2010). For instance, FXR activation inhibits breast cancer cell proliferation and negatively regulates aromatase activity reducing local estrogen production (Swales *et al.*, 2006), whereas other authors have reported that FXR activation stimulates MCF-7 cell proliferation but only in steroid-free medium (Journe *et al.*, 2008). However, the functions of FXR in breast cancer tissue are still not completely understood, and there are no data regarding its role in the endocrine-resistant breast cancer phenotype. Thus, we have investigated whether activated FXR may modulate the growth of human MCF-7 Tam-resistant breast cancer cells, a model that was developed to mimic *in vitro* the occurrence of acquired Tam resistance.

Here, we demonstrate that a specific FXR ligand chenodeoxycholic acid (CDCA) or its synthetic agonist GW4064 inhibited Tam-resistant breast cancer cell proliferation and EGF-induced growth, by reducing expression of the HER2 receptor. This occurs through an FXR-mediated inhibition of nuclear factor (NF)- $\kappa$ B binding on the human HER2 promoter region.

## Results

### *FXR expression in Tam-resistant breast cancer cells*

Acquired resistance to Tam has been associated with elevated levels of the membrane tyrosine kinase HER2 (Knowlden *et al.*, 2003; Nicholson *et al.*, 2004; Gutierrez *et al.*, 2005). In agreement with these reports, we found a marked increase in the levels of total HER2 protein content in Tam-resistant MCF-7 TR1 compared with

MCF-7 cells, whereas no differences were seen in the expression of EGFR and ER $\alpha$  (Figure 1a). We therefore evaluated anchorage-independent growth of MCF-7 and MCF-7 TR1 cells after treatment with hereceptin, a humanized monoclonal antibody directed against the extracellular domain of HER2, in the presence or not of EGF. Hereceptin had no effect on MCF-7 growth, whereas significantly inhibited anchorage-independent growth of MCF-7 TR1 cells in basal conditions as well as upon EGF treatment (Figure 1b). These data confirm that the HER2 overexpression found in the MCF-7 TR1 cells renders them more sensitive to the inhibitory effect of this selective HER2-targeted agent.

Next, we evaluated the expression of FXR in MCF-7 and MCF-7 TR1 cells. Our results revealed the presence of FXR mRNA (Figure 1c, upper panel) and protein (Figure 1c, lower panel) in both MCF-7 and MCF-7 TR1 cells. To assess the ability of FXR to be transactivated by CDCA, we transiently transfected cells with an FXR-responsive reporter gene (*FXRE-IR1*) followed by treatment with increasing doses of CDCA. The specificity of the system was tested by co-transfecting the cells with a dominant negative FXR (FXR-DN) plasmid. As shown in Figure 1d, CDCA treatment induced a dose-dependent FXR activation in both cell lines and expression of the FXR-DN completely abrogated the CDCA-induced transactivation.

### *FXR activation inhibits Tam-resistant breast cancer cell growth*

We examined, by MTT growth assays, the effects of increasing doses of CDCA and GW4064. Treatment with both ligands reduced cell proliferation in a dose-dependent manner in MCF-7 and MCF-7 TR1 cells, whereas had no effects on normal breast epithelial cells MCF-10A (Figures 2a and b). Similar results in growth inhibition were also obtained in another Tam-resistant breast cancer cell line termed MCF-7 TR2 (Supplementary Figures 2a and b). It is worth noting that the inhibitory effects exerted by FXR ligands on cell proliferation were significant at lower dose in MCF-7 TR1 cells compared with MCF-7 cells, as evidenced by half-maximal inhibitory concentration (IC<sub>50</sub>) values (Table 1). The antiproliferative effects exerted by CDCA were completely reversed in the presence of a FXR-DN plasmid, supporting the specific involvement of the FXR (Figure 2c).

Next, we tested the effects of CDCA in the presence of Tam on cell growth (Figure 2d). As expected, with anti-estrogen treatment, cell viability was significantly reduced in MCF-7 cells, whereas MCF-7 TR1 cells growth was unaffected, confirming the Tam-resistant phenotype. Interestingly, combined treatment with CDCA and Tam reduced growth of MCF-7 TR1 cells compared with treatment with Tam alone, but showed no additive effects in MCF-7 cells (Figure 2d). The ability of CDCA and Tam to inhibit Tam-resistant growth was also confirmed using anchorage-independent growth assays (Figure 2e). These results suggest that FXR activation can interfere with the cellular

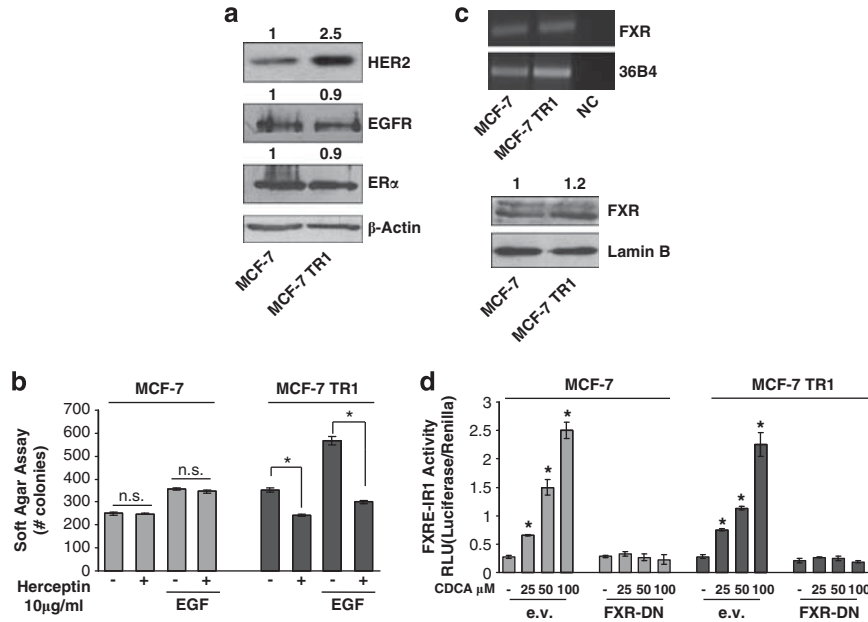


**Figure 1** FXR expression and activation in MCF-7 and MCF-7 TR1 cells. (a) Western blot analysis of HER2, EGFR, ER $\alpha$  in total protein extracts from MCF-7 and MCF-7 TR1 cells;  $\beta$ -Actin was used as loading control. (b) Soft-agar growth assay in MCF-7 and MCF-7 TR1 cells plated in 0.35% agarose and treated with EGF 100 ng/ml in the presence or absence of herceptin (10  $\mu$ g/ml). After 14 days of growth, colonies > 50  $\mu$ m diameter were counted. n.s., nonsignificant; \* $P$  < 0.05 compared with vehicle or EGF. (c) Total RNA was extracted from MCF-7 and MCF-7 TR1 cells, reverse transcribed and cDNA was subjected to PCR using primers specific for FXR or 36B4 (upper panel). NC: negative control, RNA sample without the addition of reverse transcriptase. Nuclear proteins were extracted from MCF-7 and MCF-7 TR1 and then western blotting analysis was performed using anti-FXR antibody. Lamin B was used as loading control (lower panel). (d) MCF-7 and MCF-7 TR1 cells were transiently transfected with a FXR-responsive reporter gene (*FXRE-IR1*), with either empty vector (e.v.) or FXR-DN expression plasmid. After transfection, cells were treated for 24 h with vehicle (–) or increasing doses of CDCA (25–50–100  $\mu$ M) and then luciferase activity was measured. Results represent the mean  $\pm$  s.d. of three different experiments each performed in triplicate. \* $P$  < 0.05 compared with vehicle. Numbers on top of the blots represent the average fold change versus control of MCF-7 cells normalized for  $\beta$ -Actin or Lamin B.

mechanisms by which MCF-7 TR1 cells escape antihormonal treatments.

#### CDCA reduces HER2 expression and signaling in MCF-7 TR1 cells

To understand the mechanisms associated with CDCA-mediated inhibition of Tam-resistant growth in breast cancer cells, we evaluated the possible role of FXR ligands in modulating HER2 expression. As shown in Figure 3a, treatment with CDCA downregulated HER2 protein expression in both cell lines, but with higher reduction seen in MCF-7 TR1 cells. Similar results were also observed after treatment with GW4064 (data not shown). A reduction in HER2 levels was also found upon CDCA treatment in MCF-7 TR2 cells (Supplementary Figure 2c). No differences were found in EGFR expression upon CDCA treatment (Supplementary Figure 3), confirming that activated FXR specifically target HER2 expression in breast cancer cells. In the presence of an FXR-DN the HER2 downregulation was completely abrogated, confirming FXR involvement in CDCA-induced effects on HER2 (Figure 3b). Next, we questioned whether these HER2-decreased levels could modify the responsiveness of breast cancer cells after growth factor stimulation. Thus, we investigated the effects of short-term stimulation with EGF, in the presence of CDCA treatment, on phosphorylation

levels of HER2 and MAPK, the main downstream effectors of the growth factor signaling. EGF treatment increased phosphorylation of both HER2 and MAPK, even though in higher extent in MCF-7 TR1 cells. However, pretreatment with CDCA reduced EGF-induced phosphorylation of HER2 in both cell lines and drastically prevented MAPK activation in MCF-7 TR1 cells (Figure 3c). In addition, data obtained from MTT (Figure 3d upper panel) as well as soft-agar (Figure 3d lower panel) growth assays revealed that CDCA treatment inhibited EGF-induced growth by 70% in anchorage-dependent and 50% in anchorage-independent assays in MCF-7 TR1 cells. CDCA was less effective in MCF-7 cells. These results well correlated with the downregulatory effect of CDCA on EGF-induced cyclin D1 expression, particularly in MCF-7 TR1 cells (Figure 3e).

#### Activated FXR inhibits the binding of NF- $\kappa$ B to HER2 promoter region

To explore whether HER2 downregulation relies on transcriptional mechanisms, we evaluated, using real-time reverse transcription (RT)-PCR, HER2 mRNA levels after treatment with CDCA for different times. Exposure to CDCA exhibited a time-dependent reduction in HER2 mRNA levels in both MCF-7 and MCF-7 TR1 cells (Figure 4a). Also, transcriptional activity of a

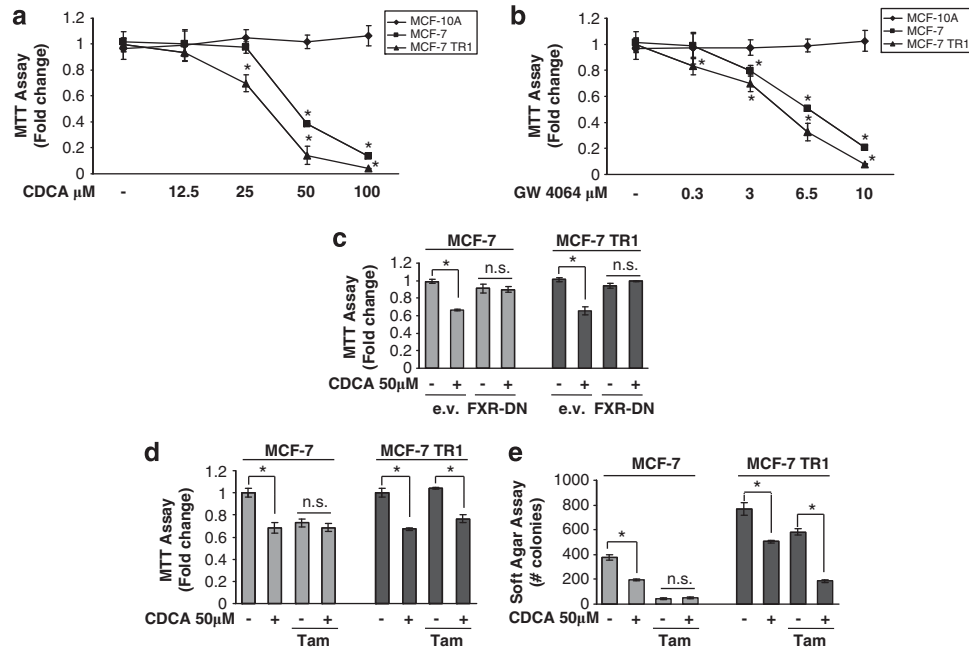


**Figure 2** FXR ligands effects on breast cancer cells proliferation. MTT growth assays in MCF-10A, MCF-7 and MCF-7 TR1 cells treated with vehicle (–) or increasing doses of CDCA (12.5–25–50–100  $\mu\text{M}$ ) (a) or GW4064 (0.3–3–6.5–10  $\mu\text{M}$ ) (b) for 7 days. Cell proliferation is expressed as fold change  $\pm$  s.d. relative to vehicle-treated cells and is representative of three different experiments each performed in triplicate. (c) MCF-7 and MCF-7 TR1 cells, transiently transfected with either empty vector (e.v.) or FXR-DN vector plasmids, were treated with vehicle (–) or CDCA 50  $\mu\text{M}$  for 4 days before testing cell viability using MTT assay. Results are expressed as fold change  $\pm$  s.d. relative to vehicle-treated cells and are representative of three different experiments each performed in triplicate. (d) MTT growth assay in MCF-7 and MCF-7 TR1 cells treated with vehicle (–) or CDCA 50  $\mu\text{M}$  in the presence or not of Tam 1  $\mu\text{M}$  for 4 days. Results are expressed as fold change  $\pm$  s.d. relative to vehicle-treated cells and are representative of three different experiments each performed in triplicate. (e) Soft-agar growth assay in MCF-7 and MCF-7 TR1 cells plated in 0.35% agarose and treated as indicated above. After 14 days of growth, colonies  $>50\mu\text{m}$  diameter were counted. n.s. (nonsignificant);  $*P < 0.05$  compared with vehicle or Tam.

**Table 1**  $\text{IC}_{50}$  of CDCA and GW4064 for MCF-7 and MCF-7 TR1 cells on anchorage-dependent growth

Cell lines	$\text{IC}_{50}$ ( $\mu\text{mol/l}$ ) CDCA	95% confidence interval	P	$\text{IC}_{50}$ ( $\mu\text{mol/l}$ ) GW4064	95% confidence interval	P
MCF-7	46	42.2–50.1		6.04	5.44–6.70	
MCF-7 TR1	31	28.6–33.9	0.0001	4.47	3.6–5.49	0.008

Abbreviations: CDCA, chenodeoxycholic acid;  $\text{IC}_{50}$ , half-maximal inhibitory concentration.

reporter plasmid containing the human HER2 promoter region (pNeuLite) was significantly reduced with CDCA treatment in both cell lines (Figures 4c and d).

The human HER2 promoter contains multiple consensus sites for several transcription factors, including Sp1, as well as activator protein (AP)-1 and NF- $\kappa\text{B}$ , the well known effectors of FXR transrepression (He *et al.*, 2006; Vavassori *et al.*, 2009) (Figure 4b). To identify the region within the HER2 promoter responsible for CDCA inhibitory effects, HER2 promoter-deleted construct (–232 pNeuLite) activity was tested (Figure 4b). We observed that the responsiveness to CDCA was still maintained, suggesting that the region from –232 to +1 containing the NF- $\kappa\text{B}$  motif might be involved in transrepression mechanisms exerted by activated FXR (Figures 4c and d). Thus, we performed site-directed mutagenesis on the NF- $\kappa\text{B}$  domain (NF- $\kappa\text{B}$  Mut) within the HER2 promoter (Figure 4b). Mutation of this

domain abrogated CDCA effects (Figures 4c and d). These latter results demonstrate that the integrity of NF- $\kappa\text{B}$ -binding site is necessary for FXR modulation of HER2 promoter activity in breast cancer cells.

The specific role of the NF- $\kappa\text{B}$  motif in the transcriptional regulation of HER2 by CDCA was investigated using electrophoretic mobility shift assays. We observed the formation of a complex in nuclear extracts from MCF-7 and MCF-7 TR1 cells using synthetic oligodeoxyribonucleotides corresponding to the NF- $\kappa\text{B}$  motif (Figure 5a, lanes 1 and 5), which was abrogated by incubation with 100-fold molar excess of unlabeled probe (Figure 5a, lanes 2 and 6), demonstrating the specificity of the DNA-binding complex. This inhibition was no longer observed when mutated oligodeoxyribonucleotide was used as competitor (Figure 5a, lanes 3 and 7). Interestingly, treatment with CDCA strongly decreased the DNA-binding protein complex compared with

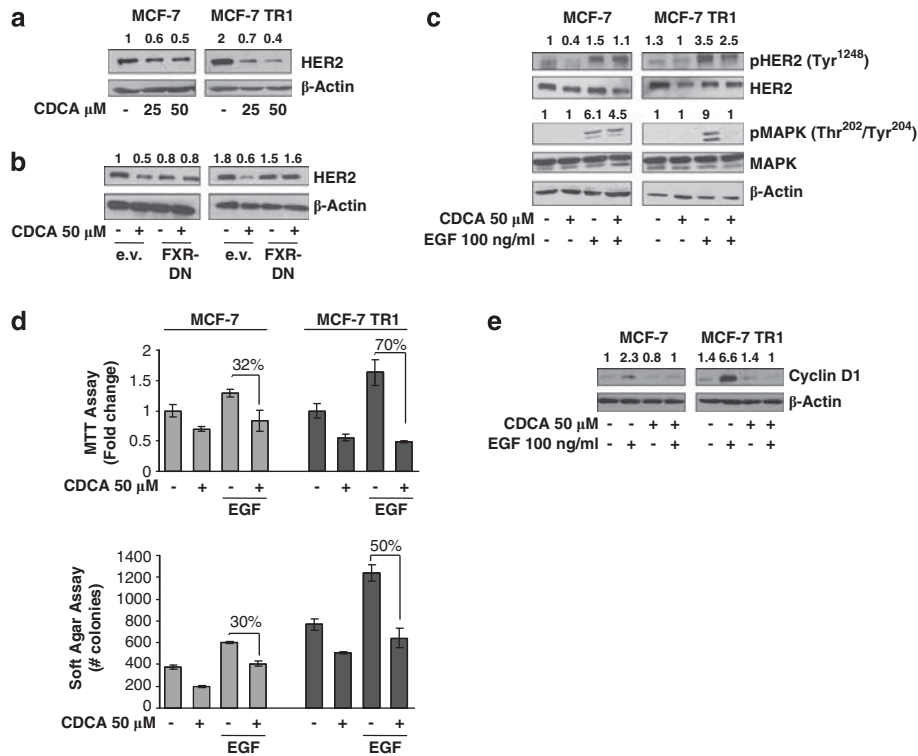


**Figure 3** Effects of CDCA on HER2 expression and its transduction pathways in MCF-7 and MCF-7 TR1 cells. (a) MCF-7 and MCF-7 TR1 cells were treated for 24h with vehicle (–) or CDCA 25 and 50 μM before lysis. Equal amounts of total cellular extract were analyzed for HER2 levels by western blotting. β-Actin was used as loading control. (b) Cells were transiently transfected with either empty vector (e.v.) or FXR-DN plasmids and then treated with vehicle (–) or CDCA 50 μM for 24h and HER2 levels were evaluated by western blotting. β-Actin was used as loading control. (c) Immunoblot analysis showing phosphorylated HER2 (pHER2 Tyr<sup>1248</sup>) and MAPK (pMAPK Thr<sup>202</sup>/Tyr<sup>204</sup>), total HER2, total MAPK in MCF-7 and MCF-7 TR1 cells pretreated for 24h with CDCA 50 μM and then treated for 10min with EGF 100 ng/ml. β-Actin was used as loading control. (d) MTT growth assay (upper panel) and soft-agar assay (lower panel) in cells treated with CDCA 50 μM with or without EGF 100 ng/ml for 4 days and 14 days, respectively. The MTT assay results are expressed as fold change ± s.d. relative to vehicle-treated cells and are representative of three different experiments each performed in triplicate. The soft-agar assay values are represented as a mean of colonies number > 50 μm diameter counted at the end of assay. Percentages of inhibition induced by CDCA versus EGF treatment alone are shown. (e) Cells were treated for 24h with vehicle (–) or EGF 100 ng/ml in the presence or not of CDCA 50 μM before lysis and then cellular extracts were analyzed for cyclin D1 levels by western blot analysis. β-Actin was used as loading control. Numbers on top of the blots represent the average fold change versus control of MCF-7 cells normalized for β-Actin.

control samples (Figure 5a, lanes 4 and 8). The inclusion of an anti-NF-κB antibody in the reaction immunodepleted the specific band, confirming the presence of NF-κB in the complex (Figure 5b, lanes 3 and 9). Nonspecific IgG did not affect NF-κB complex formation (Figure 5b, lanes 4 and 10). Recombinant NF-κB protein revealed a complex migrating at the same level as that of nuclear extracts from cells (Figure 5a, lane 9; Figure 5b, lanes 5 and 11). Of note, the CDCA-induced reduction in the DNA-binding complex was no longer observed utilizing as probe synthetic oligodeoxyribonucleotides corresponding to the AP-1 and Sp1 motifs (Supplementary Figures 1a and b). To better define the role of FXR in the inhibition of NF-κB binding on HER2 promoter, a competition assay using recombinant NF-κB protein and increasing amounts of *in vitro*-translated FXR protein (1, 3 and 5 μl) was carried out. A dose-dependent reduction in the NF-κB complex was seen (Figure 5c, lanes 1–4), suggesting that physical interaction between these two transcription factors may inhibit the binding of NF-κB to human HER2 promoter

region. To further test this possibility, we performed coimmunoprecipitation studies using nuclear protein fractions from MCF-7 and MCF-7TR1 cells treated with CDCA. As shown in Figure 6a, the formation of an FXR and NF-κB complex was detected in untreated cells, and this association was enhanced with FXR ligand treatment.

Moreover, to confirm the involvement of NF-κB in CDCA-mediated HER2-downregulation at the promoter level, ChIP assays were performed. Using specific antibodies against NF-κB and RNA-polymerase II, protein–chromatin complexes were immunoprecipitated from cells cultured with or without CDCA for 1h. The resulting precipitated DNA was then quantified using real-time PCR with primers spanning the NF-κB-binding element in the HER2 promoter region. NF-κB recruitment was significantly decreased upon CDCA treatment in both cell lines (Figure 6b). This result was well correlated with a lower association of RNA-polymerase II to the HER2 regulatory region (Figure 6c).

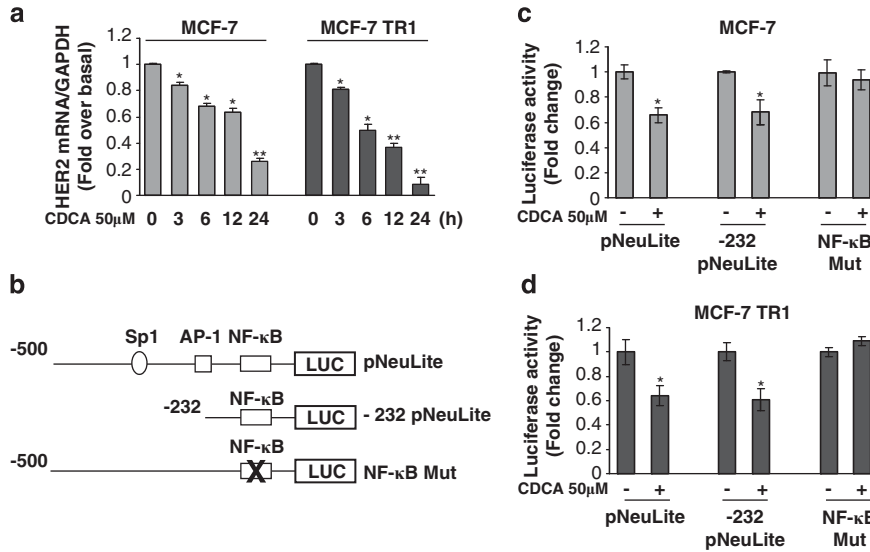


**Figure 4** Effects of CDCA on human HER2 promoter activity. (a) mRNA HER2 content, evaluated by real-time RT-PCR, after treatment with vehicle or CDCA 50  $\mu$ M, as indicated. Each sample was normalized to its GAPDH mRNA content. \* $P < 0.05$  and \*\* $P < 0.001$  compared with vehicle. (b) Schematic map of the human HER2/neu promoter region constructs used in this study. All of the promoter constructs contain the same 3' boundary. The 5' boundaries of the promoter fragments varied from -500 (pNeuLite) to -232 (-232 pNeuLite). A mutated NF- $\kappa$ B-binding site is present in NF- $\kappa$ B mut construct. HER2 transcriptional activity in MCF-7 (c) and MCF-7 TR1 (d) cells transfected with promoter constructs are shown. After transfection, cells were treated in the presence of vehicle (-) or CDCA 50  $\mu$ M for 6 h. The values represent the means  $\pm$  s.d. of three different experiments each performed in triplicate. \* $P < 0.05$  compared with vehicle.

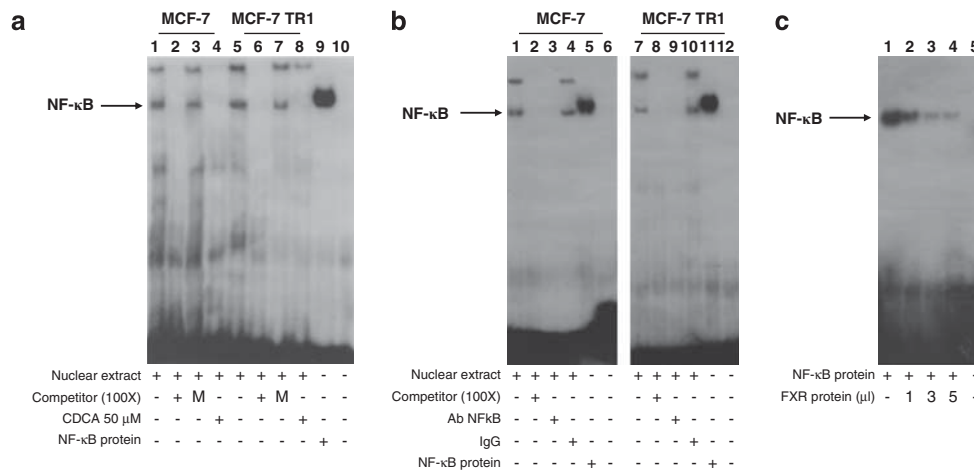


**Figure 5** Electrophoretic mobility shift assay of the NF- $\kappa$ B-binding site in the HER2 promoter region. (a) Nuclear extracts from MCF-7 and MCF-7 TR1 cells were incubated with a double-stranded NF- $\kappa$ B specific sequence probe labeled with [ $^{32}$ P]ATP and subjected to electrophoresis in a 6% polyacrylamide gel (lanes 1 and 5). Competition experiments were performed adding as competitor a 100-fold molar excess of unlabeled probe (lanes 2 and 6) or a 100-fold molar excess of unlabeled oligonucleotide containing a mutated NF- $\kappa$ B RE (lanes 3 and 7). Lanes 4 and 8, nuclear extracts from CDCA (50  $\mu$ M)-treated MCF-7 and MCF-7 TR1 cells, respectively, incubated with probe. Lane 9, NF- $\kappa$ B protein. Lane 10, probe alone. (b) Nuclear extracts from MCF-7 and MCF-7 TR1 cells were incubated with a double-stranded NF- $\kappa$ B specific sequence probe labeled with [ $^{32}$ P]ATP (lanes 1 and 7) or with a 100-fold molar excess of unlabeled probe (lanes 2 and 8). Nuclear extracts incubated with anti-NF- $\kappa$ B (lanes 3 and 9) or IgG (lanes 4 and 10). Lanes 5 and 11, NF- $\kappa$ B protein. Lanes 6 and 12, probe alone. (c) Lane 1, NF- $\kappa$ B protein. Lanes 2, 3 and 4, NF- $\kappa$ B protein incubated with increasing doses (1, 3 and 5  $\mu$ l) of transcribed and translated *in vitro* FXR protein. Lane 5, probe alone.

To further confirm the transcriptional repression mediated by activated FXR, we also evaluated the histone deacetylase 3 association on the NF- $\kappa$ B-responsive sequence within the HER2 promoter. CDCA stimulation enhanced the recruitment of histone deacetylase 3 to this NF- $\kappa$ B promoter site (Figure 6d).

*HER2 downregulation underlies the ability of FRX ligands to inhibit breast cancer cell growth*

We evaluated the effects of CDCA on cell growth in the ER $\alpha$ -negative and HER2-overexpressing breast cancer cells SKBR3. Treatment with CDCA inhibited SKBR3 anchorage-dependent growth in a dose-dependent

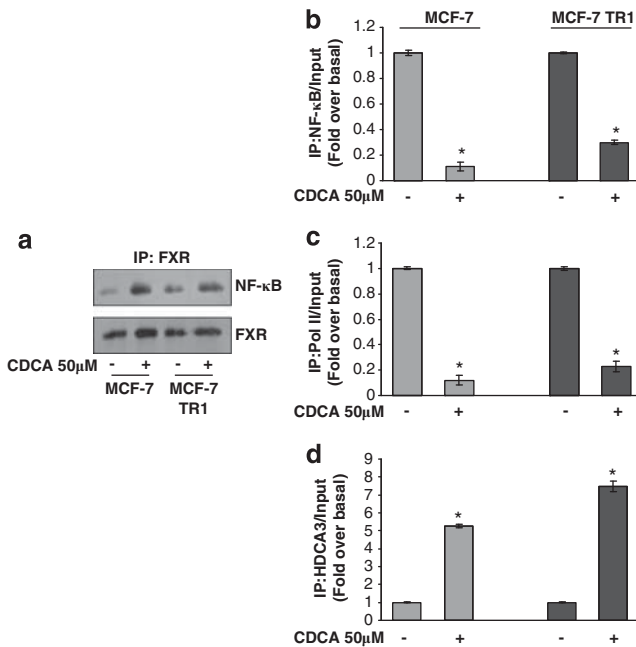


**Figure 6** FXR inhibits NF-κB recruitment to HER2 promoter. (a) MCF-7 and MCF-7 TR1 cells were treated with vehicle (–) or CDCA 50 μM for 1 h before lysis. FXR protein was immunoprecipitated using an anti-FXR polyclonal antibody (IP:FXR) and resolved in SDS–polyacrylamide gel electrophoresis. Immunoblotting was performed using an anti-NF-κB (p65 subunit) monoclonal antibody and anti-FXR antibody. MCF-7 and MCF-7 TR1 cells were treated in the presence of vehicle (–) or CDCA 50 μM for 1 h, then crosslinked with formaldehyde, and lysed. The precleared chromatin was immunoprecipitated with anti-NF-κB (b), anti-RNA polymerase II (c) and anti-HDCA3 (d) antibodies. A 5 μl volume of each sample and input was analyzed by real-time PCR using specific primers to amplify HER2 promoter sequence, including the NF-κB site. Similar results were obtained in multiple independent experiments. \**P* < 0.01 compared with vehicle.

manner (Figure 7a) and reduced colony growth in anchorage-independent assay (Figure 7b). Indeed, we found, after 48 h of treatment with CDCA, a marked decrease in both HER2 protein and mRNA levels (Figures 7c and d). In these cells, HER2 promoter activity was similarly reduced with CDCA treatment (Figure 7e).

Finally, we explored the ability of FXR ligands to inhibit proliferation using as additional model Tam-resistant derivative cell line engineered to stably overexpress HER2 (MCF-7/HER2-18). As expected, Tam-resistant growth in these cells was not affected by both CDCA and GW4064 treatments (Figure 7f). Altogether, these results well evidence how FXR-mediated downregulation of HER2 at transcriptional level is fully responsible for inhibiting breast cancer cell proliferation.

## Discussion

In this study, we show for the first time that the activated FXR downregulates HER2 expression in ERα-positive breast cancer cells resistant to Tam. This occurs through the inhibition of NF-κB binding to its responsive element located in the human HER2

promoter region and results in a significant reduction of Tam-resistant growth.

The HER2/neu transmembrane kinase receptor is a signaling amplifier of the HER family network, as activation of membrane tyrosine receptors (EGFR, HER3 and HER4) by their respective ligands determines the formation of homodimeric and heterodimeric kinase complexes into which this receptor is recruited as a preferred partner (Yarden, 2001). Multiple lines of evidences suggest a role of HER2 in the pathogenesis of breast carcinoma (Allred *et al.*, 1992; Glockner *et al.*, 2001), and clinical data suggest that breast tumors expressing elevated levels of HER2 show a more aggressive phenotype and worse outcome when treated with Tam (Arpino *et al.*, 2004; De Laurentiis *et al.*, 2005). Thus, inhibitory agents targeting HER2, such as the monoclonal antibody trastuzumab (herceptin), have been explored to improve hormonal treatment or delay emergence of endocrine resistance in estrogen-dependent breast tumors (Johnston, 2009). However, even though an increased response rate is obtained when trastuzumab is used in combination with chemotherapeutic agents (Seidman *et al.*, 2001; Slamon *et al.*, 2001), patients can still develop resistance (Slamon *et al.*, 2001). These observations highlight the importance of discovering new therapeutic tools interfering with HER2-driven signaling to overcome therapy resistance.

We have demonstrated that treatment of breast cancer cells resistant to Tam with the FXR natural ligand CDCA resulted in a reduction of HER2 protein expression. Similar results were also obtained in the ERα-negative and HER2-overexpressing SKBR3 breast cancer cells, suggesting that it may represent a general mechanism not related to cell specificity. Moreover, it assumes more relevance in Tam-resistant breast cancer cells, which are strongly dependent on HER2 activity for their growth. The complete abrogation of FXR-mediated HER2 downregulation with expression of an FXR-DN vector, along with the effects exerted by the synthetic FXR agonist GW4064, clearly demonstrated that activated FXR is involved in the regulation of HER2 expression. Furthermore, quantitative RT-PCR analysis demonstrated that HER2 mRNA levels were significantly decreased in both MCF-7 and MCF-7 TR1 cells treated with CDCA, suggesting that the FXR-induced HER2 downregulation arises via transcriptional mechanisms. Therefore, we focused on the molecular mechanisms by which FXR mediates repression of *HER2* gene expression and on the biological consequences of FXR activation on anti-estrogen-resistant growth of breast cancer cells.

FXR acts mainly by regulating the expression of target genes by binding either as a monomer or heterodimer with the retinoid X receptor to FXR response elements (Laffitte *et al.*, 2000; Ananthanarayanan *et al.*, 2001; Claudel *et al.*, 2002; Kalaany and Mangelsdorf, 2006). Human HER2 promoter did not display any FXR response elements, thus it is reasonable to hypothesize that FXR-induced downregulation of HER2 promoter activity may occur through its interaction with other transcriptional factors. For instance, it

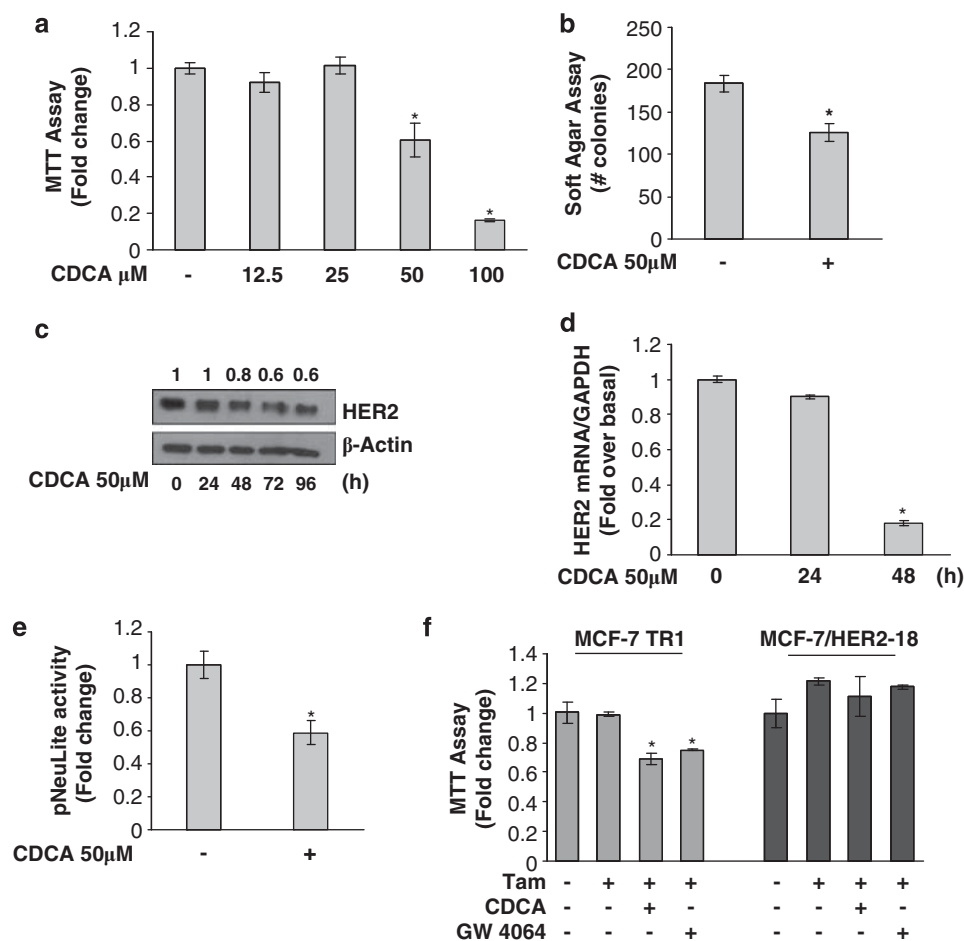


**Figure 7** Effects of FXR ligand on SKBR3 breast cancer cells. **(a)** MTT proliferation assay of SKBR3 cells treated with vehicle (–) or increasing doses of CDCA (12.5–25–50–100  $\mu\text{M}$ ) for 7 days. Results are expressed as fold change  $\pm$  s.d. relative to vehicle-treated cells and are representative of three different experiments each performed in triplicate. **(b)** Soft-agar growth assay in SKBR3 cells plated in 0.35% agarose and treated with vehicle (–) or CDCA 50  $\mu\text{M}$ . After 14 days of growth, colonies >50  $\mu\text{m}$  diameter were counted. **(c)** SKBR3 cells were treated with CDCA 50  $\mu\text{M}$  as indicated before lysis. Equal amounts of total cellular extract were analyzed for HER2 levels by western blotting.  $\beta$ -Actin was used as loading control. Numbers on top of the blots represent the average fold change relative to control normalized for  $\beta$ -Actin. **(d)** mRNA HER2 content, evaluated by real-time RT–PCR, after treatment with CDCA 50  $\mu\text{M}$  as indicated. Each sample was normalized to its GAPDH mRNA content. **(e)** SKBR3 cells were transiently transfected with pNeuLite construct. After transfection, cells were treated in the presence of vehicle (–) or CDCA 50  $\mu\text{M}$  for 24 h and the promoter activity was evaluated. The values represent the means  $\pm$  s.d. of three different experiments each performed in triplicate. \* $P$ <0.05 compared with vehicle. **(f)** MTT growth assay in MCF-7 TR1 and MCF-7/HER2-18 cells treated with vehicle (–), CDCA 50  $\mu\text{M}$  and GW4064 3  $\mu\text{M}$  in the presence or not of Tam 1  $\mu\text{M}$  for 4 days. Results are expressed as fold change  $\pm$  s.d. relative to vehicle-treated cells and are representative of three different experiments each performed in triplicate. \* $P$ <0.05 compared with Tam alone.

has been described the transrepression mechanisms for FXR-mediated inhibition of endothelin-1 expression in vascular endothelial cells (He *et al.*, 2006). In addition, it has also been demonstrated that FXR negatively regulates IL-1 $\beta$  expression by stabilizing the nuclear corepressor NCoR on the NF- $\kappa$ B sequence within the IL-1 $\beta$  promoter (Vavassori *et al.*, 2009). Several recognition elements are present within the HER2 proximal promoter (Ishii *et al.*, 1987; Hurst, 2001) and among these functional motifs we have identified both AP-1 and NF- $\kappa$ B response elements as potential targets of FXR. We have demonstrated by functional studies and site-specific mutagenesis analysis that the integrity of the NF- $\kappa$ B sequence is a prerequisite for the downregulatory effects of the FXR ligand on HER2 promoter

activity. These results were supported by electrophoretic mobility shift assays, which revealed a marked decrease in a specific DNA-binding complex in nuclear extracts from MCF-7 and MCF-7 TR1 cells treated with CDCA. *In vitro* competition studies showed that FXR protein was able to inhibit the binding of NF- $\kappa$ B to its consensus site on the HER2 promoter. Furthermore, we observed a reduced recruitment of both NF- $\kappa$ B and RNA polymerase II in CDCA-treated cells, concomitant with an enhanced recruitment of histone deacetylase 3 supporting a negative transcriptional role for FXR in modulating HER2 expression.

The physiological relevance of these effects is pointed out by proliferation studies showing that FXR activation reduced breast cancer cell growth, but did not affect

the proliferation of the non-tumorigenic breast epithelial MCF-10A cell line. MCF-7 TR1 cells exhibited lower  $IC_{50}$  values for both ligands compared with parental MCF-7 cells, suggesting a higher sensitivity of the Tam-resistant cells to the effects of FXR ligands. This suggestion is also well supported by the results obtained from growth assays, showing that combined treatment with CDCA and Tam significantly reduced Tam-resistant growth in MCF-7 TR1 cells, compared with Tam alone, but had no additive effects in MCF-7 parental cells. Moreover, FXR ligands failed to inhibit Tam-resistant growth in MCF-7/HER2-18 cells, in which HER2 expression is not driven by its own gene promoter activity. These latter results provided evidences that the downregulation of HER2 expression at transcriptional level underlies the ability of activated FXR to inhibit Tam-resistant growth in breast cancer cells.

Previous *in vitro* studies showed that enhanced EGFR/HER2 expression together with activation of downstream signaling pathways such as p42/44 MAPK are involved in acquired Tam resistance (Knowlden *et al.*, 2003; Nicholson *et al.*, 2004). Our studies showed that CDCA treatment significantly reduced the ability of EGF to activate its signal transduction cascade in MCF-7 TR1 cells, inhibiting both HER2 and MAPK phosphorylation. In addition, FXR activation was associated with a marked inhibition in EGF-induced growth, concomitant with a reduction in cyclin D1 expression in Tam-resistant breast cancer cells. All together these data demonstrate, as represented in Figure 8, that activated FXR, by preventing the binding of NF- $\kappa$ B to its response element located in the HER2 promoter sequence, abrogates HER2 expression and

signaling, resulting in an inhibition of Tam-resistant growth in breast cancer cells.

Deciphering the molecular mechanisms responsible for the development of hormonal resistance is essential for establishing the most appropriate hormone agent according to tumor characteristics and for defining the optimal sequence of endocrine therapies. Moreover, this knowledge is critical for development of new therapeutic approaches able to either overcome or prevent endocrine resistance in breast cancer patients. Over the last years, significant survival benefits for breast cancer were derived from the use of combined treatment of endocrine therapies with new targeted therapies in endocrine responsive breast cancer (Johnston, 2009). In this scenario, the sequencing or the combination of Tam with FXR ligands may represent an important research issue to explore as an alternative therapeutic strategy to treat breast cancer patients whose tumors exploit HER2 signaling to escape Tam treatment.

## Materials and methods

### Reagents and antibodies

The following components were obtained from the given respective companies, with their addresses in brackets. DMEM, L-glutamine, penicillin, streptomycin, fetal bovine serum, MTT, 4-hydroxytamoxifen, CDCA and EGF from Sigma (Milan, Italy). TRIzol by Invitrogen (Carlsbad, CA, USA). FuGENE 6 by Roche (Indianapolis, IN, USA). TaqDNA polymerase, RETROscript kit, Dual Luciferase kit, TNT master mix and NF- $\kappa$ B protein from Promega (Madison, WI, USA). SYBR Green Universal PCR Master Mix by Bio-rad (Hercules, CA, USA). Antibodies against FXR,  $\beta$ -actin, Cyclin D1, p65, ER $\alpha$ , EGFR and Lamin B by Santa Cruz

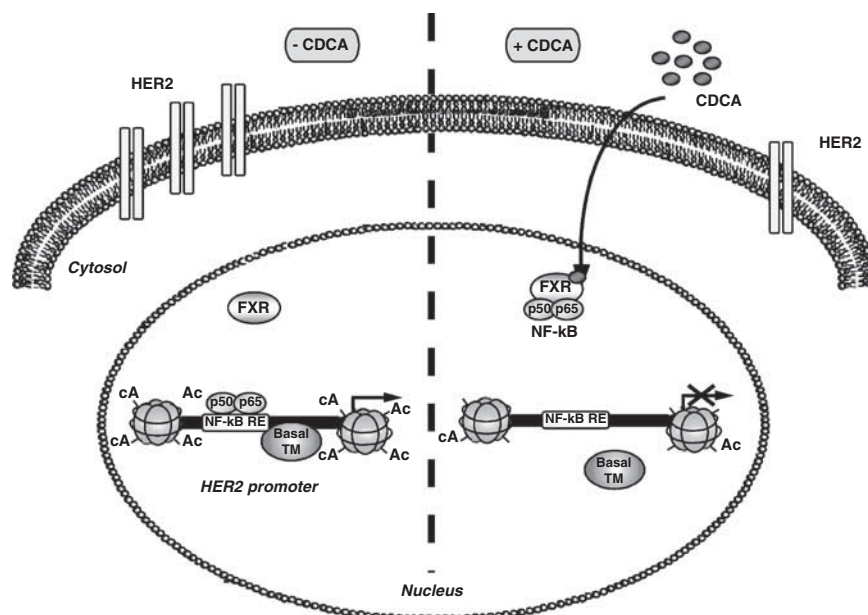


**Figure 8** Proposed working model of the FXR-mediated regulation of HER2 expression in Tam-resistant breast cancer cells. In the absence of CDCA, HER2 expression is regulated by several serum factors, including NF- $\kappa$ B, acting through a regulatory region in HER2 promoter and enabling gene transcription. Upon CDCA treatment, FXR binds NF- $\kappa$ B, inhibiting its recruitment on the response element located in the proximal HER2 promoter, causing displacement of RNA polymerase II with consequent repression of HER2 expression.

Biotechnology (Santa Cruz, CA, USA). MAPK, phosphorylated p42/44 MAPK (Thr<sup>202</sup>/Tyr<sup>204</sup>), phosphorylated HER2 (Tyr<sup>1248</sup>) from Cell Signaling Technology (Beverly, MA, USA). HER2 from NeoMarker (Fremont, CA, USA). ECL system and Sephadex G-50 spin columns from Amersham Biosciences (Buckinghamshire, UK). [ $\gamma$ -<sup>32</sup>P]ATP from PerkinElmer (Wellesley, MA, USA). Herceptin from Genentech (San Francisco, CA, USA).

#### Plasmids

The plasmid pNeuLite containing human HER2/neu promoter region was kindly provided by Dr Mien-Chie Hung (University of Texas, M.D. Anderson Cancer Center, Houston, TX, USA) (Xing *et al.*, 2000). The FXR-responsive reporter gene (*FXRE-IR1*) and FXR-DN expression plasmids were provided from Dr T.A. Kocarek (Institute of Environmental Health Sciences, Wayne State University, USA) (Kocarek *et al.*, 2002).

The -232 pNeuLite construct was generated by PCR using as template the pNeuLite plasmid with the following primers: forward 5'-GATAAGTGTGAGAACGGCTGCAGGC-3' and reverse 5'-GGGCAGATCTGGTTTCCGGTCCCAATGGA-3'. The amplified DNA fragment was digested with *Bgl*III and *Kpn*I and ligated into pGL2-basic vector. Deletion was confirmed by DNA sequencing.

#### Site-directed mutagenesis

The pNeuLite promoter plasmid-bearing NF- $\kappa$ B-responsive element-mutated site (NF- $\kappa$ B mut) was created by site-directed mutagenesis using Quick Change kit (Stratagene, La Jolla, CA, USA), according to manufacturer's method. We used as template the pNeuLite plasmid and the following primers (mutations are shown as lowercase letters): 5'-AGAGAGGGAGAAAGTGAAGCTaatcGTTGCCGACTCCCAGACTTCG-3' and 5'-CGAAGTCTGGGAGTCGGCAACgattAGCTTCACTTTCTCCCTCTCT-3'. Mutation was confirmed by DNA sequencing.

#### Cell culture

MCF-7 cells were cultured in DMEM containing 10% fetal bovine serum. MCF-7 TR1 and MCF-7 TR2 cells were generated in the laboratory of Dr Fuqua as previously described (Barone *et al.*, 2011) and maintained with 10<sup>-6</sup> M (MCF-7 TR1) and 10<sup>-7</sup> M (MCF-7 TR2) of 4-hydroxytamoxifen. SKBR3 cells were cultured in phenol red-free RPMI medium containing 10% fetal bovine serum. MCF-10A normal breast epithelial cells were grown in DMEM-F12 medium containing 5% horse serum. MCF-7/HER2-18 were kindly provided by Dr Schiff (Baylor College of Medicine, Houston, TX, USA) and maintained as described (Shou *et al.*, 2004). Before each experiment, cells were grown in phenol red-free medium, containing 5% charcoal-stripped fetal bovine serum for 2 days and treated as described.

#### Cell proliferation assays

Cell proliferation was assessed using MTT and soft-agar anchorage-independent growth assays as described (Barone *et al.*, 2009; Giordano *et al.*, 2010). The IC<sub>50</sub> values were calculated using GraphPad Prism 4 (GraphPad Software Inc., San Diego, CA) as described (Herynk *et al.*, 2006).

#### Immunoprecipitation and immunoblot analysis

Cells were treated as indicated before lysis for total protein extraction (Catalano *et al.*, 2010). Nuclear extracts were prepared as described (Morelli *et al.*, 2004). For coimmuno-

precipitation experiments, we used 1 mg of nuclear protein extract and 2  $\mu$ g of FXR antibody, followed by protein A/G precipitation. Equal amounts of cell extracts and coimmunoprecipitated protein were subjected to SDS-polyacrylamide gel electrophoresis, as described (Catalano *et al.*, 2010).

#### RT-PCR and Real-time RT-PCR assays

FXR gene expression was evaluated by the RT-PCR method using a RETROscript kit. The cDNAs obtained were amplified using the following primers: forward 5'-CGAGCCTGAAGAGTGGTACTGTC-3' and reverse 5'-CATTTCAGCCAACA TTCCCATCTC-3' (FXR); forward 5'-CTCAACATCTCCCCTTCTC-3' and reverse 5'-CAAATCCCATATCCTCGT-3' (36B4).

The PCR was performed for 35 cycles for hFXR (94 °C 1 min, 65 °C 1 min, 72 °C 1 min) and 18 cycles for 36B4 (94 °C for 1 min, 58 °C for 1 min and 72 °C for 1 min), as described (Catalano *et al.*, 2010).

*HER2* gene expression was evaluated by real-time RT-PCR. Total RNA was reverse transcribed with the RETROscript kit; 5  $\mu$ l of diluted (1:3) cDNA was analyzed in triplicates by real-time PCR in an iCycler iQ Detection System (Bio-Rad) using SYBR Green Universal PCR Master Mix, following the manufacturer's recommendations. Each sample was normalized on its GAPDH mRNA content. Primers used for the amplification were: forward 5'-CACCTACAACACAGACACGTTTGA-3' and reverse 5'-GCAGACGAGGGTGCAGGAT-3' (HER2); forward 5'-CCCCTCCTCCACCTTTGAC-3' and reverse 5'-TGTTGCTGTAGCCAAATTCGTT-3' (GAPDH). The relative gene expression levels were calculated as described (Sirianni *et al.*, 2007).

#### Transient transfection assays

MCF-7 and MCF-7 TR1 cells were transiently transfected using the FuGENE 6 reagent with FXR reporter gene (*FXRE-IR1*) in the presence or absence of FXR-DN plasmid. In a set of experiments, MCF-7, MCF-7 TR1 and SKBR3 cells were transfected with different HER2 promoter constructs. Luciferase activity was assayed as described (Catalano *et al.*, 2010).

#### Electrophoretic mobility shift assays

Nuclear extracts from cells, treated or not for 3 h with CDCA, were prepared as described (Andrews and Faller, 1991). The DNA sequences used as probe or as cold competitors are the following (nucleotide motifs of interest are underlined and mutations are shown as lowercase letters): NF- $\kappa$ B, 5'-AA GTGAAGCTGGGAGTTGCCGACTCCCAGA-3'; mutated NF- $\kappa$ B, 5'-AAGTGAAGCTaatcGTTGCCGACTCCCAGA-3'; AP-1, 5'-AGGGGGCAGAGTCAC CAGCCTCTG-3'; mutated AP-1, 5'-AGGGGGCAtcaTCACCAGCCTCTG-3'; Sp1 5'-ATCCCGGACTCCGGGGGAGGGGGC-3'; mutated Sp1, 5'-ATCCCGGACCTCattG GGAGGGGGC-3'. *In vitro*-transcribed and -translated FXR protein was synthesized using the T7 polymerase in the rabbit reticulocyte lysate system. Probe generation and the protein-binding reactions were carried out as described (Catalano *et al.*, 2010). For experiments involving anti-NF- $\kappa$ B (p65) antibody, the reaction mixture was incubated with this antibody at 4 °C for 12 h before addition of labeled probe.

#### Chromatin immunoprecipitation assays

Cells were treated with CDCA or left untreated for 1 h and then DNA/protein complexes were extracted as described (Catalano *et al.*, 2010). The precleared chromatin was immunoprecipitated with anti-NF- $\kappa$ B (p65), anti-histone

deacetylase 3 or anti-polymerase II antibodies. A normal mouse serum IgG was used as negative control. A 5 µl volume of each sample and input DNA was used for real-time PCR using the primers flanking NF-κB sequence in the human HER2 promoter region: 5'-TGAGAACGGCTGCAGGCAAC-3' and 5'-CCCACCAACTGCATTCCAA-3'. Real-time PCR was performed as described above. Final results were calculated using the  $\Delta\Delta C_t$  method, using input Ct values instead of the GAPDH mRNA. The basal sample was used as calibrator.

#### Statistical analyses

Each datum point represents the mean  $\pm$  s.d. of three different experiments. Data were analyzed by Student's *t*-test using the GraphPad Prism 4 software program.  $P < 0.05$  was considered as statistically significant.

## References

- Allred DC, Clark GM, Molina R, Tandon AK, Schnitt SJ, Gilchrist KW et al. (1992). Overexpression of HER-2/neu and its relationship with other prognostic factors change during the progression of *in situ* to invasive breast cancer. *Hum Pathol* **23**: 974–979.
- Ananthanarayanan M, Balasubramanian N, Makishima M, Mangelsdorf DJ, Suchy FJ. (2001). Human bile salt export pump promoter is transactivated by the farnesoid X receptor/bile acid receptor. *J Biol Chem* **276**: 28857–28865.
- Andrews NC, Faller DV. (1991). A rapid micropreparation technique for extraction of DNA-binding proteins from limiting numbers of mammalian cells. *Nucleic Acids Res* **19**: 2499.
- Arpino G, Green SJ, Allred DC, Lew D, Martino S, Osborne CK et al. (2004). HER-2 amplification, HER-1 expression, and tamoxifen response in estrogen receptor-positive metastatic breast cancer: a southwest oncology group study. *Clin Cancer Res* **10**: 5670–5676.
- Arpino G, Wiechmann L, Osborne CK, Schiff R. (2008). Crosstalk between the estrogen receptor and the HER tyrosine kinase receptor family: molecular mechanism and clinical implications for endocrine therapy resistance. *Endocr Rev* **29**: 217–233.
- Barone I, Brusco L, Gu G, Selever J, Beyer A, Covington KR et al. (2011). Loss of Rho GDI  $\alpha$  and resistance to tamoxifen via effects on estrogen receptor  $\alpha$ . *Journal Natl Cancer Inst* (in press).
- Barone I, Cui Y, Herynk MH, Corona-Rodriguez A, Giordano C, Selever J et al. (2009). Expression of the K303R estrogen receptor- $\alpha$  breast cancer mutation induces resistance to an aromatase inhibitor via addiction to the PI3K/Akt kinase pathway. *Cancer Res* **69**: 4724–4732.
- Bishop-Bailey D. (2004). FXR as a novel therapeutic target for vascular disease. *Drug News Perspect* **17**: 499–504.
- Blume-Jensen P, Hunter T. (2001). Oncogenic kinase signalling. *Nature* **411**: 355–365.
- Catalano S, Malivindi R, Giordano C, Gu G, Panza S, Bonfiglio D et al. (2010). Farnesoid X receptor, through the binding with steroidogenic factor 1-responsive element, inhibits aromatase expression in tumor Leydig cells. *J Biol Chem* **285**: 5581–5593.
- Chung YL, Sheu ML, Yang SC, Lin CH, Yen SH. (2002). Resistance to tamoxifen-induced apoptosis is associated with direct interaction between Her2/neu and cell membrane estrogen receptor in breast cancer. *Int J Cancer* **97**: 306–312.
- Claudel T, Sturm E, Duez H, Torra IP, Sirvent A, Kosykh V et al. (2002). Bile acid-activated nuclear receptor FXR suppresses apolipoprotein A-I transcription via a negative FXR response element. *J Clin Invest* **109**: 961–971.
- De Laurentis M, Arpino G, Massarelli E, Ruggiero A, Carlomagno C, Ciardiello F et al. (2005). A meta-analysis on the interaction between HER-2 expression and response to endocrine treatment in advanced breast cancer. *Clin Cancer Res* **11**: 4741–4748.
- Encarnacion CA, Ciocca DR, McGuire WL, Clark GM, Fuqua SA, Osborne CK. (1993). Measurement of steroid hormone receptors in breast cancer patients on tamoxifen. *Breast Cancer Res Treat* **26**: 237–246.
- Fisher B, Costantino JP, Wickerham DL, Redmond CK, Kavanah M, Cronin WM et al. (1998). Tamoxifen for prevention of breast cancer: report of the National Surgical Adjuvant Breast and Bowel Project P-1 Study. *J Natl Cancer Inst* **90**: 1371–1388.
- Forman BM, Goode E, Chen J, Oro AE, Bradley DJ, Perlmann T et al. (1995). Identification of a nuclear receptor that is activated by farnesol metabolites. *Cell* **81**: 687–693.
- Giordano C, Cui Y, Barone I, Andò S, Mancini MA, Berno V et al. (2010). Growth factor-induced resistance to tamoxifen is associated with a mutation of estrogen receptor  $\alpha$  and its phosphorylation at serine 305. *Breast Cancer Res Treat* **119**: 71–85.
- Glockner S, Lehmann U, Wilke N, Kleeberger W, Langer F, Kreipe H. (2001). Amplification of growth regulatory genes in intraductal breast cancer is associated with higher nuclear grade but not with the progression to invasiveness. *Lab Invest* **81**: 565–571.
- Gradishar WJ. (2004). Tamoxifen—what next? *Oncologist* **9**: 378–384.
- Gutierrez MC, Detre S, Johnston S, Mohsin SK, Shou J, Allred DC et al. (2005). Molecular changes in tamoxifen-resistant breast cancer: relationship between estrogen receptor, HER-2, and p38 mitogen-activated protein kinase. *J Clin Oncol* **23**: 2469–2476.
- He F, Li J, Mu Y, Kuruba R, Ma Z, Wilson A et al. (2006). Downregulation of endothelin-1 by farnesoid X receptor in vascular endothelial cells. *Circ Res* **98**: 192–199.
- Herynk MH, Beyer AR, Cui Y, Weiss H, Anderson E, Green TP et al. (2006). Cooperative action of tamoxifen and c-Src inhibition in preventing the growth of estrogen receptor-positive human breast cancer cells. *Mol Cancer Ther* **5**: 3023–3031.
- Hurst HC. (2001). Update on HER-2 as a target for cancer therapy: the ERBB2 promoter and its exploitation for cancer treatment. *Breast Cancer Res* **3**: 395–398.
- Ishii S, Imamoto F, Yamanashi Y, Toyoshima K, Yamamoto T. (1987). Characterization of the promoter region of the human c-erbB-2 protooncogene. *Proc Natl Acad Sci USA* **84**: 4374–4378.
- Johnston SR. (2009). Enhancing the efficacy of hormonal agents with selected targeted agents. *Clin Breast Cancer* **9**(Suppl 1): S28–S36.
- Journe F, Laurent G, Chaboteaux C, Nonclercq D, Durbecq V, Larsimont D et al. (2008). Farnesol, a mevalonate pathway intermediate, stimulates MCF-7 breast cancer cell growth through farnesoid-X-receptor-mediated estrogen receptor activation. *Breast Cancer Res Treat* **107**: 49–61.
- Kalaany NY, Mangelsdorf DJ. (2006). LXRS and FXR: the yin and yang of cholesterol and fat metabolism. *Annu Rev Physiol* **68**: 159–191.

## Conflict of interest

The authors declare no conflict of interest.

## Acknowledgements

This work was supported by AIRC grants, MIUR Ex 60% 2009, PRIN 2009 and Lilli Funaro Foundation. NIH/NCI R01 CA72038 and RP101251 from the Cancer Prevention and Research Institute of Texas (SAWF). We thank Dr Mien-Chie Hung for providing the pNeuLite plasmid and Dr T.A. Kocarek for providing the FXR-responsive reporter gene and FXR-DN expression plasmids. We also thank Dr Rachel Schiff for providing the MCF-7/HER2-18 cells.

- Kirkegaard T, McGlynn LM, Campbell FM, Muller S, Tovey SM, Dunne B *et al.* (2007). Amplified in breast cancer 1 in human epidermal growth factor receptor—positive tumors of tamoxifen-treated breast cancer patients. *Clin Cancer Res* **13**: 1405–1411.
- Knowlden JM, Hutcheson IR, Jones HE, Madden T, Gee JM, Harper ME *et al.* (2003). Elevated levels of epidermal growth factor receptor/c-erbB2 heterodimers mediate an autocrine growth regulatory pathway in tamoxifen-resistant MCF-7 cells. *Endocrinology* **144**: 1032–1044.
- Kocarek TA, Shenoy SD, Mercer-Haines NA, Runge-Morris M. (2002). Use of dominant negative nuclear receptors to study xenobiotic-inducible gene expression in primary cultured hepatocytes. *J Pharmacol Toxicol Methods* **47**: 177–187.
- Laffitte BA, Kast HR, Nguyen CM, Zavacki AM, Moore DD, Edwards PA. (2000). Identification of the DNA binding specificity and potential target genes for the farnesoid X-activated receptor. *J Biol Chem* **275**: 10638–10647.
- Makishima M, Okamoto AY, Repa JJ, Tu H, Learned RM, Luk A *et al.* (1999). Identification of a nuclear receptor for bile acids. *Science* **284**: 1362–1365.
- Meng S, Tripathy D, Shete S, Ashfaq R, Haley B, Perkins S *et al.* (2004). HER-2 gene amplification can be acquired as breast cancer progresses. *Proc Natl Acad Sci USA* **101**: 9393–9398.
- Morelli C, Garofalo C, Sisci D, del Rincon S, Cascio S, Tu X *et al.* (2004). Nuclear insulin receptor substrate 1 interacts with estrogen receptor alpha at ERE promoters. *Oncogene* **23**: 7517–7526.
- Nicholson RI, Staka C, Boyns F, Hutcheson IR, Gee JM. (2004). Growth factor-driven mechanisms associated with resistance to estrogen deprivation in breast cancer: new opportunities for therapy. *Endocr Relat Cancer* **11**: 623–641.
- Osborne CK, Bardou V, Hopp TA, Chamness GC, Hilsenbeck SG, Fuqua SA *et al.* (2003). Role of the estrogen receptor coactivator AIB1 (SRC-3) and HER-2/neu in tamoxifen resistance in breast cancer. *J Natl Cancer Inst* **95**: 353–361.
- Parks DJ, Blanchard SG, Bledsoe RK, Chandra G, Consler TG, Kliewer SA *et al.* (1999). Bile acids: natural ligands for an orphan nuclear receptor. *Science* **284**: 1365–1368.
- Sabnis GJ, Jelovac D, Long B, Brodie A. (2005). The role of growth factor receptor pathways in human breast cancer cells adapted to long-term estrogen deprivation. *Cancer Res* **65**: 3903–3910.
- Schiff R, Massarweh SA, Shou J, Bharwani L, Mohsin SK, Osborne CK. (2004). Cross-talk between estrogen receptor and growth factor pathways as a molecular target for overcoming endocrine resistance. *Clin Cancer Res* **10**: 331S–336S.
- Seidman AD, Fornier MN, Esteva FJ, Tan L, Kaptain S, Bach A *et al.* (2001). Weekly trastuzumab and paclitaxel therapy for metastatic breast cancer with analysis of efficacy by HER2 immunophenotype and gene amplification. *J Clin Oncol* **19**: 2587–2595.
- Shou J, Massarweh S, Osborne CK, Wakeling AE, Ali S, Weiss H *et al.* (2004). Mechanisms of tamoxifen resistance: increased estrogen receptor-HER2/neu cross-talk in ER/HER2-positive breast cancer. *J Natl Cancer Inst* **96**: 926–935.
- Sirianni R, Chimento A, Malivindi R, Mazzitelli I, Ando S, Pezzi V. (2007). Insulin-like growth factor-I, regulating aromatase expression through steroidogenic factor 1, supports estrogen-dependent tumor Leydig cell proliferation. *Cancer Res* **67**: 8368–8377.
- Slamon DJ, Godolphin W, Jones LA, Holt JA, Wong SG, Keith DE *et al.* (1989). Studies of the HER-2/neu proto-oncogene in human breast and ovarian cancer. *Science* **244**: 707–712.
- Slamon DJ, Leyland-Jones B, Shak S, Fuchs H, Paton V, Bajamonde A *et al.* (2001). Use of chemotherapy plus a monoclonal antibody against HER2 for metastatic breast cancer that overexpresses HER2. *N Engl J Med* **344**: 783–792.
- Staka CM, Nicholson RI, Gee JM. (2005). Acquired resistance to oestrogen deprivation: role for growth factor signalling kinases/oestrogen receptor cross-talk revealed in new MCF-7X model. *Endocr Relat Cancer* **12**(Suppl 1): S85–S97.
- Swales KE, Korbonits M, Carpenter R, Walsh DT, Warner TD, Bishop-Bailey D. (2006). The farnesoid X receptor is expressed in breast cancer and regulates apoptosis and aromatase expression. *Cancer Res* **66**: 10120–10126.
- Vavassori P, Mencarelli A, Renga B, Distrutti E, Fiorucci S. (2009). The bile acid receptor FXR is a modulator of intestinal innate immunity. *J Immunol* **183**: 6251–6261.
- Xing X, Wang SC, Xia W, Zou Y, Shao R, Kwong KY *et al.* (2000). The ets protein PEA3 suppresses HER-2/neu overexpression and inhibits tumorigenesis. *Nat Med* **6**: 189–195.
- Yarden Y. (2001). Biology of HER2 and its importance in breast cancer. *Oncology* **61**(Suppl 2): 1–13.

Supplementary Information accompanies the paper on the Oncogene website (<http://www.nature.com/onc>)